

Phosphine—Phosphinite and Phosphine—Phosphite Ligands: Preparation and Applications in Asymmetric Catalysis

Héctor Fernández-Pérez,[†] Pablo Etayo,[†] Armen Panossian,[†] and Anton Vidal-Ferran^{*,†,‡}

[†]Institute of Chemical Research of Catalonia (ICIQ), Avda. Països Catalans 16, 43007 Tarragona, Spain

[‡]Catalan Institution for Research and Advanced Studies (ICREA), Passeig Lluís Companys 23, 08010 Barcelona, Spain

CONTENTS

1. Introduction	2119	3.2.4. Asymmetric Hydroformylations of Heteroatom-Substituted Olefins or Alkenes That Contain Substituents with Functional Groups	2147
2. Preparation of Enantiopure Phosphine—Phosphinites and Phosphine—Phosphites	2124	3.2.5. Rationalization of the Stereochemical Outcome	2150
2.1. Synthesis of Phosphino Alcohols and Subsequent O-Phosphorylation with Electrophilic Phosphorus Reagents (Chlorophosphines and Chlorophosphites)	2125	3.2.6. Comparative Tables in Hydroformylations	2151
2.1.1. Preparation of Enantiopure Phosphine—Phosphinites	2125	3.3. Copper-Mediated Conjugate Additions	2151
2.1.2. Preparation of Enantiopure Phosphine—Phosphites	2126	3.3.1. Comparative Tables in Conjugate Additions	2152
2.2. Synthesis of Phosphine—Phosphinites and Phosphine—Phosphites by C- and O-Phosphorylation with Electrophilic Phosphorus Reagents	2129	3.4. Polymerizations of Alkenes with CO	2153
2.3. Synthesis of Phosphine—Phosphites by Supramolecular Interactions	2130	3.4.1. Alternating Copolymerizations of CO with Propene	2153
3. Applications in Asymmetric Catalysis	2132	3.4.2. Alternating Copolymerizations of CO with Higher Aliphatic 1-Alkenes	2155
3.1. Hydrogenations of Prochiral C=C and C=N Bonds	2133	3.4.3. Alternating Copolymerizations of CO with Vinyl Arenes	2156
3.1.1. Asymmetric Hydrogenations of Prochiral C=C Bonds Mediated by Phosphine—Phosphinite and Phosphine—Phosphite Ligands	2133	3.4.4. Terpolymerizations of Aliphatic Alkenes, Vinyl Arenes, and CO	2157
3.1.2. Asymmetric Hydrogenations of Prochiral Imines and Related Compounds Mediated by Phosphine—Phosphite Ligands	2138	3.5. Palladium-Mediated Allylic Substitutions	2159
3.1.3. Mechanistic Considerations and Origin of the Enantioselectivity	2138	3.5.1. Comparative Table in Allylic Substitutions	2165
3.1.4. Comparative Table in Asymmetric Hydrogenations	2141	3.6. Rhodium-Mediated Hydroborations of Alkenes	2165
3.2. Hydroformylations	2141	3.6.1. Comparative Table in Hydroborations	2166
3.2.1. Asymmetric Hydroformylations of Aryl-Substituted Alkenes	2141	3.7. Palladium-Mediated Hydrophosphorylations of Vinyl Arenes	2166
3.2.2. Asymmetric Hydroformylations of Alkyl-Substituted Alkenes	2145	3.8. Miscellaneous Reactions	2168
3.2.3. Asymmetric Hydroformylations of Conjugated Dienes and Heteroaryl Alkenes	2145	3.9. Most Recent Progress	2170
		4. Conclusions and Outlook	2170
		Author Information	2171
		Biographies	2171
		Acknowledgment	2172
		References	2172

1. INTRODUCTION

Over the past few decades transition metal-mediated transformations have become extremely powerful tools in organic

Special Issue: 2011 Frontiers in Transition Metal Catalyzed Reactions

Received: July 31, 2010

Published: January 20, 2011

synthesis, with many classes of efficient chiral nonracemic ligands having been developed for an ever-growing number of asymmetric transformations.¹ The key step in most metal-mediated asymmetric processes is the formation of a new species around the metallic center, which involves the substrate, the reagent(s), and an enantiomerically pure molecule (the ligand) usually bound to the metal center through one or more functional groups. As in every supramolecular process, reversible interactions (i.e., hydrogen

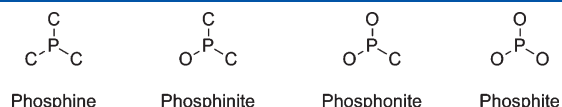


Figure 1. Various trivalent phosphorus ligand families.

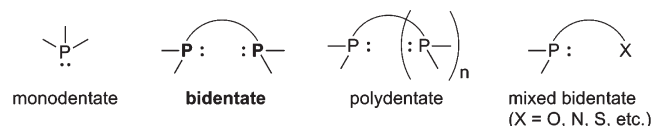


Figure 2. Trivalent phosphorus ligands classified by coordination mode.

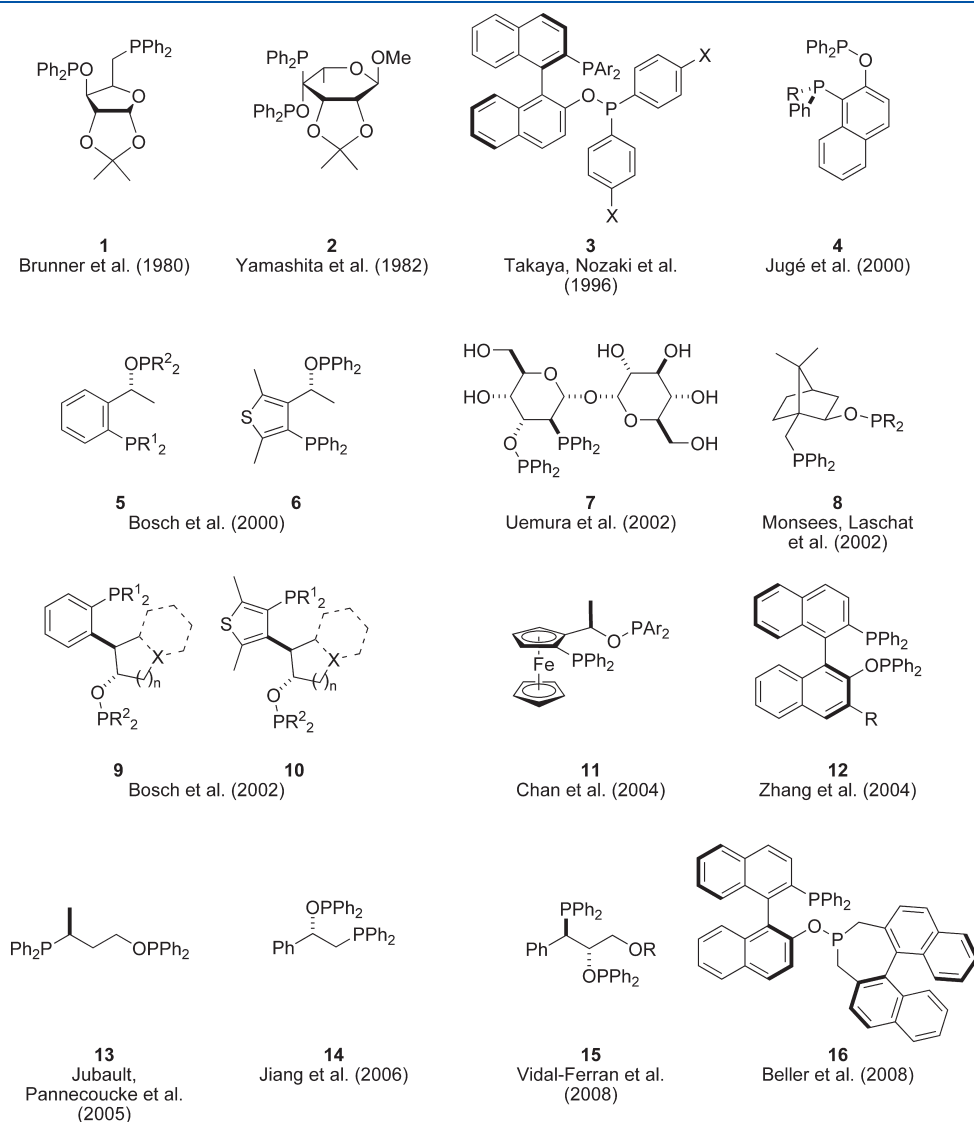
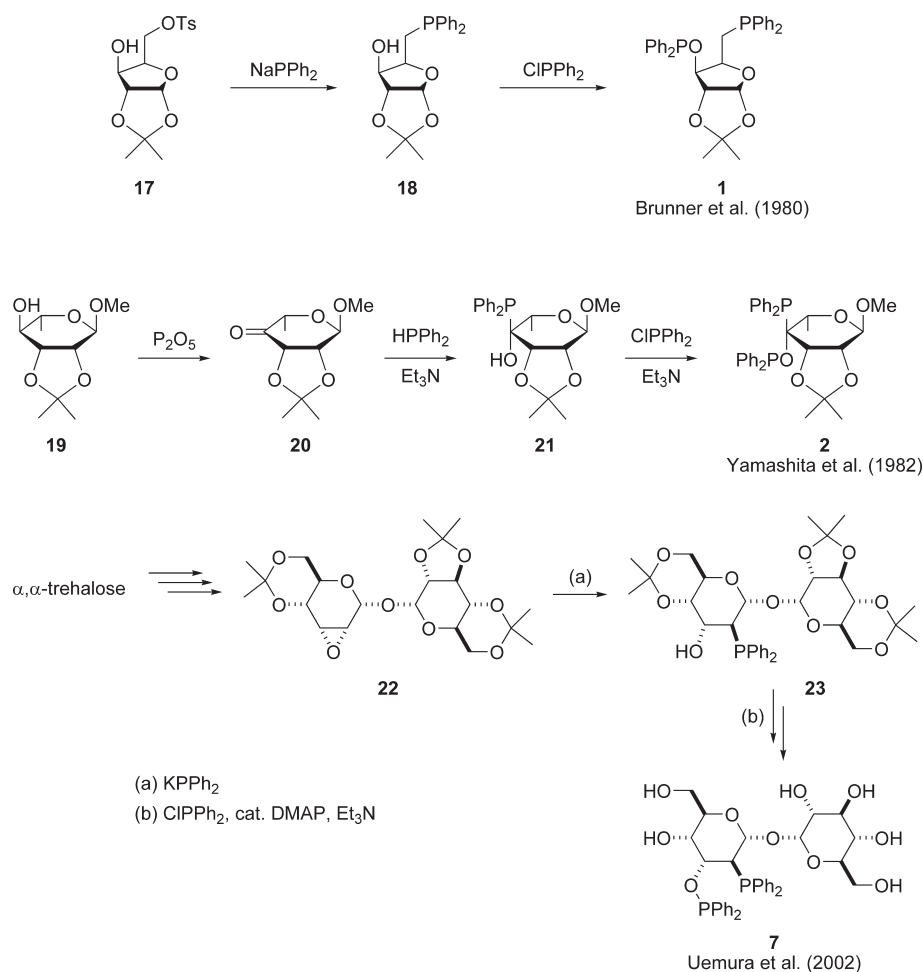


Figure 3. Known enantiopure phosphine-phosphinite ligands.

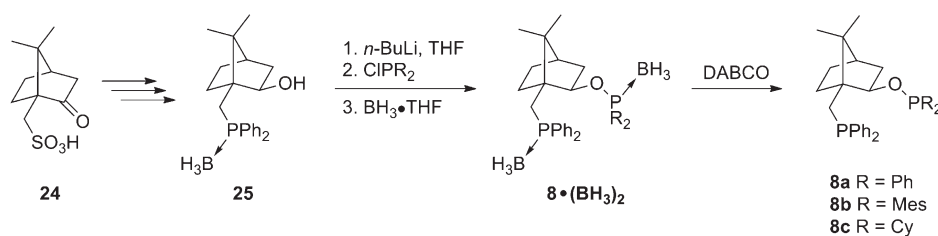
bonding, π - π stacking, or metal-ligand bonding) are responsible for the assembly of the elements of the catalytic system. The nature and strength of the binding forces by which the reagents assemble around the catalyst are highly dependent on the nature of the catalyst, the chemical transformation, and the mechanism of stereinduction. In such a catalytic system, the metal provides a low-energy reaction pathway to the products, whereas the ligand modulates the reactivity of the metal and also creates an asymmetric (or dissymmetric) environment around the metal center, thereby allowing for the preferential recognition of one of the enantiotopic elements (atom, group, or face) in the substrate.

The first ligands that were employed in asymmetric catalysis mostly derived from natural products. However, researchers soon realized that because of the limited structural diversity among those ligands, it was unlikely that they could provide a satisfactory response in terms of selectivity to all the conceivable situations in catalysis (reactions, metals, substrates, reagents, etc.). Thus, asymmetric synthesis was harnessed to broaden the repertoire of available ligand scaffolds, incorporate every conceivable type of molecular chirality, and functionalize ligands with a myriad of binding groups for the majority of metal centers. Indeed, enantiomerically

Scheme 1. Carbohydrate-Derived Phosphine–Phosphinites



Scheme 2. Terpene-Derived Phosphine–Phosphinite Ligands

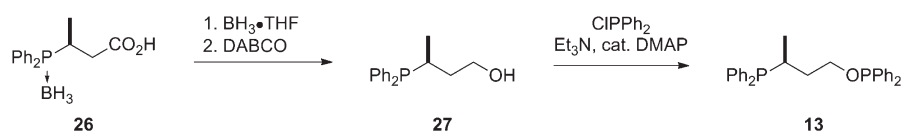


pure C-, N-, O-, P-, and S-containing ligands of synthetic origin have enabled major advances in asymmetric catalysis for nearly every synthetic transformation amenable to catalysis.

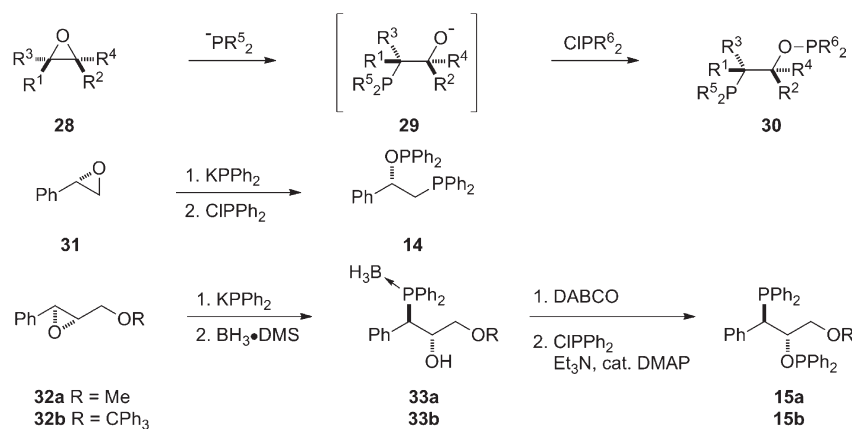
Owing to the special metal ligation properties of phosphorus derivatives, trivalent phosphorus ligands have played and still play an important role as metal binders in asymmetric homogeneous organometallic catalysis. These trivalent phosphorus compounds offer chemists the unique opportunity to modify the steric and electronic properties of the ligands. In terms of electronic structure, the π -accepting properties of the phosphorus group can be strongly modified via replacement of the P–C bonds with P–O (Figure 1), leading to phosphinites, phosphonites, or phosphites.

Ligands, in general, and more specifically P-derivatives can also be differentiated according to their coordinating mode (i.e., monodentate, bidentate, or polydentate; see Figure 2). In the early 1970s, Kagan devised the C_2 -symmetric chelating diphosphine DIOP² and demonstrated that rhodium complexes of chelating diphosphines catalyzed the asymmetric hydrogenation of C=C bonds with higher enantioselectivities than monodentate analogs. The topology of DIOP (chelating coordination and C_2 -symmetry) strongly influenced the design of future ligands for asymmetric catalysis, of which C_2 -symmetric ligands have been predominant.³ C_2 -Ligands might aid in reducing the number of possible catalyst–substrate adducts (and transition states), and

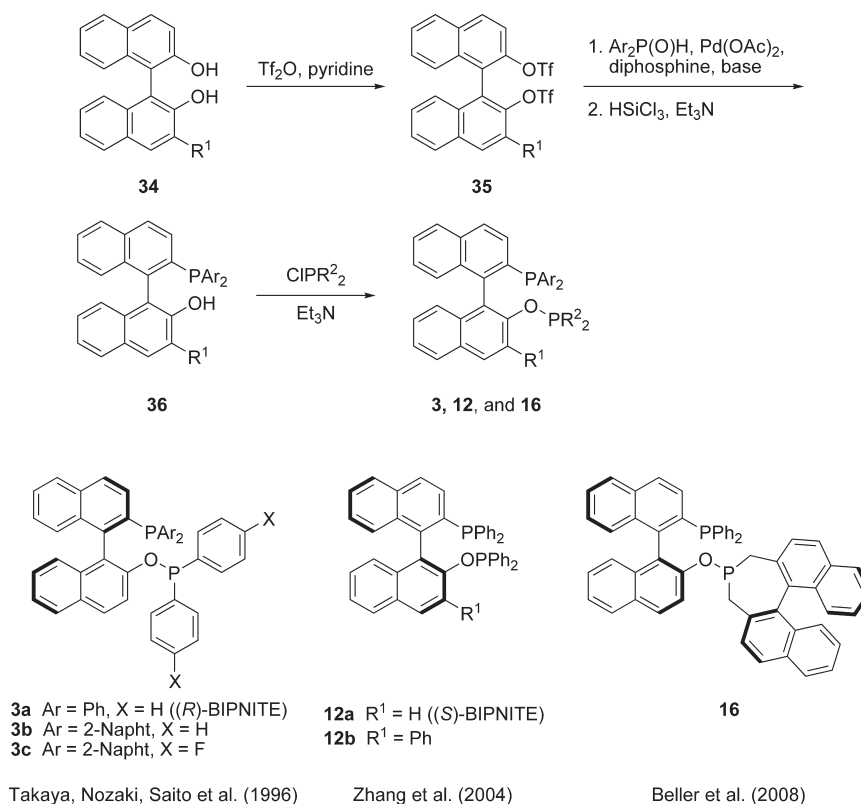
Scheme 3. Preparation of P–OP Ligand 13 by Reduction of a Phosphorus-Containing Intermediate



Scheme 4. Preparation of Phosphine–Phosphinites by Ring-Opening of Non-natural Epoxides



Scheme 5. General Strategy for Synthesizing the Phosphine–Phosphinites 3, 12, and 16 from Optically Pure BINOLs



this was believed to have favorable effects on the asymmetric bias of the transformation. Later advancements in the field of asymmetric catalysis demonstrated that, regarding enantioselectivities,

C₂-symmetric ligands are not necessarily intrinsically better than their analogs lacking any symmetry element (i.e., C₁-ligands).⁴ In certain situations, ligands with two different coordinating groups

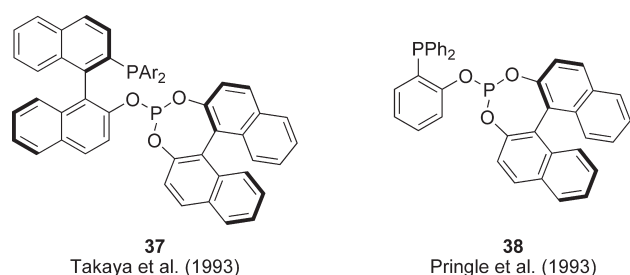


Figure 4. The first reported chiral phosphine–phosphites.

should allow for a better stereocontrol.⁵ This has led to growing interest in the design, preparation, and study of the catalytic properties of C_1 -symmetric bidentate ligands.

Phosphine–phosphinites and phosphine–phosphites are examples of nonsymmetric ligands that differ in the electronics and the sterics of their respective binding groups. Since the reports of the seminal phosphine–phosphite designed by Takaya⁶ and Pringle,⁷ and the phosphine–phosphinites developed by Brunner,⁸ several other related ligands have been described. These P–OP ligands encompass diverse carbon backbones and stereogenic elements as well as different distances between

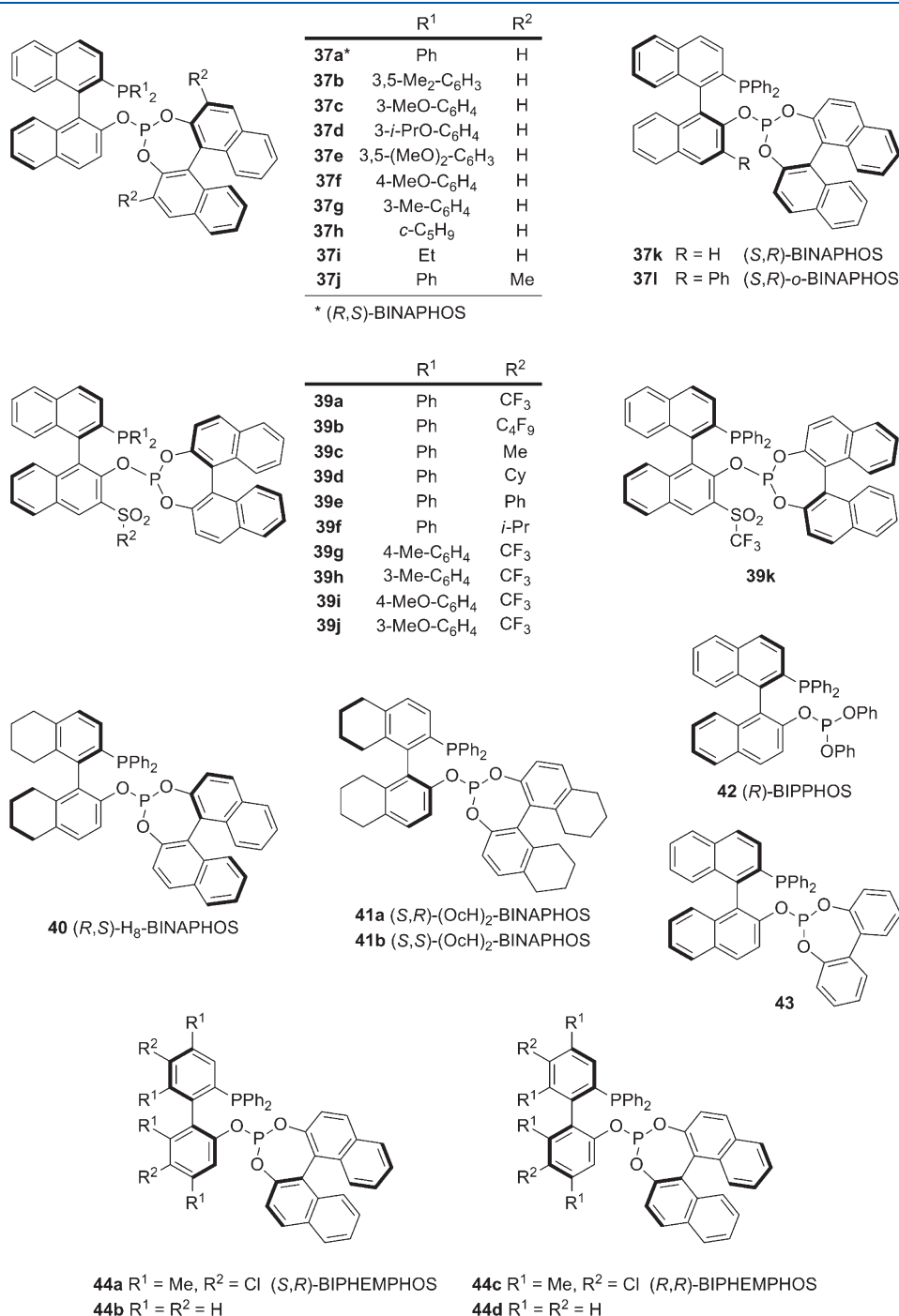


Figure 5. BINAPHOS-related ligands.

the two phosphorus functionalities. These compounds have been widely studied in enantioselective catalysis, for which they have afforded excellent results in various asymmetric transformations.

Although several reviews have dealt with phosphine–phosphinites and phosphine–phosphites derived from carbohydrates,⁹ highlighted their activity in a given asymmetric transformation,¹⁰ or included phosphine–phosphinites and phosphine–phosphites in a general review on phosphorus ligands,¹¹ none of these articles

provide a comprehensive overview on the different methods for preparing these ligands in enantiomerically pure form. Furthermore, the literature is lacking an updated summary of their performance in asymmetric catalysis. Thus, this review was devised to summarize the results obtained with enantiopure bidentate phosphine–phosphinite and phosphine–phosphite ligands in well-studied, transition metal-mediated asymmetric transformations and to describe their synthesis. However, symmetric bisphosphorus derivatives, polydentate ligands that contain the phosphine–phosphinite or phosphine–phosphite units, and mixed P–N, P–S, or P–O–bidentate ligands are all outside the scope of this text.

2. PREPARATION OF ENANTIOPURE PHOSPHINE–PHOSPHINITES AND PHOSPHINE–PHOSPHITES

This section reviews the strategies for synthesizing phosphine–phosphinites and phosphine–phosphites, in which phosphino alcohols or their phenolic analogs are often key intermediates (preparation of enantiomerically pure P–OH derivatives is detailed in the following sections). Subsequent O-phosphorylation of the P–OH intermediates with electrophilic trivalent derivatives (chlorophosphines or chlorophosphites) readily affords the target ligands. Routes that do not involve P–OH intermediates are also described in the following sections.

In homogeneous catalysis, there is a need for catalyst recycling and product separation, especially for expensive catalysts that involve transition metals. The few known examples on heterogenization strategies for phosphine–phosphites and phosphine–phosphinites are highlighted in the following sections.

Several groups have recently reported the construction of the ligand backbone via modular attachment of building blocks using noncovalent and metal–ligand interactions. These building blocks

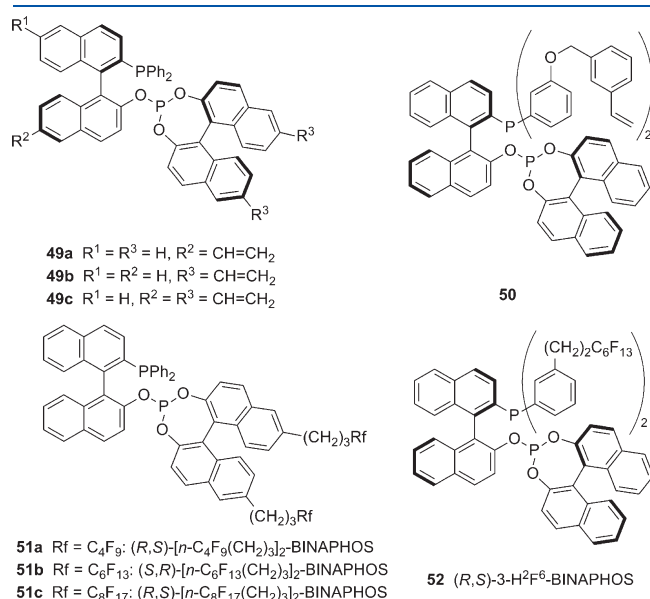


Figure 6. Developments in catalyst recycling involving BINAPHOS analogs.

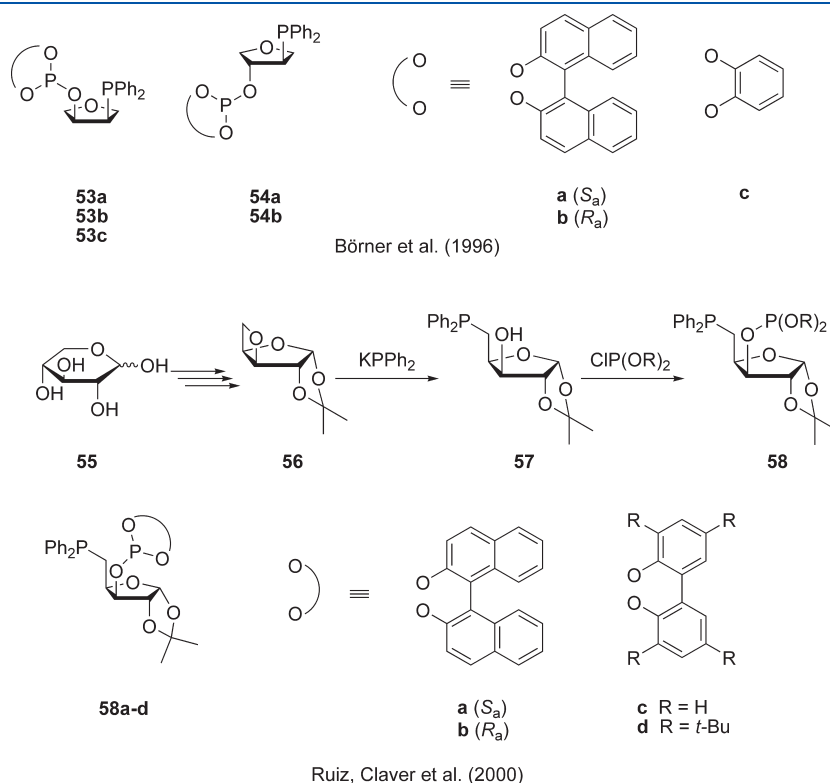


Figure 7. Enantiomerically pure phosphine–phosphite ligands derived from the chiral pool.

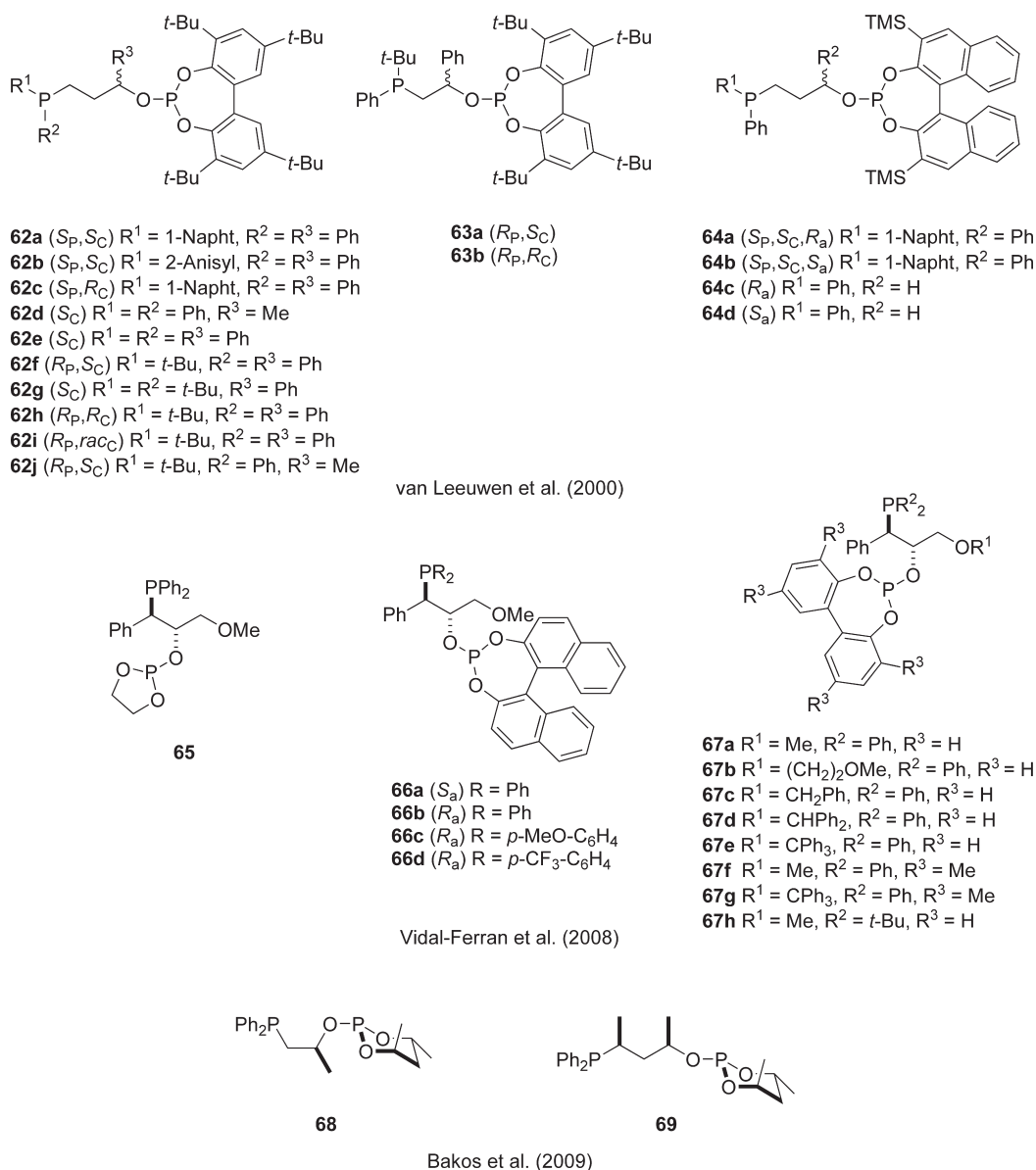


Figure 8. Phosphine—phosphite ligands derived from enantiomerically pure epoxides (or, in the case of ligand **69**, from an enantiopure cyclic sulfate).

contain the functional groups required for the desired catalysis (phosphine, phosphinite, and phosphite functionalities) as well as the motifs necessary for the supramolecular assembly. This methodology has enabled preparation of libraries of structurally diverse phosphine—phosphinites and phosphine—phosphites with unprecedented ease relative to standard covalent chemistry. Supramolecular routes to P—OP ligands are also detailed in the following sections.

2.1. Synthesis of Phosphino Alcohols and Subsequent O-Phosphorylation with Electrophilic Phosphorus Reagents (Chlorophosphines and Chlorophosphites)

2.1.1. Preparation of Enantiopure Phosphine—Phosphinites. Numerous phosphine—phosphinite ligands are known in the literature (Figure 3). They are typically synthesized via derivatization of the corresponding phosphino alcohols or their phenolic analogs. The phosphino functionality is normally introduced by attacking a suitably functionalized chiral backbone with a nucleophilic phosphorus reagent. The synthesis mainly

differs according to the transformation used to introduce the phosphino group:

- Nucleophilic substitution
- Nucleophilic addition onto C=O groups
- Epoxide ring-opening

Once the P—OH intermediate has been prepared, the phosphinite functionality is typically introduced by O-phosphorylation of a hydroxy group with the required chlorophosphine in the presence of a base.

Many of the known phosphine—phosphinite ligands are derived from the chiral pool, which has provided a diverse range of carbon backbones. Phosphine—phosphinite ligands **1**, **2**, and **7** were synthesized from readily accessible carbohydrates (Scheme 1), from which compound **1** was the first phosphine—phosphinite ligand reported in the literature by Brunner et al.⁸ Carbohydrates or sugar derivatives contain numerous hydroxy groups; therefore, a fundamental challenge in preparing these ligands comprised the selective transformation of a limited number of hydroxy groups into

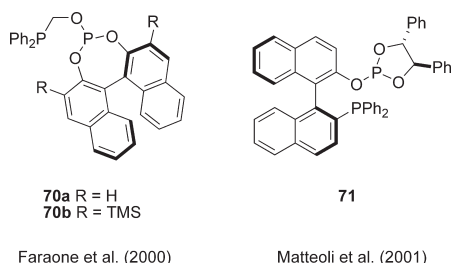


Figure 9. Chiral phosphine–phosphite ligands derived from BINOL or (*R,R*)-1,2-diphenyl-1',2'-ethanediol.

phosphino groups, which normally required a very careful planning of the synthetic strategy. The examples depicted in Scheme 1 nicely illustrate several strategies to introduce the phosphino functionality onto suitably modified carbohydrates using phosphides or the combination of a secondary phosphine and a base: whereas in the synthesis of **1**, Brunner et al.⁸ introduced the PPh₂ group via nucleophilic displacement of a tosyl group, to prepare ligand **2**, Yamashita et al.¹² generated the geminal phosphino alcohol **21** by diastereoselective addition of diphenylphosphine onto a C=O group, and last Uemura et al.¹³ prepared the 1,2-phosphino alcohol **23** by ring-opening of the epoxide **22** (derived from α,α -trehalose) with KPPH₂. The synthesis of phosphine–phosphinites **1**, **2**, and **7** was completed by O-phosphorylation of compounds **18**, **21**, and **23**, respectively, with chlorodiphenylphosphine and an auxiliary base.

The rich chemistry of terpenes, and their availability from the chiral pool have made them attractive starting materials for the synthesis of chiral ligands. For example, the phosphine–phosphinites **8a–c** were obtained in six steps from (1*S*)-(+)-camphorsulfonic acid (Scheme 2) by Monsees, Laschat, et al.¹⁴ Their route enabled incorporation of different phosphinite moieties in the final steps, facilitating the study of electronic and steric effects on asymmetric catalysis.

Interestingly, Jubault, Pannecoucke et al. synthesized ligand **13** by reduction of the carboxylic acid in P-containing intermediate **26** followed by O-phosphorylation of the resulting phosphino alcohol **27** (Scheme 3).¹⁵

Another convenient path to phosphine–phosphinite ligands is ring-opening of epoxides **28**, which proceeds by an S_N2 mechanism,¹⁶ followed by O-phosphorylation (Scheme 4), whereby alkali metal (Li or K) phosphides are normally employed as the phosphorus nucleophiles. Further derivatization of the resulting alkoxide **29** or its parent phosphino alcohol analog with the appropriate chlorophosphine leads to the desired phosphine–phosphinite ligands **30**. Jiang et al.¹⁷ and Vidal-Ferran et al.¹⁸ have used this chemistry to prepare phosphine–phosphinites from styrene oxide or Sharpless epoxy ethers, respectively. Vidal-Ferran et al. reported that ring-opening of the Sharpless epoxy ethers **32** at $-30\text{ }^{\circ}\text{C}$ to room temperature proceeded smoothly and in good yield. Phosphino alcohols generated from the ring-opening reactions were rather prone to oxidation; subsequent protection as the corresponding borane adducts **33** facilitated handling and storage. X-ray analysis¹⁹ of the borane adducts confirmed the regioselectivity of the ring-opening (nucleophilic attack at the benzylic position) and an *anti* arrangement of the hydroxy and phosphino substituents in **33**, as expected for a stereospecific S_N2-like oxirane ring-opening (inversion at the attacked carbon and retention at the other). Free phosphino alcohols were obtained by decomplexation of the borane adduct using DABCO and then derivatized using catalytic amounts of DMAP, an auxiliary base, and chlorodiphenylphosphine.

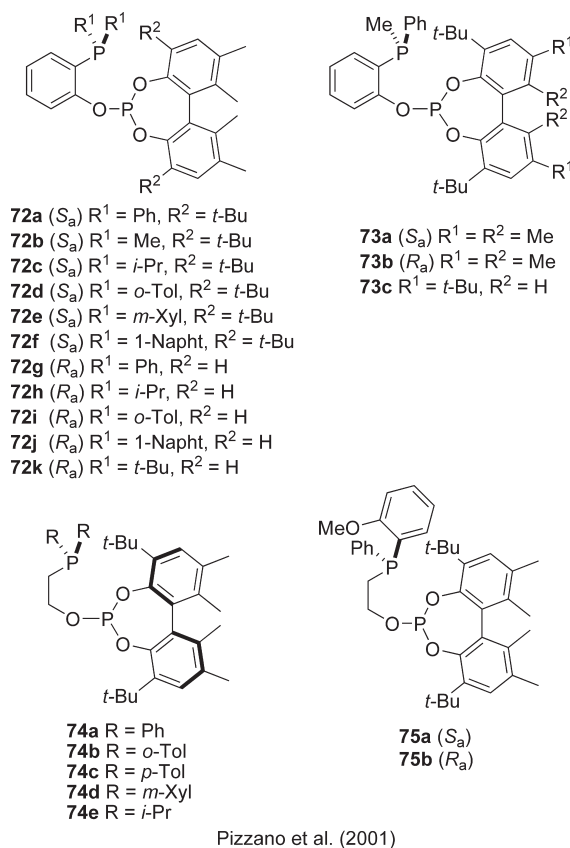


Figure 10. Phosphine–phosphite ligands synthesized by Pizzano et al.

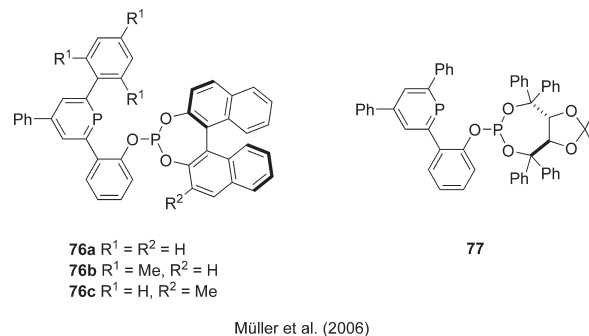
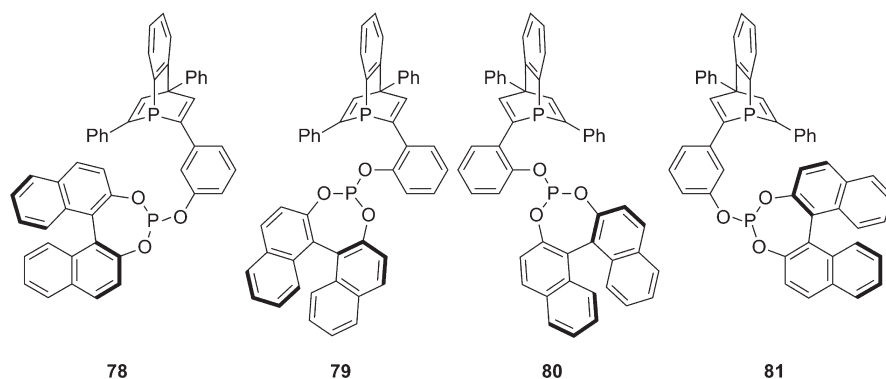


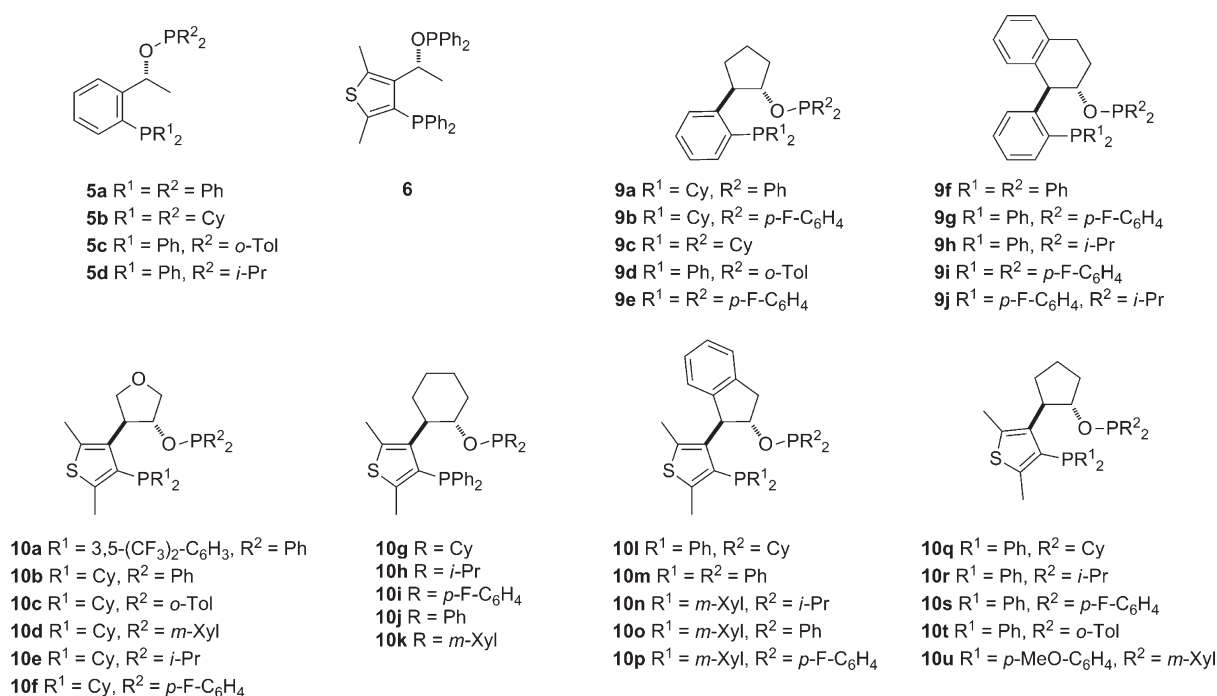
Figure 11. Phosphine–phosphite ligands designed by Müller et al.

Ligands with a conformationally stable biaryl group (e.g., a binaphthyl backbone) have been widely used in asymmetric catalysis, providing excellent conversion rates and enantioselectivities. Various binding groups have been attached to the binaphthyl backbone. In 1996, the late Takaya and Nozaki, Saito et al. developed the phosphine–phosphinite **3** (Scheme 5),²⁰ containing a stereogenic axis. Following Takaya's synthetic methodology, ligands **12**²¹ and **16**²² were readily synthesized by reacting the corresponding phosphino phenol **36** with the appropriate chlorophosphine, using triethylamine as base. Compounds **3**, **12**, and **16** were prepared from enantiomerically pure BINOLs **34**, through generation of the bistriflate **35**, followed by palladium-mediated phosphorus–carbon bond formation and, finally, reduction of the resulting phosphine oxide with HSiCl₃/Et₃N (Scheme 5).

2.1.2. Preparation of Enantiopure Phosphine–Phosphites. Compared with phosphine–phosphinites, far more



Breit et al. (2006)

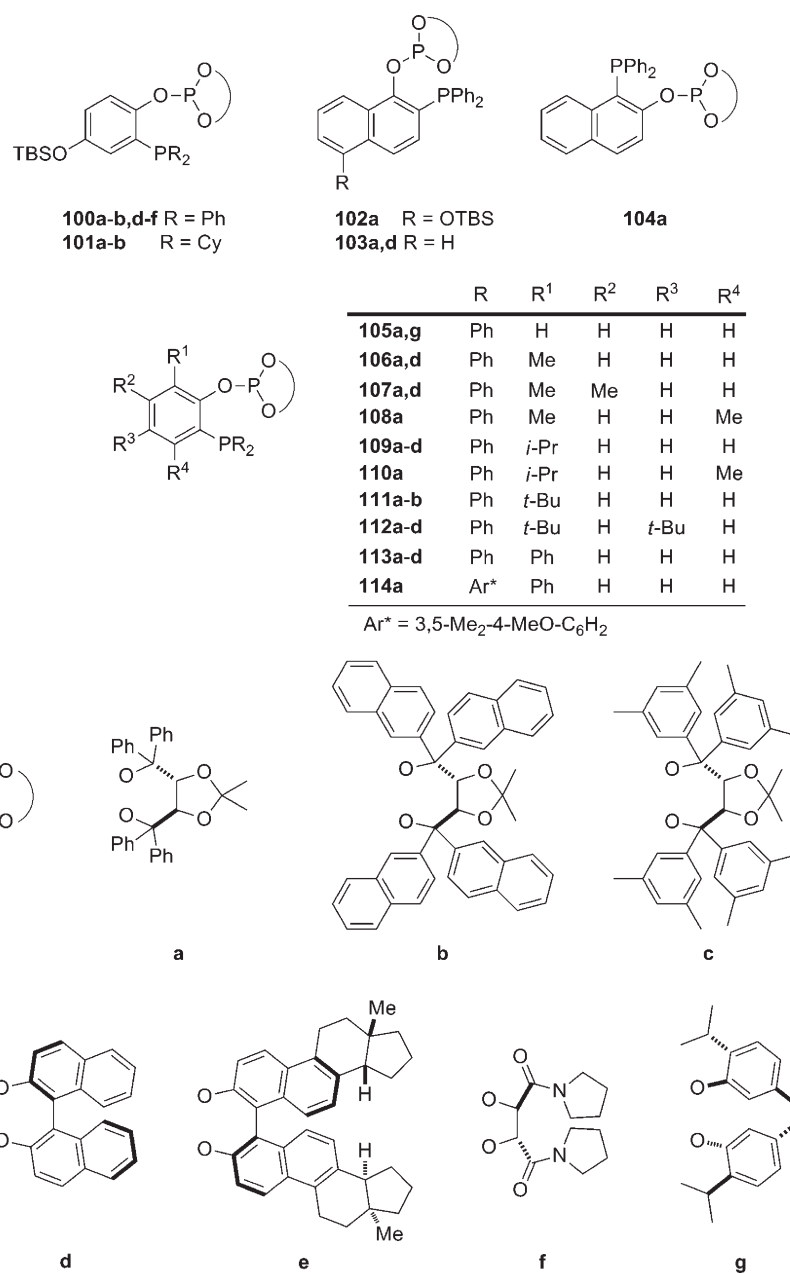
Figure 12. Phosphabarrelene-phosphite ligands developed by Breit et al.**Figure 13.** Phosphine–phosphinite ligands **5**, **6**, **9**, and **10** containing different backbones.

phosphine–phosphite ligands (see Figures 4–15 and Schemes 6–15) have been reported and evaluated in asymmetric catalysis. The most common strategy for synthesizing phosphine–phosphites is quite similar to that described in section 2.1.1: O-phosphorylation of phosphino alcohols or their phenolic analogs with chlorophosphites (rather than chlorophosphines).

Compounds **37** and **38**, the first examples of enantiopure phosphine–phosphites, were simultaneously reported in 1993 by the Takaya⁶ and Pringle⁷ groups, respectively. In these compounds, the two phosphorus groups are situated on structurally diverse carbon backbones. They both contain an axis as the stereogenic element that confers the stereodifferentiating properties to the ligand.

To the best of the author's knowledge, catalytic applications for phosphine–phosphite **38** are scarce in the literature.²³ Conversely, (*R,S*)-BINAPHOS (**37a**, Ar = Ph; Figure 4) is the most extensively studied phosphine–phosphite ligand in enantioselective catalysis and has afforded excellent results in many

asymmetric transformations. Thus, it should be regarded as a “privileged chiral ligand”.²⁴ The impact of BINAPHOS in the field of asymmetric catalysis not only lies in its outstanding catalytic properties, but also results because it has served as inspiration for the preparation of related phosphine–phosphite ligands, such as **37b**,⁶ **37c–g**,²⁵ **37h,i**,²⁶ **37j**,²⁷ **37k**,⁶ **37l**,²¹ **39**,²⁸ **40**,²⁶ **41**,²⁹ **42**,⁶ **43**,³⁰ and **44**.^{31,32} (Figure 5). (*R,S*)-BINAPHOS **37a** and its analogs **40–44** were prepared similarly to phosphine–phosphinites **3**, **12**, and **16** (see Scheme 5) from the corresponding P–OH derivatives, except that a chlorophosphite was used instead of a chlorodiarylphosphine in the O-phosphorylation of compound **36** and its analogs. Notably, the key intermediates **48** for the synthesis of ligands **39** developed by Leitner, Lloyd-Jones, et al.²⁸ were prepared via a thia-Fries rearrangement, via migration of a sulfonyl group from one oxygen atom in **47** to its *ortho* position, which had first been selectively deprotonated³³ (Scheme 6). O-Phosphorylation of these sulfonyl-containing P–OH derivatives **48** afforded BINAPHOS analogs **39a–k**.



Schmalz et al. (2000)

Figure 14. Structurally diverse phosphine–phosphite ligands prepared by Schmalz et al.

Given the impact of BINAPHOS in asymmetric catalysis, numerous heterogenization strategies for BINAPHOS and its analogs have been devised. Ligands **49a–c** and **50** contain vinyl groups at one or both of the binaphthyl moieties or at the phenyl substituents tethered to the phosphino group (Figure 6), enabling incorporation of the chiral ligand into a polymeric network, thereby making heterogeneous versions of these ligands possible.³⁴ In contrast, ligands **51a–c**³⁵ and **52**³⁶ contain perfluoroalkyl-substituted groups in either the phosphino or phosphite moieties (Figure 6), permitting their use in supercritical carbon dioxide, which facilitates catalyst recovery.

Several phosphine–phosphite ligands were later prepared in multistep reactions from chiral pool-derived compounds, thereby obviating the tedious step of resolving racemic compounds.

Ligands **53–54** (Figure 7) were prepared from enantiomerically pure *cis*- and *trans*-tetrahydrofuran derivatives, respectively, which are readily available from *L*-ascorbic or *D*-isoascorbic acids, respectively.³⁷ Starting from a different chiron, also derived from the chiral pool, Ruiz, Claver, et al. synthesized the new family of phosphine–phosphite ligands **58a–d**, based on the carbohydrate *D*-(+)-xylose **55**³⁸ (Figure 7).

Phosphine–phosphite ligands have also been synthesized via ring-opening of epoxides with phosphorus-containing nucleophilic reagents, followed by derivatization of the resulting phosphino alcohols with a chlorophosphite reagent, analogously to the preparation of phosphine–phosphinite ligands (see Scheme 4 in section 2.1.1). This procedure has been used by the groups of van Leeuwen, Vidal-Ferran, and Bakos to prepare the enantiomerically

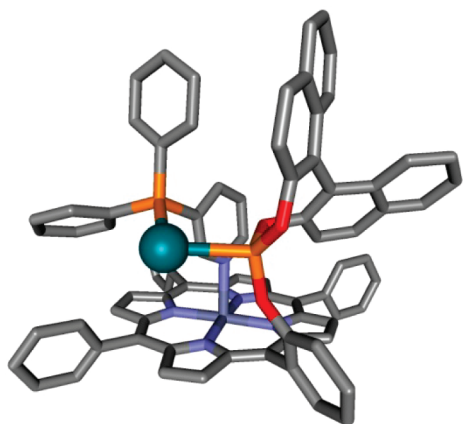


Figure 15. CAChe-minimized 3D structure of the rhodium-124b,u complex (other ligands from the metal omitted for clarity).

pure phosphine–phosphite ligands **62–68** (Figure 8). Several types of epoxides and, more interestingly, of phosphorus-containing nucleophiles have been employed (Scheme 7): whereas phosphides have provided access to numerous 1,2-phosphine–phosphite ligands **59**, a lithiated methylphosphine, used as nucleophile to open the epoxide, enabled preparation of 1,3-phosphine–phosphites **61**.

Van Leeuwen et al. synthesized the phosphine–phosphite ligands **62–64** from enantiomerically pure epoxides (propene oxide or styrene oxide) and phosphorus-containing carbon nucleophiles or nucleophilic phosphorus reagents, some of which were enantiomerically pure (Figure 8).³⁹ These nucleophiles enabled elegant synthesis of compounds **64a,b**, which contain three stereogenic elements (a stereogenic carbon center arising from the epoxide ring-opening, a stereogenic phosphorus atom, and a configurationally stable biaryl unit).

Vidal-Ferran et al. utilized ring-opening of the Sharpless epoxy ethers **32** with various phosphorus nucleophilic reagents (see Scheme 4), followed by O-phosphorylation with several chlorophosphites, to create a small library of highly modular phosphine–phosphite ligands, compounds **65–67** (Figure 8).^{18,19,40} Bakos et al. recently reported preparation of enantiopure phosphine–phosphite ligand **68** starting from (*S*)-propylene oxide and employing epoxide ring-opening and O-phosphorylation as key steps in the synthetic route. Likewise, these authors synthesized the phosphine–phosphite ligand **69** from an enantiomerically pure cyclic sulfate (Figure 8).⁴¹

The phosphine–phosphite ligands **70** and **71** (Figure 9), derived from BINOL or (*R,R*)-1,2-diphenyl-1',2'-ethanediol, respectively, were prepared via O-phosphorylation of P–OH derivatives with readily available chlorophosphites.⁴²

Pizzano et al.⁴³ have developed a versatile route to a new class of chiral phosphine–phosphite ligands, compounds **72–75** (Figure 10), by O-phosphorylation of a phosphino alcohol or its phenolic analog bridged by an oxyethylene or an *o*-oxyphenyl fragment, respectively. Notably, their methodology also enabled preparation of enantiopure ligands **75a** and **75b** from P-stereogenic phosphine fragments.

More recently, two new types of phosphine–phosphite ligands, **76** and **77**⁴⁴ and **78–81**,⁴⁵ derived from phosphinines and phosphabarrelenes, respectively, were synthesized (Figures 11 and 12). These ligands are notable in that the nonphosphite P-groups form a heterocycle, making them electronically different from those in other ligands. These phosphinines and phosphabarrelenes

are interesting π -acceptor ligands for homogeneous catalysis, with electronic properties closer to those of phosphites.

The corresponding P–OH intermediates **86** and **87** required to synthesize P–OP ligands indicated in Figures 11 and 12 were elegantly prepared from the pyrylium salts **84** by O–P exchange using phosphine or tris(trimethylsilyl)phosphine, respectively. Subsequent cleavage of the methoxy group in **85** with BBr_3 , followed by O-phosphorylation, afforded Müller's phosphinine–phosphite ligands **76–77** (Scheme 8).⁴⁴ Breit's P–OP ligands were prepared from P–OH intermediates **87**, which in turn were obtained by Diels–Alder reaction of **85** and benzyne (generated *in situ*), followed by cleavage of the methoxy group. The target ligands **78–81** were then readily synthesized by O-phosphorylation of **87**.⁴⁵

2.2. Synthesis of Phosphine–Phosphinites and Phosphine–Phosphites by C- and O-Phosphorylation with Electrophilic Phosphorus Reagents

The phosphine–phosphinites and phosphine–phosphites highlighted in the previous section have been prepared by introducing the two phosphorus functionalities onto a (normally) chiral backbone using a nucleophilic phosphorus reagent (to afford the phosphine) and an electrophilic trivalent phosphorus derivative (to afford the phosphinite or phosphite). During retrosynthetic analysis of a target P–OP ligand, strategies for the introduction of the two phosphorus functionalities from electrophilic trivalent phosphorus should be considered, providing that the desired starting material for preparing the ligand enables selective metalation of one of the carbons. In these cases, two sequential C- and O-phosphorylations would yield phosphine–phosphinites or phosphine–phosphites, depending on the reagent used for the O-phosphorylation. This section summarizes the synthetic details of the ligands prepared to date following this methodology.

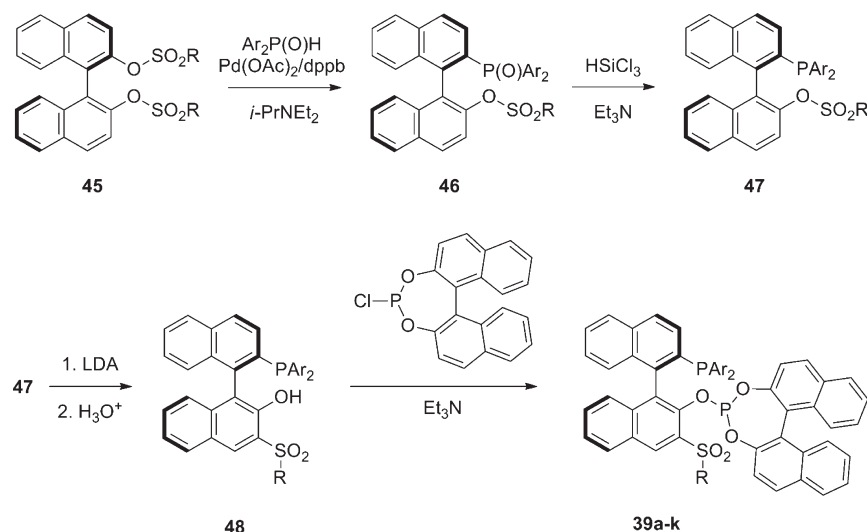
P-stereogenic derivatives with an *o*-hydroxyaryl group have recently gained attention as ligands in various asymmetric reactions and as precursors to other phosphorus ligands.⁴⁶ The ligands **4** were synthesized rather elegantly⁴⁷ (Scheme 9): first, the C–Br bond in **88** was lithiated, inducing an *ortho* Fries-like rearrangement, which led to migration of the phosphorus group from the *ortho*-oxy position to the metalated carbon with retention of configuration; second, the rearranged product was trapped with chlorodiphenylphosphine and subsequently protected with borane to give intermediates **89**; and finally, the resulting borane complex was cleaved with DABCO.

In a related procedure, Bosch et al. reported various structurally diverse enantiopure P–OP ligands, the compounds **5**, **6**, **9**, and **10** (Figure 13), encompassing different kinds of chiral backbones.⁴⁸ In this case, the two P-donor functionalities were introduced without any rearrangement (Scheme 10).

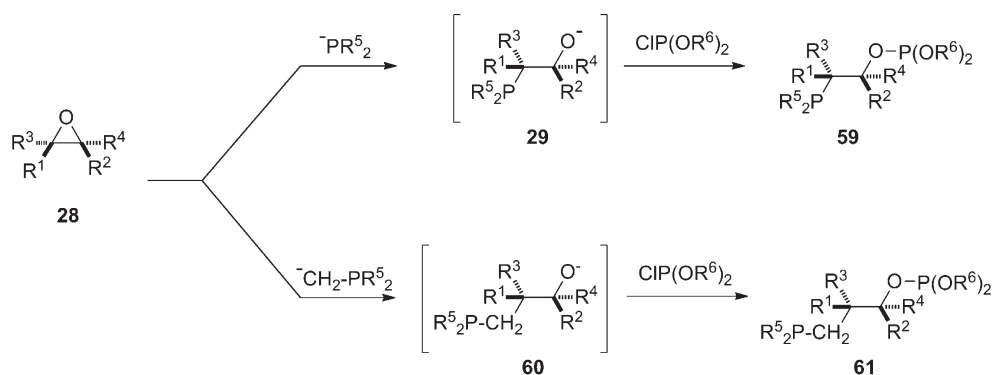
Ferrocene-based chiral ligands have proven invaluable in several transition metal-mediated asymmetric reactions. Yeung and Chan et al.⁴⁹ prepared the chiral phosphine–phosphite **99** and the phosphine–phosphinites **11a** and **11b** starting from Ugi's amine (see **96** in Scheme 11). These ferrocene-containing ligands are very attractive for asymmetric catalysis, owing to their straightforward synthesis and their stability to air and moisture.

New ligand structures are typically rationally designed and then individually synthesized. However, this is rather time-consuming, especially considering that many of the ligands will not provide an efficient catalyst. Thus, to accelerate ligand development, Schmalz et al. devised a broad library of structurally diverse

Scheme 6. Synthesis of Leitner's and Lloyd-Jones' BINAPHOS Analogs 39



Scheme 7. Preparation of Phosphine–Phosphite Ligands by Epoxide Ring-Opening



ligands (**100–114**) derived from modular ligand architectures (Figure 14).⁵⁰

ortho-Lithiation on either phenol- or naphthol-derived backbones provided the key intermediate **116**, onto which two phosphorus donor moieties were separately introduced to generate the phosphine–phosphite ligands **100–105** (Scheme 12).

However, this original methodology failed for the preparation of phosphine–phosphites **106–114**, all of which contain a bulky substituent R^1 . Alternatively, a phospho-Fries rearrangement^{47,51} of **120** to **121** (see section 2.2, Scheme 9) did provide ready access to **106–114** (Scheme 13).

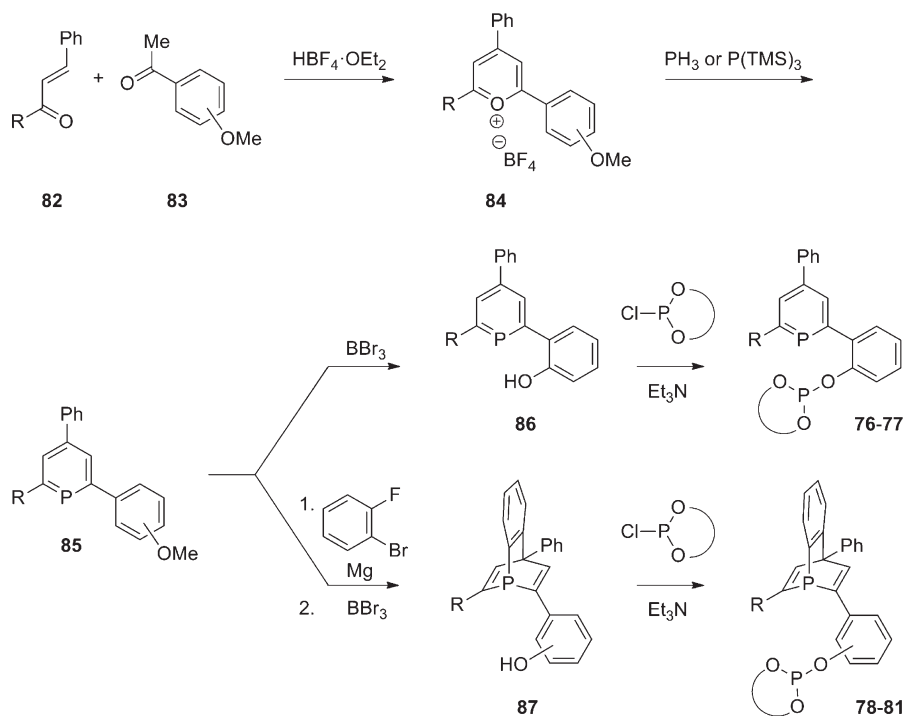
2.3. Synthesis of Phosphine–Phosphites by Supramolecular Interactions

Noncovalent and metal–ligand interactions are increasingly being used in construction of the asymmetric backbone of the catalyst via modular attachment of building blocks by the supramolecular interactions previously mentioned. These building blocks contain the functional groups required for the desired catalysis as well as motifs necessary for the supramolecular assembly. This methodology has enabled synthesis of libraries of structurally diverse supramolecular ligands with far greater ease than for standard covalent chemistry.

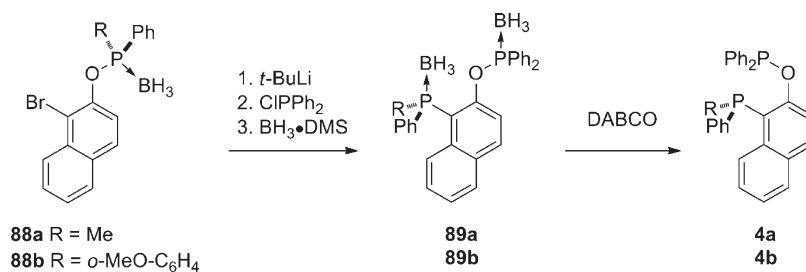
Van Leeuwen, Reek, et al. have pioneered a new and efficient supramolecular strategy for preparing bidentate ligands,⁵² whereby two suitably designed monomeric ligands are simply mixed. Phosphine–phosphites and other kinds of supramolecular bidentate ligands have been formed by a system comprising one porphyrin unit functionalized with one covalently bonded phosphite (**123** in Scheme 14) and a ditopic ligand **122** that contains nitrogen and phosphorus binding groups. Ligand **122** coordinated with its hard nitrogen atom to Zn in the porphyrin unit, whereas the phosphorus functionality did not intervene in the assembly process, thereby remaining free for catalysis. Libraries made this way were named *SUPRAPHOS*. A first generation library of ligands (Scheme 14) was successfully synthesized with this strategy and tested in allylic substitutions. This library was recently extended to ca. 500 members, which have been evaluated in many other catalytic reactions,^{11c,53} in which the supramolecular P–OP ligands behaved as bidentate ligands—specifically, wide-bite angle bidentates (Figure 15). The catalysis results are discussed in detail in the following sections.

Nishibayashi et al.⁵⁴ recently devised another supramolecular approach for preparing chelating ligands for homogeneous

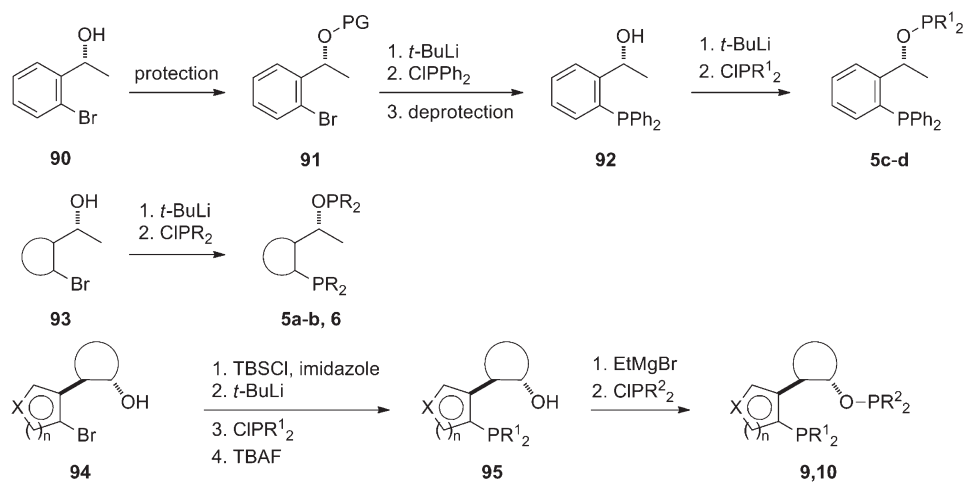
Scheme 8. Synthesis of the Required P–OH Intermediates for Müller's and Breit's P–OP Ligands



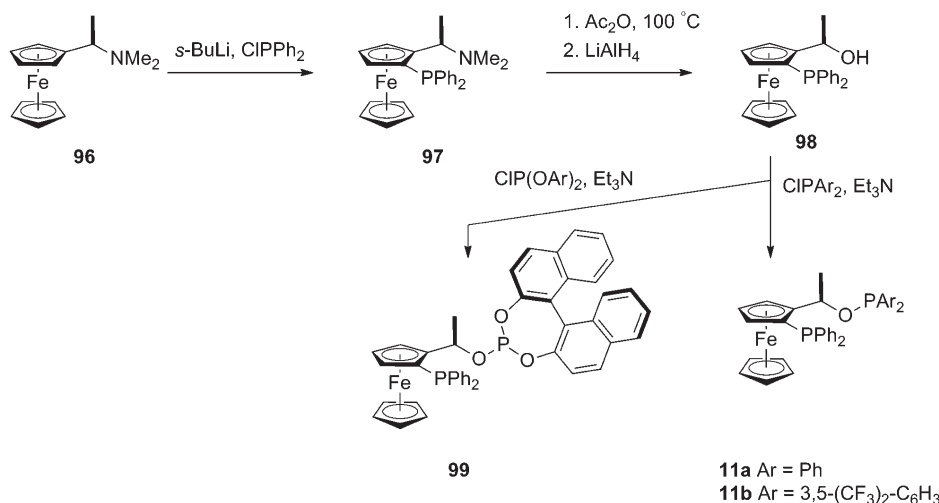
Scheme 9. Synthesis of the Phosphine–Phosphinite Ligands 4



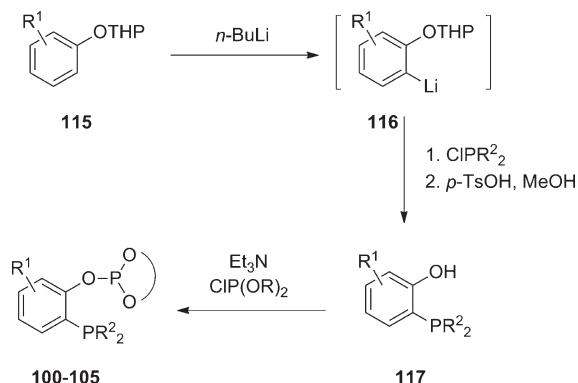
Scheme 10. Different Synthetic Procedures for Synthesizing Phosphine–Phosphinites 5, 6, 9, and 10



Scheme 11. Preparation of Ferrocene-Based Phosphine–Phosphites and Phosphine–Phosphinites



Scheme 12. Original Synthetic Strategy for Schmalz's Ligands



catalytic asymmetric transformations. They interlocked crown ether **125**, which contains a BINOL-derived phosphite group, with the phosphine-substituted ammonium derivatives **126** to form the supramolecular phosphine–phosphites **127a–c**, which have a pseudorotaxane structure. They exploited the high stability of the crown ether–ammonium salt interaction to link the two building blocks, each of which contributed one functional group to the final supramolecular bidentate ligand.

Both the *wheel* (**125**) and the *axle* (**126**) moieties from the pseudorotaxanes were synthesized in good yields using well-established synthetic methodologies.⁵⁴ Mixing equimolar amounts of these moieties afforded a mixture of two diastereoisomeric supramolecular complexes **127** due to the generation of a stereogenic plane in the pseudorotaxane skeleton.⁵⁵ Addition of a cationic rhodium complex to this diastereomeric mixture gave quantitative formation of a single diastereomeric rhodium chelate **128a,a** (Scheme 15) whose stereochemistry has not yet been determined. This result suggests that the diastereomeric formation of only one rhodium chelate is achieved by thermodynamic control through a reversible step within its formation.

Using this same strategy, Fan et al. have reported some more examples of pseudorotaxane-based phosphine–phosphites.⁵⁶

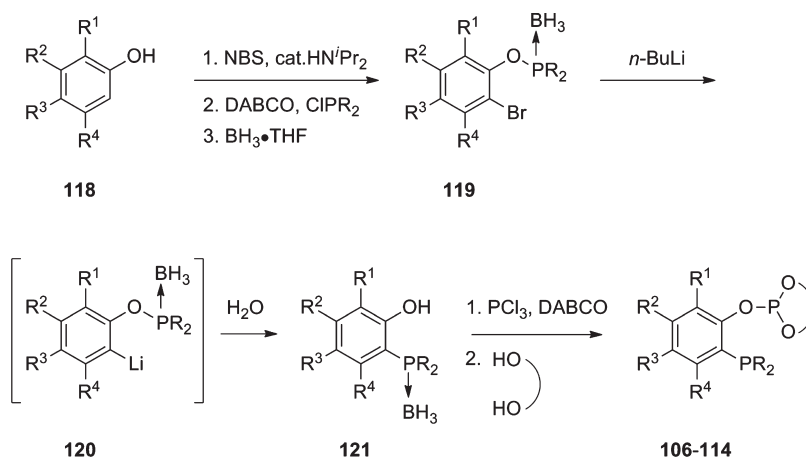
3. APPLICATIONS IN ASYMMETRIC CATALYSIS

With the advent of transition-metal based catalysts, asymmetric catalysis has expanded to encompass an ever-growing scope of substrates and chemical transformations. In fact, in the past 30 years, enantioselective catalysts have been developed for nearly every chemical transformation imaginable, enabling major breakthroughs in almost every one. Despite the remarkably advanced state of the field, many research groups continue to pursue new catalytic systems for challenging substrates, higher activity, or improved enantioselectivity.

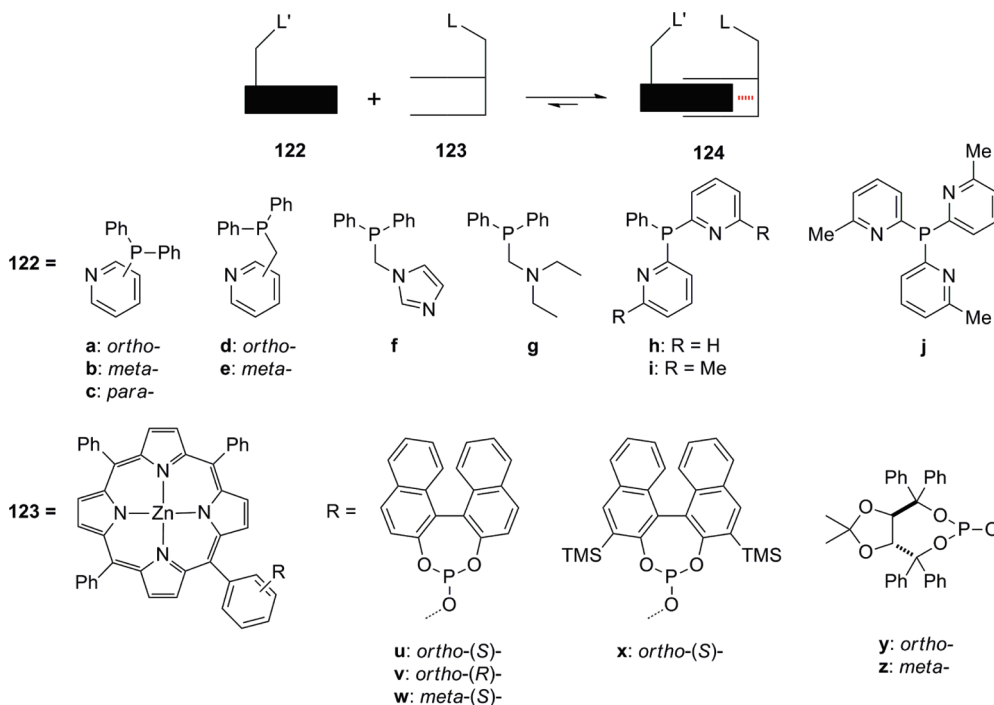
Ligand tuning in asymmetric catalysis has facilitated rapid development of efficient catalytic systems.^{19,57,58} When a catalytic process is developed or improved via catalyst tuning, it is crucial to progressively move to more efficient catalytic systems according to mechanistic and molecular interaction principles. Ideally, ligand design should incorporate several independent modules or molecular fragments orchestrated around a chiral skeleton. If these modules are designed such that they can influence the catalytic site, then modification of their steric and electronic properties should provide a higher performing catalytic system (i.e. one that offers higher conversion and regio- and enantioselectivity). Indeed, the sterics and electronics of the constituent modules/molecular fragments can be considered the *input parameters* in the optimization process. Complementarily, combinatorial and high-throughput synthetic strategies have led to numerous highly efficient ligands that utilize either standard covalent chemistry⁵⁹ or supramolecular interactions.^{52–54,56,60}

Phosphine–phosphite and phosphine–phosphinite ligands contain two different phosphorus-containing modules, whose sterics and coordination relative to a catalytic metal center can be modified by changing their substituents. This section provides an overview of the literature precedent on the application of enantiomerically pure phosphine–phosphinite and phosphine–phosphite ligands in asymmetric catalysis, highlighting, when necessary, the strategy employed during catalyst optimization.

Scheme 13. Improved General Synthesis of Schmalz's Ligands



Scheme 14. Preparation of Supramolecular Phosphine–Phosphite Ligands

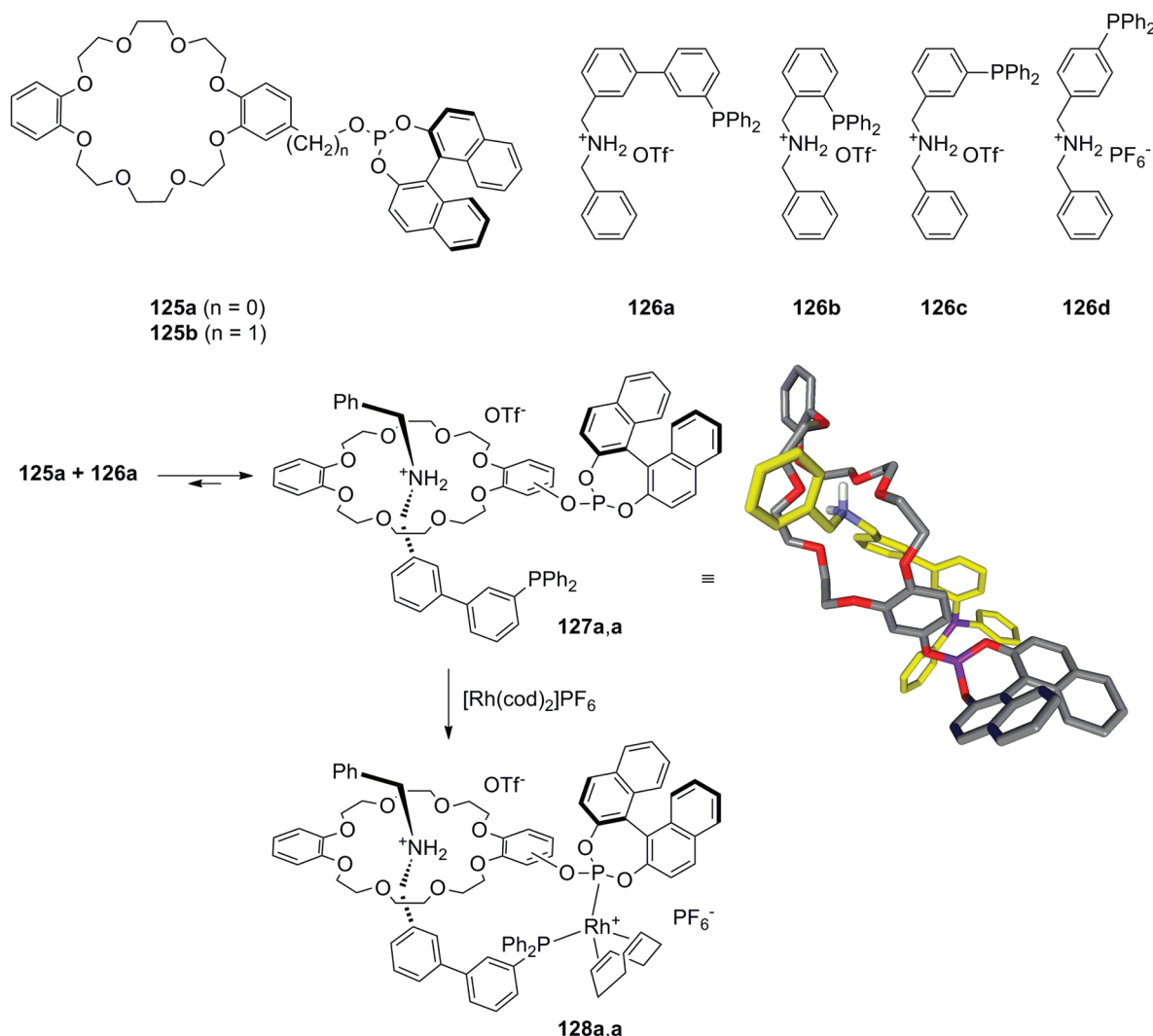


3.1. Hydrogenations of Prochiral C=C and C=N Bonds

Transition metal-mediated asymmetric hydrogenation is a well-established and efficient methodology for the catalytic reduction of prochiral alkenes, imines, and ketones.⁶¹ From a practical perspective, asymmetric hydrogenation has many advantages for generating new stereogenic centers, including broad substrate scope, high reactivity and selectivity, and simplified workup. There have been several significant breakthroughs in the field and a myriad of Ru-, Rh-, and Ir-coordination compounds (mostly phosphorus-containing derivatives) that can mediate these transformations with very high enantioselectivities are known.⁶¹ Most remarkably, the development of commercial processes has rendered this transformation highly desirable to both academia and industry.⁶²

3.1.1. Asymmetric Hydrogenations of Prochiral C=C Bonds Mediated by Phosphine–Phosphinite and Phosphine–Phosphite Ligands. Enantiopure phosphine–phosphinite ligands have been studied in rhodium-mediated asymmetric hydrogenation of functionalized alkenes. The corresponding 1:1 chelates between a phosphine–phosphinite and a Rh(I) precursor (mainly $[\text{Rh}(\text{cod})_2]\text{BF}_4$) should be regarded as the precatalysts in these asymmetric hydrogenations. These species are typically formed *in situ* by mixing the corresponding Rh(I) precursor with a slight excess of P–OP ligand. The diene ligand in the Rh(I) precatalyst is hydrogenated, and the two resulting vacant coordination sites on the metal center are subsequently occupied by solvent molecules: the resulting rhodium complex is

Scheme 15. Building Blocks for Assembling Pseudorotaxane-Based Supramolecular Phosphine–Phosphite Ligands **127** and a Representative Final Supramolecular Complex (**127a,a**)^a

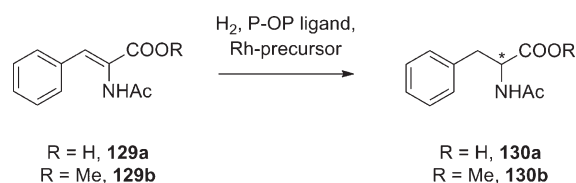


^a The 3D structure has been obtained by minimization with CAChe software and represents one of the two possible diastereoisomers.

considered the first species in the catalytic cycle of rhodium-mediated hydrogenations.⁶³

The behavior in catalysis of phosphine–phosphinite ligands has been tested in the asymmetric hydrogenation of benchmark substrates, the 2-acetamido-3-arylacrylate derivatives **129** (see Scheme 16). However, to the best of the author's knowledge, published studies on the asymmetric hydrogenation of topologically distinct prochiral alkenes mediated by this kind of P–OP ligands are very scarce. Results obtained for substrates **129a** and **129b** are shown in Table 1, whereby the results listed correspond to those obtained with the lead structure from a family of ligands. All of the phosphine–phosphinites studied offered excellent conversion; however, they varied widely in enantioselectivity, from low to excellent, depending on ligand structure. Ligand **11b**,⁴⁹ containing a ferrocene unit, and ligand **12b**,²¹ incorporating a binaphthyl moiety, gave the highest enantioselectivities for the 2-acetamido-3-phenylacrylate derivatives **129**. The substituents on the substrate's phenyl group did not affect the enantioselectivity (ligand **11b**, entry 6 and eight more examples,⁴⁹ ee's ranging from 95 to >99%; ligand **12b**, entry 8 and five more

Scheme 16. 2-Acetamido-3-phenylacrylate Derivatives as Substrates in Asymmetric Hydrogenation



examples,²¹ ee's 95 to >99%). Remarkably, Zhang's ligand also tolerates the free acid in substrates **129** without any loss of enantioselectivity (ligand **12b**, entry 7 and five more examples with the free carboxylic group,²¹ ee's >99%). None of the other phosphine–phosphinite ligands tested (Figure 16) fulfilled the steric and electronic requirements around the rhodium center to achieve such high enantioselectivities.

Phosphine–phosphite ligands have been more widely used in rhodium-mediated asymmetric hydrogenation than their

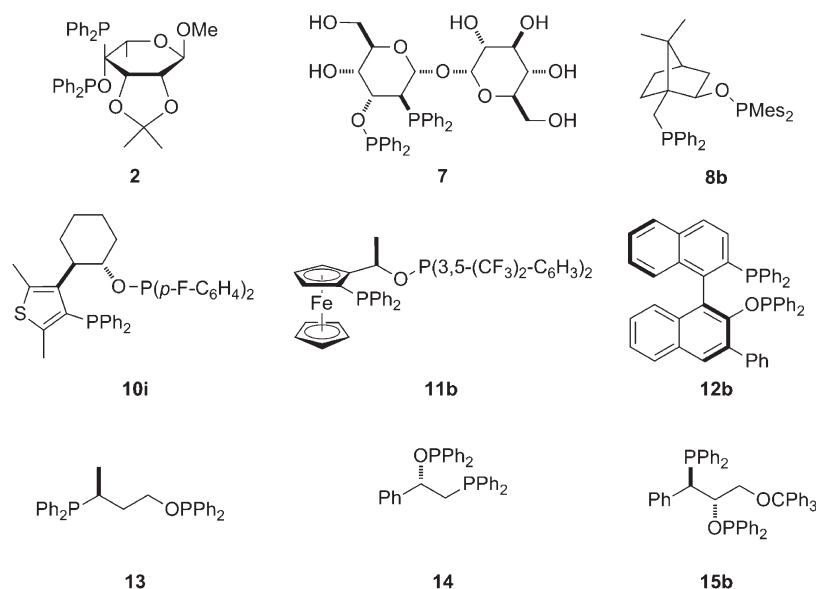


Figure 16. Phosphine–phosphinite ligands studied in asymmetric hydrogenation.

Table 1. Rhodium-Mediated Asymmetric Hydrogenation of Dehydroarylalanines Mediated by Phosphine–Phosphinite Ligands

entry	ligand	substrate	reaction conditions	conv. (%)	% ee of 130 (config.)
1	2 ¹²	129a	1 mol % [RhCl(cod)(P–OP)], 6 mol % Et ₃ N, rt, 50 atm H ₂ , 0.2 M in benzene–ethanol (1:1)	100	5 (R)
2	7 ¹³	129a	2 mol % [Rh(cod)(P–OP)]BF ₄ , rt, 50 atm H ₂ , 0.1 M in EtOAc–H ₂ O (1:1)	100	50 (R)
3	7 ¹³	129b	2 mol % [Rh(cod)(P–OP)]BF ₄ , rt, 50 atm H ₂ , 0.1 M in EtOAc–H ₂ O (1:1)	100	73 (R)
4	8b ^{14b}	129b	0.5 mol % [Rh(cod)(P–OP)]OTf, rt, 4.9 atm H ₂ , 0.2 M in toluene	100	89 (S)
5	10i ^{48b}	129b	0.2 mol % [Rh(cod)(P–OP)]OTf, rt, 4.9 atm H ₂ , 0.3 M in methanol	100	69 (nd)
6	11b ⁴⁹	129b	1 mol % [Rh(cod)(P–OP)]BF ₄ , 5 °C, 10.2 atm H ₂ , 0.5 M in toluene–DCM	100	97 (S)
7	12b ²¹	129a	1 mol % [Rh(cod)(P–OP)]PF ₆ , rt, 1.0 atm H ₂ , 0.2 M in THF	100	>99 (S)
8	12b ²¹	129b	1 mol % [Rh(cod)(P–OP)]PF ₆ , rt, 1.0 atm H ₂ , 0.2 M in THF	100	>99 (S)
9	13 ¹⁵	129b	0.5 mol % [Rh(cod)(P–OP)]BF ₄ , rt, 1.0 atm H ₂ , 0.2 M in DCM	100	91 (S)
10	14 ¹⁷	129a	1 mol % [Rh(cod)(P–OP)]PF ₆ , rt, 9.9 atm H ₂ , 0.6 M in DCM	100	70 (S)
11	14 ¹⁷	129b	1 mol % [Rh(cod)(P–OP)]PF ₆ , rt, 9.9 atm H ₂ , 0.6 M in DCM	100	77 (S)
12	15b ¹⁸	129b	1 mol % [Rh(nbd)(P–OP)]BF ₄ , rt, 19.7 atm H ₂ , 0.2 M in DCM	100	52 (S)

phosphinite counterparts. The corresponding 1:1 chelates between a phosphine–phosphite ligand and the usual rhodium(I) precursors in asymmetric hydrogenation should also be regarded as the precatalysts in this transformation. Analogously to the case of phosphine–phosphinites explained above, the corresponding chelates are typically generated *in situ* by reacting the corresponding Rh(I) precursor with the P–OP derivative.^{19,43g} Alternatively, precatalytic [Rh(diene)(P–OP)]⁺ complexes can be easily prepared in good yields following well-established procedures.⁶⁴ Complexes preformed this way have demonstrated equivalent catalytic performance in asymmetric hydrogenation as precatalysts prepared *in situ*.¹⁹

The catalytic activity of rhodium complexes bearing enantio-pure phosphine–phosphites in asymmetric hydrogenation has been evaluated against a wider variety of alkenes than for their phosphinite counterparts. Table 2 shows the results obtained for related phosphine–phosphites in the rhodium-mediated asymmetric hydrogenation of substrates **129a** and **129b** (Scheme 16), whereby the results listed in Table 2 correspond to those obtained with the lead structure from a family of ligands (Figure 17). The catalytic activity of a rhodium complex derived from a given P–OP ligand has normally been assessed in the hydrogenation

of methyl 2-acetamidoacrylate and **129** as benchmark substrates. Results on the asymmetric hydrogenation of methyl 2-acetamidoacrylate normally follow the same trend as do its phenyl-substituted analogs **129**, and for the results obtained with this substrate, the reader is referred to the original articles.

Diverse phosphine–phosphites have provided excellent conversions and enantioselectivities in the hydrogenation of 2-acetamido-3-phenylacrylate derivatives **129**. For example, P–OP ligands from Zhang (**371**),²¹ Ruiz and Claver (**58a** and **58d**),³⁸ van Leeuwen (**62e** and **63b**),⁶⁴ and Vidal-Ferran (**66a**)¹⁸ have all provided enantiomeric excesses greater than 95%. Ligands **371** and **66a** were also tested in the hydrogenation of a set of β -aryl dehydro- α -amino acids **129** with excellent conversions and enantioselectivities (ligand **371**, entry 2 in Table 2 and six more examples,²¹ ee's from 95% to >99%; ligand **66a**, entry 8 in Table 2 and five more examples,^{18,19} ee's 99%). Ligands **371** and **66a** tolerate as well the free acid group in substrate **129a** without any loss of enantioselectivity (ligand **371**, entry 1 in Table 2 and five more examples with the free carboxylic group,²¹ ee's >99%; ligand **66a** entry 7 in Table 2). An important feature of the phosphine–phosphite ligand **66a** is its tolerance to a broad variety of carbamate-type amino-protecting groups (Boc, Cbz,

Table 2. Rhodium-Mediated Asymmetric Hydrogenation of Dehydroarylalanines Mediated by Phosphine–Phosphite Ligands

entry	ligand	substrate	reaction conditions	conv. (%)	% ee of 130 (config.)
1	37 ²¹	129a	1 mol % [Rh(cod)(P–OP)]PF ₆ , rt, 1 atm H ₂ , 0.2 M in THF	100	99 (S)
2	37 ²¹	129b	1 mol % [Rh(cod)(P–OP)]PF ₆ , rt, 1 atm H ₂ , 0.2 M in THF	100	>99 (S)
3	58a ³⁸	129b	1 mol % [Rh(cod)(P–OP)]BF ₄ , rt, 1 atm H ₂ , 0.2 M in DCM	100	98 (S)
4	58d ³⁸	129b	1 mol % [Rh(cod)(P–OP)]BF ₄ , rt, 1 atm H ₂ , 0.2 M in DCM	100	99 (R)
5	62e ⁶⁴	129b	1 mol % [Rh(cod)(P–OP)]BF ₄ , rt, 1 atm H ₂ , 0.2 M in DCM	100	97 (R)
6	63b ⁶⁴	129b	2 mol % [Rh(cod)(P–OP)]BF ₄ , rt, 1 atm H ₂ , 0.2 M in DCM	100	95 (R)
7	66a ¹⁸	129a	1 mol % [Rh(nbd)(P–OP)]BF ₄ , rt, 19.7 atm H ₂ , 0.2 M in THF	>99	99 (R)
8	66a ¹⁸	129b	1 mol % [Rh(nbd)(P–OP)]BF ₄ , rt, 19.7 atm H ₂ , 0.2 M in THF	>99	99 (R)
9	72a ^{43b}	129b	0.2 mol % [Rh(cod)(P–OP)]BF ₄ , rt, 4 atm H ₂ , 0.2 M in DCM	100	>99 (R)
10	73b ^{43b}	129b	0.2 mol % [Rh(cod)(P–OP)]BF ₄ , rt, 4 atm H ₂ , 0.2 M in DCM	100	99 (S)
11	76a ^{44a}	129b	1 mol % [Rh(cod)(P–OP)]BF ₄ , 40 °C, 9.9 atm H ₂ , 0.1 M in DCM	>99	62 (R)
12	79 ⁴⁵	129b	1 mol % [Rh(cod)(P–OP)]BF ₄ , rt, 1 atm H ₂ , 0.1 M in DCM	100	88 (S)
13	99 ⁴⁹	129b	1 mol % [Rh(cod)(P–OP)]BF ₄ , rt, 20.4 atm H ₂ , 0.5 M in THF	100	89 (S)
14	127a , ^a ⁵⁴	129b	1 mol % [Rh(cod)(P–OP)]PF ₆ , rt, 1 atm H ₂ , 0.2 M in DCM	>99	77 (R) ^a
15	127b , ^d ⁵⁶	129b	0.2 mol % [Rh(cod)(P–OP)]BF ₄ , rt, 1 atm H ₂ , 0.1 M in DCM	100	80 (R)

^a 90% ee (R) was observed at 0 °C in a 0.1 M solution in DCM.

and Fmoc) as demonstrated in the excellent enantioselectivities observed (Table 3, Scheme 17).^{18,19,65}

Functionalized alkenes that are topologically distinct from **129** have been tested in phosphine–phosphite-mediated asymmetric hydrogenations. Itaconate derivatives (Scheme 18) are another class of compounds that give interesting enantiopure derivatives upon asymmetric hydrogenation. Excellent enantioselectivities (equal or higher than 99% ee) were obtained in the hydrogenation of dimethyl itaconate **131a** with rhodium complexes derived from ligands **66a**¹⁸ (entry 1 in Table 4) and **72a**^{43a} (entry 7 in Table 4). Several itaconate derivatives **131b–d** (entries 2–4 in Table 4) and the related compounds **131e** and **131f** (entries 5 and 6 in Table 4) were also hydrogenated with high levels of stereoselection by the rhodium complex derived from **66a**.^{19,65} Contrariwise, lower ee's were obtained with ligands **76a**^{44a} (entry 8 in Table 4) and **79**⁴⁵ (entry 9 in Table 4).

High enantioselectivities were observed in the asymmetric hydrogenation of α -aryl enamides **133a–e** (entries 1–5 in Table 5) catalyzed by the rhodium complex derived from ligand **66a** (Scheme 19);^{18,19,65} however, this complex failed for enamides **133f** and **133g** (entries 6 and 7 in Table 5). Remarkably, the readily available rhodium complex derived from SUPRAPHOS ligand **124b,u** (see Scheme 14 in section 2.3),^{53b} which can be easily prepared by supramolecular guided assembly of two P-containing components, proved successful for the difficult substrate **133h**, for which only a few highly selective metal-based hydrogenation catalysts are known (entry 8 in Table 5).^{53b,66}

Pizzano's ligands (Figure 18) can efficiently mediate the hydrogenation of various unsaturated phosphonates (Scheme 20), some of which have proven difficult to hydrogenate using other kinds of trivalent phosphorus ligands.^{43d,g,h,67} Hydrogenation of functionalized unsaturated phosphonates leads to α - or β -hydroxyphosphonates, which have numerous biological applications. Results obtained with the best P–OP ligand for each substrate are shown in Table 6 (17 examples, ee's from 86% to 99%). Whereas Pizzano's results demonstrate that ligand **72c** was the optimal one for the asymmetric hydrogenation leading to β -hydroxyphosphonates **136i–p** (entries 9–16 in Table 6), no single catalyst performed universally well for the hydrogenation of unsaturated phosphonates to afford α -hydroxy-substituted

derivatives **136a–h** (entries 1–8 in Table 6): the enantioselectivities achieved with rhodium complexes derived from ligands **72a**, **72g**, and **72h** are clearly substrate dependent.

There is a pressing need for catalyst recycling and easy product separation in homogeneous catalysis, especially in the case of expensive catalysts involving enantiomerically pure ligands and transition metals. *Multiphase catalysis* is one of the most innovative approaches for easy catalyst recycling and product separation.⁶⁸ In this method, the catalyst resides in one of the phases, while the products and substrates are distributed between the first (catalyst-containing) phase and a second, immiscible phase: by simple separation of these phases, the catalyst can be recovered and the product isolated.

Leitner et al. have designed and developed an innovative and efficient catalytic system for asymmetric hydrogenation based on ligand (R,S)-3-H²F⁶-BINAPHOS **52** (a structurally modified version of the phosphine–phosphite BINAPHOS, see Figure 6 in section 2.1.2), which was designed for operation in a H₂O/scCO₂ biphasic catalytic system. Incorporation of perfluoroalkyl groups in the ligand skeleton of BINAPHOS and use of [Rh(cod)₂]BAR_F as rhodium precursor conferred the required CO₂-philicity to the corresponding catalytic system, which they showed to be soluble in compressed CO₂ as solvent and to provide high enantioselectivity in the asymmetric hydrogenation of methyl 2-acetamidoacrylate **137** among other substrates.^{36b,69} With an optimal stationary phase for catalytically active rhodium complexes of 3-H²F⁶-BINAPHOS **52** in hand, Leitner's group then pursued an inverted supercritical CO₂/aqueous biphasic media for asymmetric hydrogenation (Scheme 21). The [Rh(cod)(**52**)]BAR_F or [Rh(cod)(**52**)]BF₄ precatalytic species was dissolved in a mixture of scCO₂ and compressed H₂ at required pressure and temperature in an autoclave. An aqueous solution of the substrate was then introduced against pressure using a pump, thereby forming a H₂O/scCO₂ biphasic system. Stirring generated an intimate mixture, allowing asymmetric hydrogenation to proceed. Full conversions were observed for itaconic acid (**131b**) and for methyl 2-acetamidoacrylate (**137**) after 1 hour at 40 or 56 °C, respectively, using 0.5 mol % of catalyst (*V*_{tot} = 100 mL, 55 g CO₂, P(H₂) = 29.6 atm; Scheme 21). The aqueous layer that contained the hydrogenated product was removed from the reactor, into

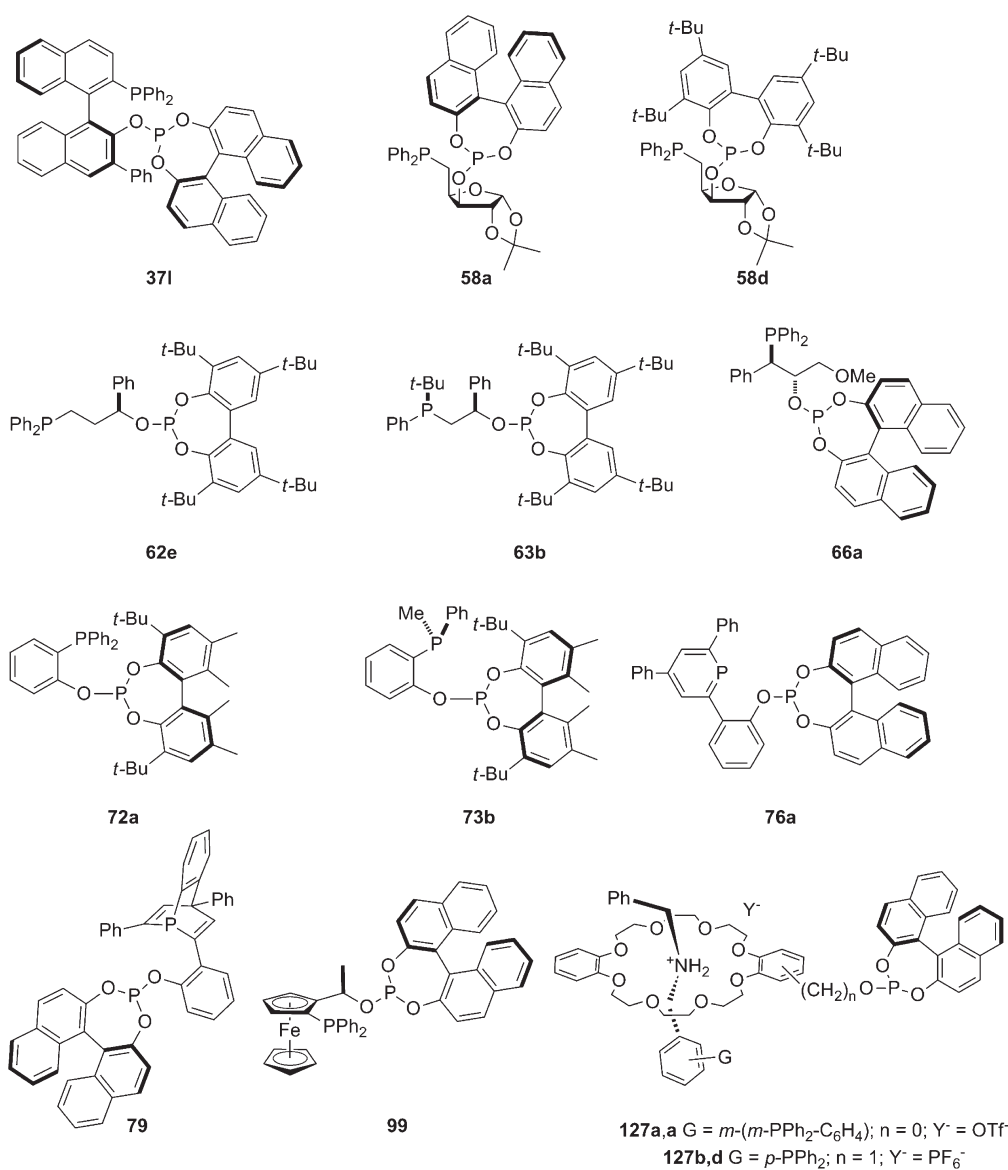


Figure 17. Phosphine–phosphite ligands studied in asymmetric hydrogenation of alkenes 129.

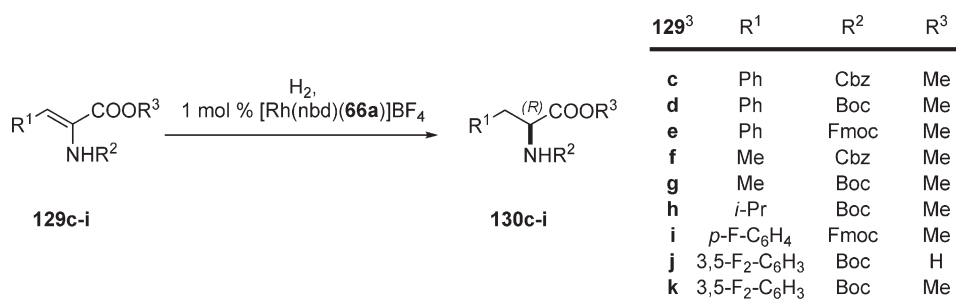
Table 3. Tolerance to *N*-Protecting Groups in the Asymmetric Hydrogenation of 129c–i Mediated by the Rhodium Complex Derived from Ligand 66a

entry	substrate	reaction conditions	conv. (%)	% ee of 130 (config.)
1	129c ¹⁸	rt, 19.7 atm H ₂ , 0.2 M in THF	>99	99 (<i>R</i>)
2	129d ¹⁸	rt, 19.7 atm H ₂ , 0.2 M in THF	>99	96 (<i>R</i>)
3	129e ¹⁸	rt, 39.5 atm H ₂ , 0.2 M in THF	99	98 (<i>R</i>)
4	129f ⁶⁵	rt, 19.7 atm H ₂ , 0.2 M in THF	>99	98 (<i>R</i>)
5	129g ⁶⁵	rt, 19.7 atm H ₂ , 0.2 M in THF	>99	98 (<i>R</i>)
6	129h ¹⁹	rt, 39.5 atm H ₂ , 0.2 M in THF	70	92 (<i>R</i>)
7	129i ¹⁸	rt, 39.5 atm H ₂ , 0.2 M in THF	94	97 (<i>R</i>)
8	129j ¹⁹	rt, 19.7 atm H ₂ , 0.2 M in THF	>99	96 (<i>R</i>)
9	129k ¹⁹	rt, 19.7 atm H ₂ , 0.2 M in THF	>99	96 (<i>R</i>)

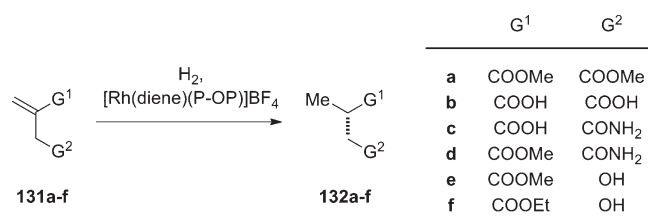
which a fresh solution of substrate was then added, which generated a new catalytic cycle. Leitner et al. demonstrated the efficient recycling of the catalytic systems under these conditions: for methyl 2-acetamidoacrylate **137** they observed an average

enantiomeric excess of 98.4% ± 0.6% throughout five cycles. Remarkably, leaching of rhodium and phosphorus into the aqueous layer was 1.4 ppm and 5.2 ppm, respectively, during the first cycle, but became undetectable in all following cycles.

Scheme 17. Tolerance to *N*-Protecting Groups in the Asymmetric Hydrogenation of **129c–i** Mediated by the Rhodium Complex Derived from Ligand **66a**



Scheme 18. Rhodium-Mediated Asymmetric Hydrogenation of Itaconic Acid Derivatives and Related Compounds Employing Phosphine–Phosphite Ligands



Continuous processing is possible in Leitner's approach. The resulting method, which is relatively straightforward and cost-effective, offers high reaction rates (TOF = ca. 10² h^{−1}) and excellent asymmetric inductions, all of which underscore the value of this novel approach in multiphase enantioselective catalysis.

Vidal-Ferran et al. recently described a less-sophisticated, yet effective, procedure for catalyst reuse and product recovery in the asymmetric hydrogenation of dimethyl itaconate **131a** catalyzed by the rhodium complex derived from ligand **66a**.¹⁹ This work was based on the finding that rhodium complexes such as the catalytic species derived from **66a** are soluble in propylene carbonate, which has proven to be an ideal solvent for hydrogenation.⁷⁰ If the hydrogenation product is sufficiently soluble in nonpolar solvents (e.g., alkanes), which in turn are nonmiscible with propylene carbonate, then the hydrogenated products can be separated from the reaction mixture by liquid–liquid extraction: the catalyst remains in the propylene carbonate solution, whereas the product can be extracted into the nonpolar phase. Dimethyl itaconate **131a** was thus reduced in propylene carbonate under standard hydrogenation conditions (1.0 mol % of [Rh(nbd)(**66a**)]BF₄, rt, 19.7 atm of hydrogen) in five consecutive cycles, followed by liquid–liquid extraction of the hydrogenated product, and finally, addition of more substrate to start a new cycle. Vidal-Ferran et al. reported an average enantiomeric excess of 97.4% ± 0.7% throughout five cycles, observing almost no change in the catalytic activity.¹⁹

Both catalyst reuse approaches are efficient, although they cannot be considered as general, because they suffer from the same intrinsic limitation: restrictions on the solubility of the hydrogenated product. Leitner's approach demands that the substrate and product be water-soluble,^{36b,69} whereas Vidal-Ferran's strategy following Börner's procedure^{70a} requires that the

hydrogenation product be soluble in a nonpolar solvent such as cyclohexane.¹⁹ Hence, general strategies for catalyst recovery are still being actively sought.

3.1.2. Asymmetric Hydrogenations of Prochiral Imines and Related Compounds Mediated by Phosphine–Phosphite Ligands. Asymmetric catalytic hydrogenation of C=N bonds is a very attractive method for synthesizing enantiomerically enriched chiral amines.⁷¹ It offers many of the advantages of the hydrogenation of C=C bonds,⁶¹ enabling simple and efficient generation of a stereogenic center α to an NH group. However, the asymmetric hydrogenation of C=N bonds has not been developed to the extent of that for C=C and C=O bonds. Indeed, despite intense research efforts, no catalytic system has yet been developed for C=N bonds that offers robustness, high conversion rates and enantioselectivities, and a broad substrate scope. Thus, identification of efficient ligands for this transformation is of great interest.

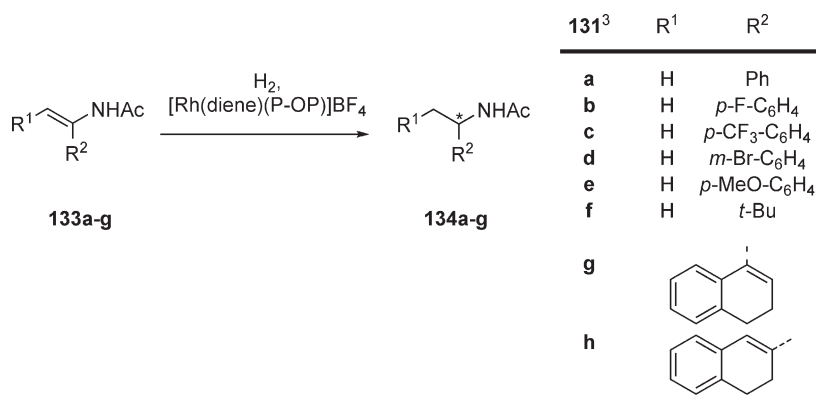
Pizzano et al. prepared a diverse set of their modular phosphine–phosphites and then studied these in the iridium-mediated asymmetric hydrogenation of imines.^{43c,e,72} An ethane-bridged ligand backbone between the two phosphorus functionalities, a P-stereogenic phosphino group and a conformationally stable phosphite moiety (as indicated in **75a**) were identified as being crucial for achieving high enantioselectivity for *N*-aryl imine substrates (Scheme 22). The results obtained for substrates **139a–f** are shown in Table 7, whereby only the results obtained with the iridium complex derived from lead ligand **75a** are listed. Enantioselectivities ranging from 72% to 85% ee were obtained in the hydrogenation of various *N*-aryl imines mediated by the lead catalyst.

Recently, Vidal-Ferran et al. have assessed the catalytic activity of their highly modular P–OP ligands in the enantioselective hydrogenation of heteroaromatic compounds, specifically in the case of quinolines, which is a convenient and challenging route for the preparation of enantiomerically enriched heterocyclic compounds (Scheme 23).⁷³ Thereby, from the whole ligand library, iridium complexes derived from phosphine–phosphite **66b** mediated the hydrogenation of several substituted quinolines **141** with high enantioselectivities, ranging from 71% to 92% ee (Table 8). The nature of the solvent, the temperature, and the use of anhydrous HCl as additive proved to have an important role in determining the enantioselectivity of the process. Optimized reaction conditions for the hydrogenation of a variety of quinolines have been summarized in Table 8.

3.1.3. Mechanistic Considerations and Origin of the Enantioselectivity. To shed light on the correlation between the enantioselection mechanisms operating in asymmetric

Table 4. Rhodium-Mediated Asymmetric Hydrogenation of Itaconic Acid Derivatives and Related Compounds

entry	ligand	substrate	reaction conditions	conv. (%)	% ee of 132 (config.)
1	66a ¹⁸	131a	1 mol % [Rh(nbd)(P-OP)]BF ₄ , rt, 19.7 atm H ₂ , 0.2 M in DCM	>99	99 (S)
2	66a ⁶⁵	131b	1 mol % [Rh(nbd)(P-OP)]BF ₄ , rt, 19.7 atm H ₂ , 0.2 M in THF	>99	95 (S)
3	66a ⁶⁵	131c	1 mol % [Rh(nbd)(P-OP)]BF ₄ , rt, 19.7 atm H ₂ , 0.2 M in THF	>99	95 (S)
4	66a ⁶⁵	131d	1 mol % [Rh(nbd)(P-OP)]BF ₄ , rt, 19.7 atm H ₂ , 0.2 M in THF	>99	99 (S)
5	66a ¹⁹	131e	1 mol % [Rh(nbd)(P-OP)]BF ₄ , 0 °C, 19.7 atm H ₂ , 0.2 M in THF	>99	95 (S)
6	66a ⁶⁵	131f	1 mol % [Rh(nbd)(P-OP)]BF ₄ , 0 °C, 19.7 atm H ₂ , 0.2 M in THF	>99	94 (S)
7	72a ^{43a}	131a	0.01 mol % [Rh(cod)(P-OP)]BF ₄ , rt, 5.0 atm H ₂ , 0.5 M in DCM	>95	>99 (S)
8	76a ^{44a}	131a	0.1 mol % [Rh(cod)(P-OP)]BF ₄ , rt, 9.9 atm H ₂ , 0.1 M in DCM	>99	79 (S)
9	79 ⁴⁵	131a	1 mol % [Rh(cod)(P-OP)]BF ₄ , rt, 1 atm H ₂ , 0.1 M in DCM	100	19 (S)

Scheme 19. Rhodium-Mediated Asymmetric Hydrogenation of α -Substituted EnamidesTable 5. Rhodium-Mediated Asymmetric Hydrogenation of α -Substituted Enamides

entry	ligand	substrate	reaction conditions	conv. (%)	% ee of 134 (config.)
1	66a ¹⁸	133a	1 mol % [Rh(nbd)(P-OP)]BF ₄ , rt, 19.7 atm H ₂ , 0.2 M in THF	>99	98 (R)
2	66a ⁶⁵	133b	1 mol % [Rh(nbd)(P-OP)]BF ₄ , rt, 19.7 atm H ₂ , 0.2 M in THF	>99	98 (R)
3	66a ⁶⁵	133c	1 mol % [Rh(nbd)(P-OP)]BF ₄ , rt, 19.7 atm H ₂ , 0.2 M in THF	>99	98 (R)
4	66a ⁶⁵	133d	1 mol % [Rh(nbd)(P-OP)]BF ₄ , rt, 19.7 atm H ₂ , 0.2 M in THF	>99	97 (R)
5	66a ¹⁹	133e	1 mol % [Rh(nbd)(P-OP)]BF ₄ , rt, 19.7 atm H ₂ , 0.2 M in THF	>99	97 (R)
6	66a ⁶⁵	133f	1 mol % [Rh(nbd)(P-OP)]BF ₄ , rt, 19.7 atm H ₂ , 0.2 M in THF	>99	23 (S)
7	66a ¹⁹	133g	1 mol % [Rh(nbd)(P-OP)]BF ₄ , rt, 19.7 atm H ₂ , 0.2 M in THF	>99	57 (R)
8	124b,u ^{53b}	133h	5 mol % [Rh(cod)(P-OP)]BF ₄ , 40 °C, 11.8 atm H ₂ , 20 equiv. DIPEA, 0.2 M in DCM	100	94 (nd)

hydrogenation and the nature of the P-OP ligands, theoretical studies into the reactivity of rhodium catalysts derived from phosphine-phosphinites and phosphine-phosphites with methyl 2-acetamidoacrylate **137** have been carried out by Maseras et al.¹⁹ In contrast with the systems studied in the majority of investigations on asymmetric hydrogenation, P-OP ligands are not C₂ symmetric. Whereas with C₂ symmetric ligands there are only two distinct modes of binding the chelating substrate to the catalyst, C₁ ligands as the ones considered here lead to four possible binding modes in the catalyst-substrate adduct complexes, **143a-d**, as shown in Figure 19. Two sets of catalyst-substrate complexes can be expected depending on the coordination of the C=C double bond of the substrate *trans* to the P group (phosphine, **143a** and **143b**) or *trans* to the PO group (phosphinite or phosphite, **143c** and **143d**) in the rhodium complex. Lastly, each of these two coordination modes (C=C *trans* to the PO and C=C *trans* to P groups) may lead to two

complexes, depending on the prochirality of the α -carbon of methyl 2-acetamidoacrylate **137** (pro-(R) or pro-(S)).

The mechanism for rhodium-mediated hydrogenation of enamides such as methyl 2-acetamidoacrylate **137** is complex, but fortunately, it has been extensively explored by a number of research groups,^{61a,63,74} resulting in the generally accepted "unsaturated" mechanism. Previous computational studies on asymmetric hydrogenation have shown that the approach of dihydrogen to the substrate-catalyst adduct takes place in a direction parallel to the P-Rh-olefin bonds and that for substrates such as methyl 2-acetamidoacrylate, the first hydride addition is made to the β carbon of the substrate (Figure 19).⁷⁴ Theoretical studies on hydrogenation observe competition between oxidative addition and migratory insertion as possible rate-determining steps.⁷⁵ This observation was confirmed by studying the energy profile in the asymmetric hydrogenation of methyl 2-acetamidoacrylate catalyzed by the rhodium complex derived from

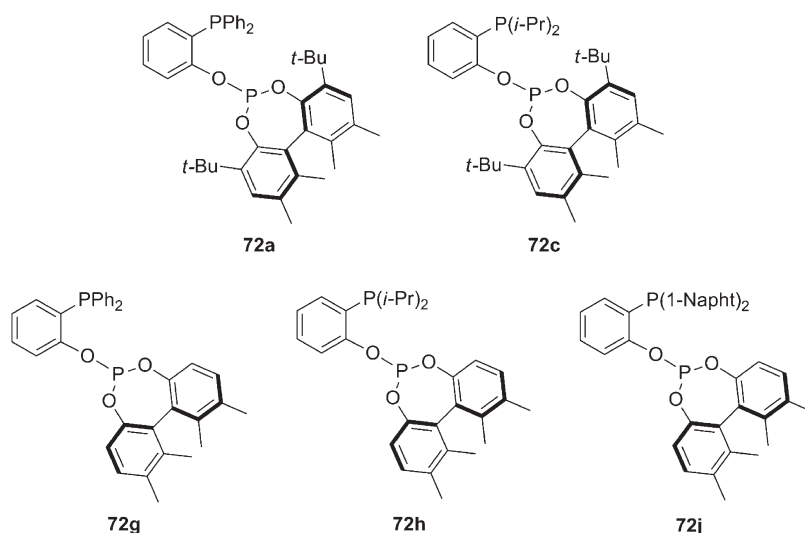
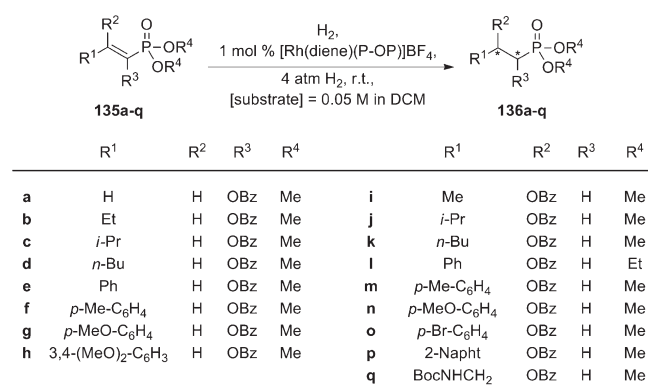


Figure 18. Lead P–OP ligands for the hydrogenation of unsaturated phosphonates.

Scheme 20. Rhodium-Mediated Asymmetric Hydrogenation of Unsaturated Phosphonates



phosphine–phosphinite ligand **15a** for the complete catalytic cycle and for the different reaction manifolds derived from the different substrate–catalyst complexes (Figure 19).^{19,76} These studies revealed that oxidative addition had higher activation energies (1–3 kcal·mol^{−1}) than the ones for migratory insertion for the asymmetric hydrogenation of methyl 2-acetamidoacrylate catalyzed by the rhodium complex derived from ligand **15a**. Transition states for oxidative addition had also a higher energy (less than 1 kcal·mol^{−1}) than the migratory insertion ones in the asymmetric hydrogenation catalyzed by the rhodium complex derived from phosphine–phosphite ligand **66a**. Similar conclusions have been also obtained by Claver, van Leeuwen, et al., who experimentally determined that oxidative addition of hydrogen gas was the rate-determining step in hydrogenations catalyzed by rhodium complexes bearing phosphine–phosphites **58** and **62–64**.^{64,77}

Having already determined that oxidative addition is rate-determining, a detailed conformational study of the oxidative addition transition states for all four reaction manifolds (Figure 19) for the asymmetric hydrogenation of methyl 2-acetamidoacrylate catalyzed by the rhodium complex derived from ligand **66a** revealed that enantiodiscrimination arises from a fine balance between electronic and steric effects.

Primarily, the electronic asymmetry of the P–OP ligand establishes a discrimination in two out of the four possible manifolds, since the phosphite group hinders binding of the

Table 6. Rhodium-Mediated Asymmetric Hydrogenation of **135**

entry	ligand	substrate	conv. (%)	% ee of 136 (config.)
1	72a ^{43g}	135a	100	93 (S)
2	72j ^{43g}	135b	100	98 (R)
3	72h ^{43d}	135c	100	98 (R)
4	72h ^{43d}	135d	100	96 (R)
5	72h ^{43d}	135e	100	92 (R)
6	72g ^{43g}	135f	100	87 (R)
7	72h ^{43d}	135g	43	91 (R)
8	72h ^{43g}	135h	60	86 (R)
9	72c ^{43h}	135i	90 ^a	99 (R)
10	72c ^{43h}	135j	82 ^a	99 (R)
11	72c ^{43h}	135k	55 ^a	99 (R)
12	72c ^{43h}	135l	93 ^a	99 (R)
13	72c ^{43h}	135m	85 ^a	99 (R)
14	72c ^{43h}	135n	73 ^a	95 (R)
15	72c ^{43h}	135o	87 ^a	99 (R)
16	72c ^{43h}	135p	86 ^a	99 (R)
17	72c ^{43h}	135q	87 ^a	99 (R)

^a Isolated yield (%).

substrate in its *trans* position (manifolds derived from **143c** and **143d** in Figure 19). This can be visualized in the quadrant diagram depicted in Figure 20 by saying that the two right-hand sites are electronically disfavored with respect to placement of the C_α and C_β olefin carbon atoms of the substrate. The difference within each of the two remaining manifolds with electronically similar properties (manifolds derived from **143a** and **143b** in Figure 19) is associated with steric effects. The lower-left quadrant is far from the steric congestion produced by BINOL, and the oxidative addition transition state having the C_α carbon in this quadrant is energetically favored: it is accepted⁷⁴ that in the oxidative addition transition state, steric hindrance develops in the quadrant occupied by the C_α olefin carbon. Steric congestion at the oxidative addition stage in the manifold derived from structure **143b** (C_α carbon in the upper left quadrant) increased the energy by 2.2 kcal·mol^{−1} with respect to manifold

derived from **143a**, in which the C $_{\alpha}$ carbon is placed in the lower left quadrant (Figure 20).

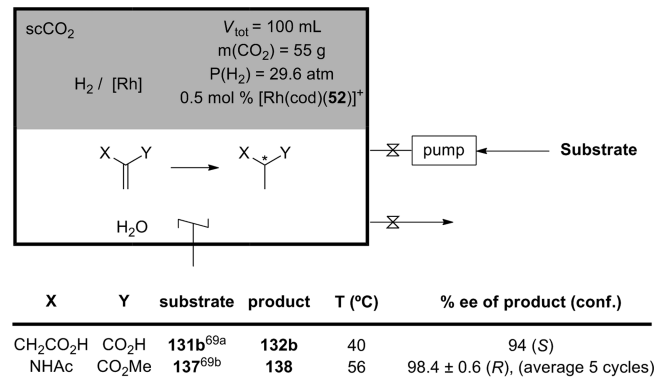
Finally, the computational studies carried out by Maseras et al. also revealed that the asymmetric hydrogenation of methyl 2-acetamidoacrylate mediated by rhodium complexes bearing phosphine–phosphite ligand **66a** follows an anti-lock-and-key behavior in this system. The most stable catalyst–substrate adduct (and thus most abundant) is **143b**, but product formation proceeds by means of the manifold derived from **143a**.

3.1.4. Comparative Table in Asymmetric Hydrogenations. Rhodium complexes of P–OP ligands have efficiently catalyzed the asymmetric hydrogenation of a broad array of functionalized alkenes (section 3.1.1), and Table 9 provides comparison between the enantioselectivity obtained with rhodium complexes of P–OP ligands and the ee values attained with so-called *milestone ligands* in rhodium-mediated asymmetric hydrogenations.⁷⁸ Metal complexes of P–OP ligands compare very favorably (in terms of enantioselectivity) with those derived from ligands **144**–**149** in rhodium-mediated asymmetric hydrogenations of structurally diverse functionalized alkenes (Figure 21).

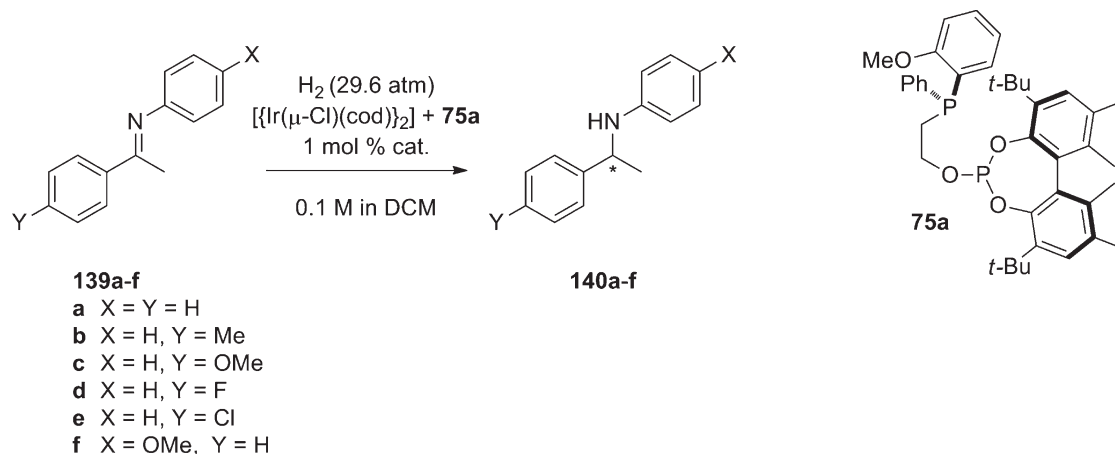
3.2. Hydroformylations

Asymmetric hydroformylation of alkenes remains one of the most powerful transformations for preparing enantiopure aldehydes,⁹³ which are valuable precursors of active pharmaceutical ingredients (APIs) and agrochemicals. This transformation involves elongation of the carbon skeleton by one unit from one of the two possible sp² carbons of the alkene, via addition of CO and H₂. Thus, for nonsymmetric alkene substrates, two regioisomers

Scheme 21. Leitner's H₂O/scCO₂ Biphasic Catalytic System



Scheme 22. Hydrogenation of *N*-Aryl Imines Catalyzed by the Iridium Complex Derived from P–OP Ligand **75a**



of aldehydes are possible (see Scheme 24) and either zero, one, or two stereogenic centers can be generated, depending on the position at which the CHO unit is incorporated and on the topology of the starting alkene. Though asymmetric hydroformylation has great potential for preparing diverse chiral products, it is only synthetically valuable if used with catalysts that offer excellent regio- and enantiocontrol; this is especially true on the industrial scale. Nonetheless, the applicability of hydroformylation can be limited by poorly reactive alkenes (namely, from the decrease in reactivity consequent to the increase in number of substituents⁹⁴), insufficiently active catalysts, and the difficulty in simultaneously controlling regio- and enantioselectivity.

Research in enantioselective hydroformylation remains focused on rhodium as the catalyst metal, because it offers high activity and selectivity in complexes with bidentate P ligands.^{6,10,93} Given that rhodium-mediated asymmetric hydroformylations have already been generally covered in other reviews,^{10,95} in this section, we have focused on the results obtained with rhodium complexes of phosphine–phosphite ligands used with various structurally diverse substrates.⁹⁶ Furthermore, since the stereochemical outcome of the reaction is greatly influenced by the regioselectivity of the reaction, which in turn is affected by inherent substrate preferences or by directing effects from the substrate's functional groups, we have organized this section according to substrate topology.

3.2.1. Asymmetric Hydroformylations of Aryl-Substituted Alkenes. Phosphine–phosphite ligands have been tested to a greater extent than phosphine–phosphinites in the rhodium-mediated asymmetric hydroformylation of olefins. In this transformation, the corresponding catalyst precursors [Rh(acac)(P–OP)] were usually prepared *in situ* by adding variable amounts of the desired P–OP ligand to a Rh(I) precursor (mainly [Rh(acac)(CO)₂]).

Table 7. Hydrogenation of *N*-Aryl Imines Catalyzed by the Iridium Complex Derived from Ligand **75a**

entry	substrate	conv. (%)	% ee of 140 (conf.)
1	139a ^{43e}	100	84 (R)
2	139b ^{43e}	100	72 (nd)
3	139c ^{43e}	100	85 (nd)
4	139d ^{43e}	100	79 (nd)
5	139e ^{43e}	100	82 (nd)
6	139f ^{43e}	100	81 (nd)

Scheme 23. Hydrogenation of Quinolines Mediated by the Iridium Complex Derived from Ligand 66b

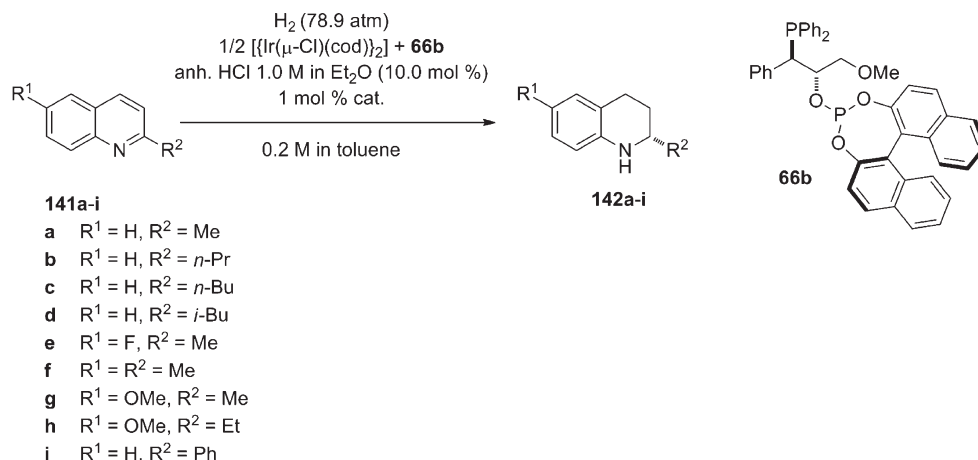


Table 8. Hydrogenation of Quinolines Catalyzed by the Iridium Complex Derived from Ligand 66b

entry	substrate	conv. (%)	% ee of 140 (config.)
1	141a ⁷³	>99	91 (S)
2	141b ⁷³	98	71 (S)
3	141c ⁷³	99	85 (S)
4	141d ⁷³	>99	88 (S)
5	141e ⁷³	92	88 (S)
6	141f ⁷³	74	92 (S)
7	141g ⁷³	38	89 (S)
8	141h ⁷³	23	87 (S)
9	141i ⁷³	>99	84 (R)

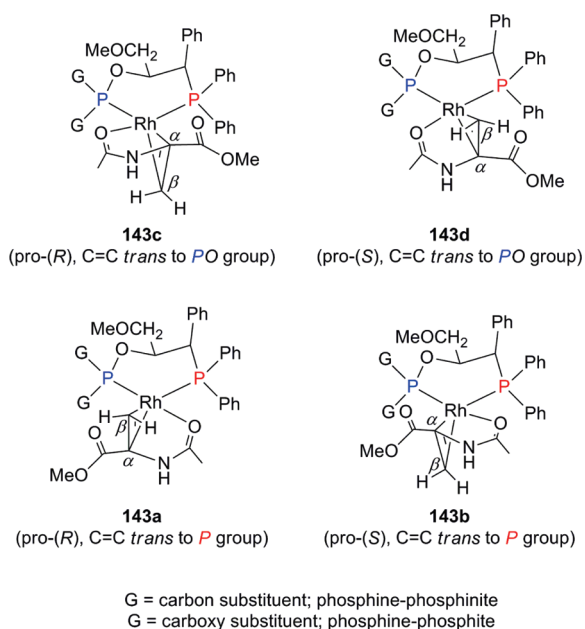


Figure 19. The four possible binding modes for methyl 2-acetamidoacrylate with P–OP-ligated catalysts.

Over the past few decades, rhodium-mediated enantioselective hydroformylation of styrene (**150a**) and its derivatives has

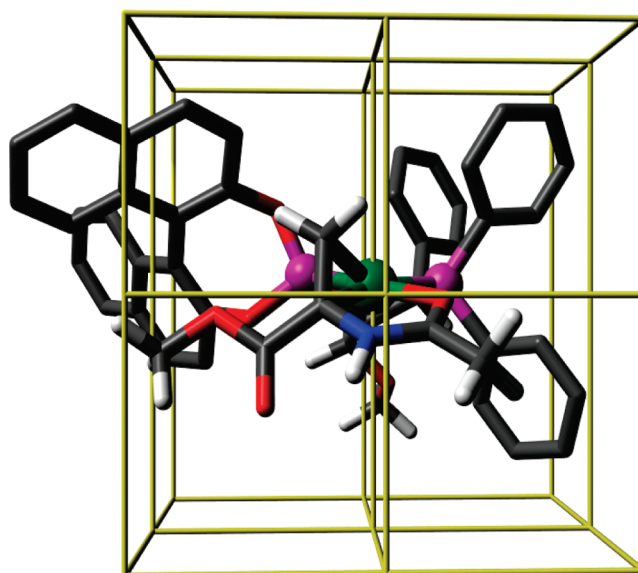


Figure 20. Quadrant diagram for the catalyst–substrate adduct, which leads to the major enantiomer of the hydrogenation product of methyl 2-acetamidoacrylate (the structure of the catalyst–substrate adduct has been calculated at the full DFT level).¹⁹

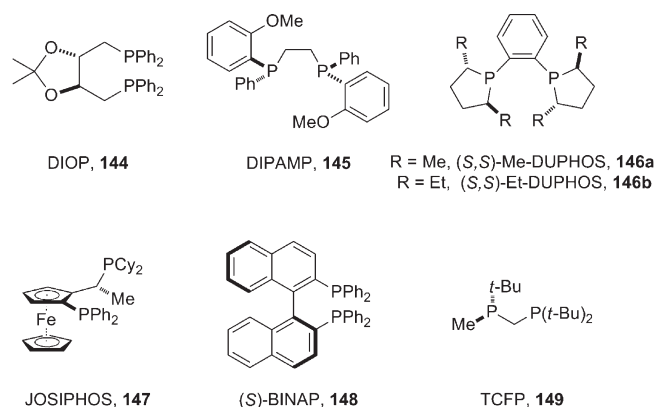
been extensively investigated, using a broad range of chelating phosphorus ligands. The phosphine–phosphite ligands studied in the hydroformylation of styrene are shown in Figure 22, and the results are listed in Table 10. Rh(I) complexes of BINAPHOS (**37k**), typically generated by mixing $[\text{Rh}(\text{acac})(\text{CO})_2]$ with an excess of the ligand, were the first to be reported for asymmetric hydroformylation of styrene (Scheme 25), providing high activity and regio- and enantioselectivity (entry 1 in Table 10).⁶ Rh(I) complexes of enantiopure BINAPHOS were the first truly efficient and general enantioselective catalysts for hydroformylation, representing an important breakthrough in this transformation.

The potential of this BINAPHOS-based catalyst was also demonstrated against various *p*-substituted styrene derivatives, for which it offered high regio- and enantioselectivity.^{6,30,99} The results for the hydroformylation of *p*-methylstyrene **150b** are the best reported (97% conv., 95% ee, 86% branched product; Scheme 26).⁶

Table 9. Comparison of the Enantioselectivity (% ee) Obtained with Selected P–OP Ligands to Those Obtained with Milestone Ligands 144–149 in Rhodium-Mediated Asymmetric Hydrogenations of Several Alkenes

	ligands									
	144	145	146b	147	148	149	37l	62e	66a	72a
129a	72 (R) ⁷⁹	94 (S) ⁸⁰		84 (S) ⁸¹	96 (R) ^{82,a}	>99 (R) ⁸³	99 (S) ²¹		99 (R) ¹⁸	
129b	68 (R) ⁸⁴	96 (S) ⁸⁰	99 (S) ⁸⁵	96 (S) ⁸¹	93 (R) ^{82,a}	>99 (R) ⁸³	>99 (S) ²¹	97 (R) ⁶⁴	99 (R) ¹⁸	>99 (R) ^{43b}
137			>99 (S) ⁸⁵	88 (S) ⁸¹	21 (R) ⁸⁶	>99 (R) ⁸³	>99 (S) ²¹	99 (R) ⁶⁴	99 (R) ¹⁸	
133a	53 (S) ⁸⁷		95 (S) ^{88,b}		11 (R) ⁸⁶	98 (R) ⁸³			98 (R) ¹⁸	
131a	25 (R) ⁸⁹	88 (R) ⁹⁰	97 (R) ⁹¹	98 (S) ⁸¹	94 (S) ^{92,c}	98 (S) ⁸³			99 (S) ¹⁸	>99 (S) ^{43a}

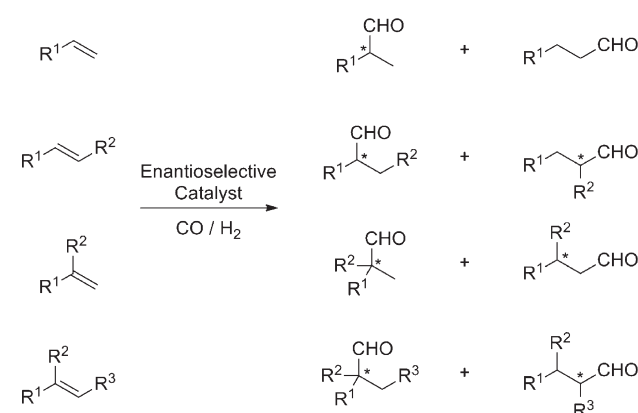
^a The ee values correspond to the hydrogenation of the *N*-benzoyl-protected derivatives rather than the *N*-acetyl ones. ^b Compound 133a was reduced using ligand 146a. ^c The ee values for the hydrogenation of itaconic acid 131b.

**Figure 21.** Milestone ligands in asymmetric hydrogenations.

Modification of the steric and electronic properties of the phosphine group in BINAPHOS by introducing different substituents into the P-aryl groups of the ligands 37b–g did not affect either the enantioselectivity or the ratio of branched to linear product (entries 2–7 in Table 10).^{25,30} However, the rhodium complex of the other seminal phosphine–phosphite 38 (Pringle's ligand)^{23b} behaved rather distinctly from BINAPHOS in the hydroformylation of styrene **150a**, offering only poor enantioselectivity (entry 8 in Table 10). It is worth mentioning that a lower enantioselectivity was achieved in the hydroformylation of styrene **150a** with *mismatched* (*R,R*)-BINAPHOS (25% ee)³⁰ than that observed with *matched* (*S,R*)-BINAPHOS 37k (94% ee, entry 1 in Table 10).

High regio- and enantioselectivities were achieved by using a rhodium complex of phosphine–phosphite **44a**, which is based on an atropisomerically stable biphenyl backbone (entry 11 in Table 10).³¹ However, lower enantiomeric excesses were observed when a biphenyl unit, whose corresponding conformers are capable of interconversion, was placed either between the phosphine and phosphite functionalities (**44b/44d**)^{31,32} or at the phosphite fragment (**43**)³⁰ (entries 10 and 12 in Table 10, respectively).

The aforementioned outstanding results with BINAPHOS and related ligands inspired researchers to design and synthesize new P–OP ligands for asymmetric hydroformylation. For example, Ruiz, Claver, et al. developed the sugar-based phosphine–phosphite ligands **58** (see Figure 7 in section 2.1.2), among which ligand **58d** (Figure 22) proved to be the best. The bulky *tert*-butyl groups at the phosphite fragment were crucial for providing high regio- and moderate enantioselectivities (entry 13 in Table 10).⁹⁷ Moreover, **58d** mediated the hydroformylation of styrene under mild conditions (pressure and temperature). Similar activity and selectivity were obtained by using rhodium

Scheme 24. Hydroformylation of Topologically Diverse Alkenes

complexes of the phosphine–phosphites **62–64** described by van Leeuwen et al. (see Figure 8 in section 2.1.2). Hydroformylation of styrene (**150a**) catalyzed by [RhH(CO)₂](**62a**) afforded the branched aldehyde **151a** with high regio- and good enantioselectivity (entry 14 in Table 10).^{39a} The combination of a stereogenic phosphine fragment, containing a naphthyl group, and the matched configuration of the stereocenter in the ligand backbone enabled the efficient stereoselection.

Faraone et al. reported the rhodium complex of ligand **70b** to be an efficient catalyst for the branched aldehyde **151a** (entry 15 in Table 10).⁹⁸ Although the conversion and the chemo- and regioselectivities were extremely high, the enantioselectivity was only moderate (20% ee). The authors used NMR to explain the low selectivity, showing that the rhodium complexes contained monodentate rather than the desired bidentate ligands. They deduced that the monodentate phosphorus species could have been formed via ligand hydrolysis. Matteoli et al. studied the catalytic activity of the rhodium complex of the ligand **71** in the enantioselective hydroformylation of styrene **150a** (entry 16 in Table 10).^{42b} The results were very similar (in terms of chemo-, regio-, and enantioselectivity) to those obtained by the other researchers with the aforementioned P–OP ligands **58**, **62**, and **70**.

In 2007, Pizzano et al. described hydroformylation of aryl alkenes catalyzed by rhodium complexes of the phosphine–phosphite ligands **72–75** (see Figure 10 in section 2.1.2).^{43f} The best enantioselectivity that they obtained for the hydroformylation of substrate **150a** was 71% ee (entry 17 in Table 10), using the 1-naphthyl P-substituted ligand **72f** under standard conditions

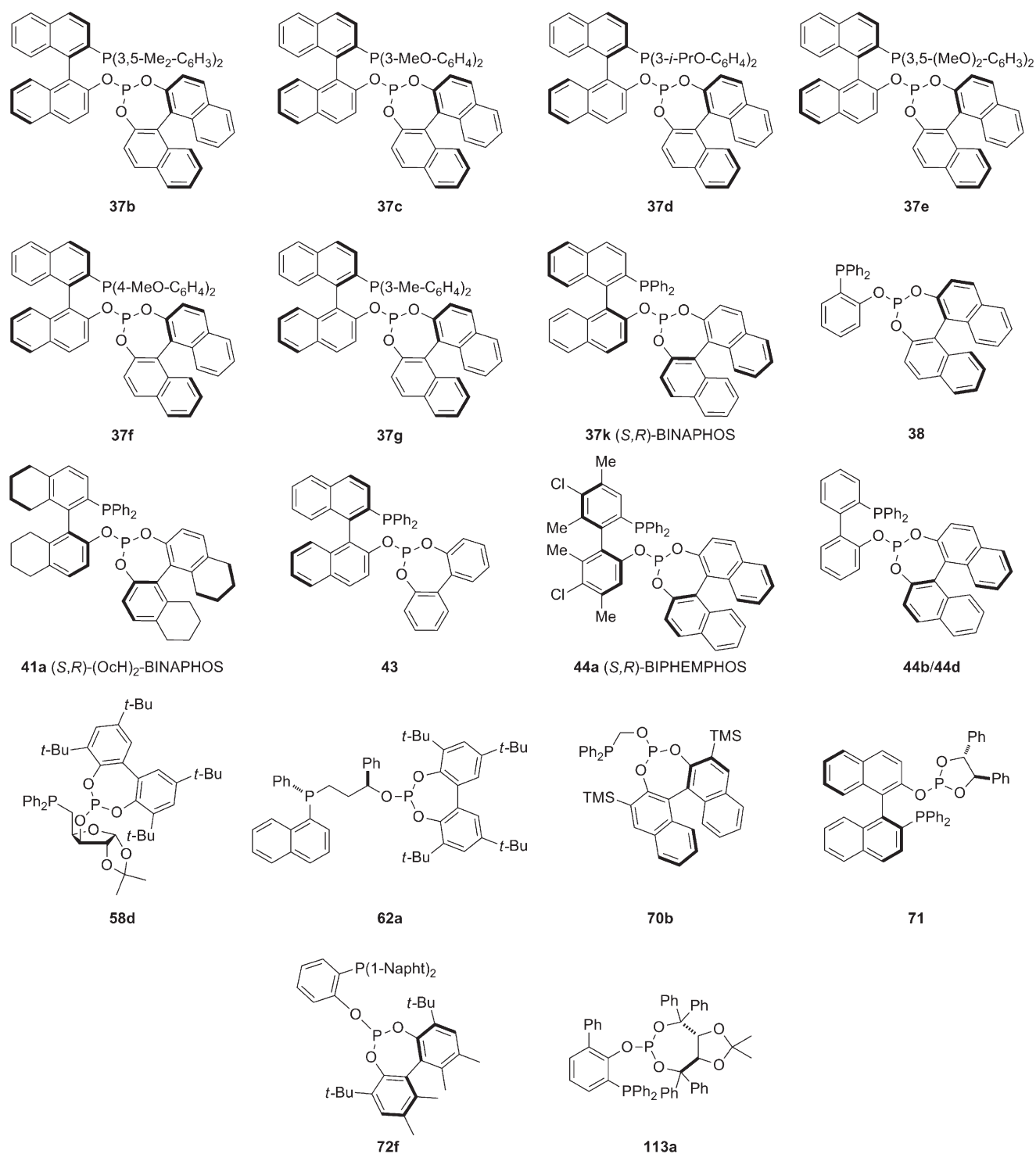


Figure 22. P–OP ligands used in rhodium-mediated asymmetric hydroformylation.

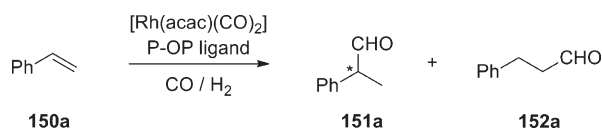
(50 °C and 19.7 atm of syngas). These substituents are responsible for the improved selectivity of the catalyst, via formation of π – π stacking interactions between the aryl groups on the phosphine and the styrene substrate. This positive effect was confirmed by the high performance of the rhodium catalyst incorporating ligand **72f** in the carbonylation of 1-vinyl naphthalene **150c** (100% conversion, 89% ee, and 99% for the branched aldehyde, Scheme 27).

Very recently, the potential of Schmalz's phosphine–phosphites **100**–**114** (see Figure 14 in section 2.2) were evaluated in

rhodium-mediated asymmetric hydroformylations of styrene.^{50d} High regioselectivity and good enantioselectivity (80% ee, entry 18 in Table 10) were obtained with a rhodium complex of the TADDOL-based ligand **113a**. This ligand contains a phenyl group *ortho* to the phosphite fragment, which strongly influences the stereochemical outcome of the reaction. By running the hydroformylation at 20 °C, the authors were able to enhance the enantioselectivity (up to 85% ee) of the catalyst, although this came at the expense of poorer reactivity (9% conversion). Despite

Table 10. Rhodium-Mediated Asymmetric Hydroformylation of Styrene **150a** Using P–OP Ligands

entry	ligand	reaction conditions	conv. (%)	ratio of 151a to 152a	% ee of 151a (config.)
1	37k ⁶	0.05 mol % [Rh(acac)(CO) ₂], 0.2 mol % 37k , 60 °C, 100 atm CO/H ₂ (1/1), 20.0 M in benzene	>99	88/12	94 (S)
2	37b ³⁰	0.05 mol % [Rh(acac)(CO) ₂], 0.2 mol % 37b , 60 °C, 100 atm CO/H ₂ (1/1), 20.0 M in benzene	>99	90/10	85 (R)
3	37c ²⁵	0.05 mol % [Rh(acac)(CO) ₂], 0.2 mol % 37c , 60 °C, 19.7 atm CO/H ₂ (1/1), 20.0 M in benzene	>99	92/8	95 (R)
4	37d ²⁵	0.05 mol % [Rh(acac)(CO) ₂], 0.2 mol % 37d , 60 °C, 19.7 atm CO/H ₂ (1/1), 20.0 M in benzene	>99	91/9	96 (R)
5	37e ²⁵	0.05 mol % [Rh(acac)(CO) ₂], 0.2 mol % 37e , 60 °C, 19.7 atm CO/H ₂ (1/1), 20.0 M in benzene	>99	93/7	93 (R)
6	37f ²⁵	0.05 mol % [Rh(acac)(CO) ₂], 0.2 mol % 37f , 60 °C, 19.7 atm CO/H ₂ (1/1), 20.0 M in benzene	>99	88/12	92 (R)
7	37g ²⁵	0.05 mol % [Rh(acac)(CO) ₂], 0.2 mol % 37g , 60 °C, 19.7 atm CO/H ₂ (1/1), 20.0 M in benzene	>99	89/11	92 (R)
8	38 ^{23b}	0.5 mol % [Rh(acac)(CO) ₂], 1.0 mol % 38 , 60 °C, 79.0 atm CO/H ₂ (1/1), 0.4 M in toluene	>99	95/5	5 (nd)
9	41a ^{29a}	0.1 mol % [Rh(acac)(41a)], 60 °C, 100 atm CO/H ₂ (1/1), 1.0 M in benzene	84	92/8	89 (S)
10	43 ³⁰	0.05 mol % [Rh(acac)(CO) ₂], 0.2 mol % 43 , 60 °C, 100 atm CO/H ₂ (1/1), 20.0 M in benzene	>99	91/9	83 (R)
11	44a ³¹	0.1 mol % [Rh(acac)(CO) ₂], 0.4 mol % 44a , 60 °C, 100 atm CO/H ₂ (1/1), 20.0 M in benzene	>99	90/10	94 (S)
12	44b/44d ^{31,32}	0.1 mol % [Rh(acac)(CO) ₂], 0.4 mol % 44b/44d , 60 °C, 100 atm CO/H ₂ (1/1), 20.0 M in benzene	98	89/11	69 (S)
13	58d ⁹⁷	0.1 mol % [Rh(acac)(CO) ₂], 0.11 mol % 58d , 25 °C, 24.7 atm CO/H ₂ (2/1), 0.9 M in toluene	58	95/5	49 (S)
14	62a ^{39a}	0.05 mol % [Rh(acac)(CO) ₂], 0.2 mol % 62a , 50 °C, 19.7 atm CO/H ₂ (1/1), 1.0 M in toluene	55	92/8	63 (S)
15	70b ⁹⁸	[Rh(acac)(CO) ₂]/ 70b (1/4), 40 °C, 100 atm CO/H ₂ (1/1), benzene	>99	97/3	20 (S)
16	71 ^{42b}	0.05 mol % [Rh(acac)(CO) ₂], 0.1 mol % 71 , 25 °C, 100 atm CO/H ₂ (1/1), 2.0 M in benzene	53	96/4	40 (R)
17	72f ^{43f}	0.1 mol % [Rh(acac)(CO) ₂], 0.4 mol % 72f , 50 °C, 19.7 atm CO/H ₂ (1/1), 1.1 M in toluene	48	98/2	71 (S)
18	113a ^{50d}	0.1 mol % [Rh(acac)(CO) ₂], 0.4 mol % 113a , 35 °C, 9.9 atm CO/H ₂ (1/1), 1.1 M in toluene	77	97/3	80 (S)

Scheme 25. Hydroformylation of Styrene **150a** Using Rhodium Complexes of P–OP Ligands

their high chemo- and regioselectivities, these complexes never provided comparable enantioselectivities (ee up to 80% with ligand **113a**) to those obtained with BINAPHOS (compare entries 1 and 18 in Table 10).

Studies on catalyst recycling, catalyst reuse, and product separation within asymmetric hydroformylation ran almost in parallel to the development of standard phosphine–phosphite ligands for homogeneous catalysis. For example, in 1998 Nozaki et al. reported the highly efficient rhodium-mediated enantioselective hydroformylation of styrene **150a** using the polymer-immobilized enantiopure phosphine–phosphite ligands **49** and **50** (Figure 23).³⁴ These heterogeneous catalysts provided comparable results (see Table 11) to those obtained with the homogeneous analogs, although the catalytic efficiency depended heavily on mechanical considerations: the catalyst could be reused up to four times with almost no change in catalytic activity, but only at low stirring rates. The catalytic complexes of **49** and **50** also performed well for asymmetric hydroformylation in the vapor phase (i.e., in the absence of organic solvents).^{34c–e}

The Leitner^{36a,b} and Ojima³⁵ groups independently reported a similar approach, using supercritical CO₂¹⁰⁰ in fluorinated solvents for enantioselective hydroformylation. The catalysts formed from [Rh(acac)(CO)₂] and either of the perfluoroalkyl-substituted phosphine–phosphite ligands, **51** or **52**, provided excellent regio- and enantioselectivities (up to 94% ee with **52**) for the hydroformylation of several *p*-substituted styrene derivatives.

3.2.2. Asymmetric Hydroformylations of Alkyl-Substituted Alkenes. Hydroformylation of terminal aliphatic alkenes with rhodium catalysts has not been as widely explored as that of aryl alkenes (see section 3.2.1), probably because of the lower regio- and enantioselectivities obtained for the alkyl branched aldehydes compared with their aryl analogs.^{10,93} The few literature reports on the use of rhodium complexes of P–OP ligands in the hydroformylation of alkyl-substituted alkenes (Scheme 28) mainly relate to BINAPHOS and analogous ligands (see Table 12 for catalysis results and Figure 22 for ligand structures).

Low regioselectivities and high enantioselectivities were generally observed (Table 12), irrespective of the ligand used (**37a**, **37c**, or **44a**); however, the highest enantioselectivity (>99% ee, 60% of the branched aldehyde, entry 10 in Table 12) was observed for substrate **153h**, which contains a triphenylmethyl substituent at the allylic position.

Asymmetric hydroformylation of 1,2-disubstituted aliphatic alkenes is more complicated, because of the numerous reactions pathways possible. For example, the rhodium catalyst could mediate the isomerization of the initial substrate to the corresponding terminal aliphatic alkenes (Scheme 29), whereby hydroformylation products both from the internal (**157**) and from the terminal alkenes (**159** and **160**) would be expected.

Remarkably, the catalyst using the BINAPHOS analog **37c** afforded high enantioselectivities and total chemo- and regioselectivities in the enantioselective hydroformylation of internal aliphatic alkenes.²⁵ These results were better than those obtained with the rhodium complex of (*R,S*)-BINAPHOS **37a**.¹⁰² As a representative example, for the substrate (*Z*)-2-butene (**156a**), the only product obtained was the enantiomerically enriched branched aldehyde **157a** in 90% ee (Scheme 29), the highest ee value ever described for this type of substrate. The absence of linear product indicated that no isomerization had occurred during the catalytic transformation.

3.2.3. Asymmetric Hydroformylations of Conjugated Dienes and Heteroaryl Alkenes. Taking into consideration the excellent performance of Rh(I)-BINAPHOS complexes,

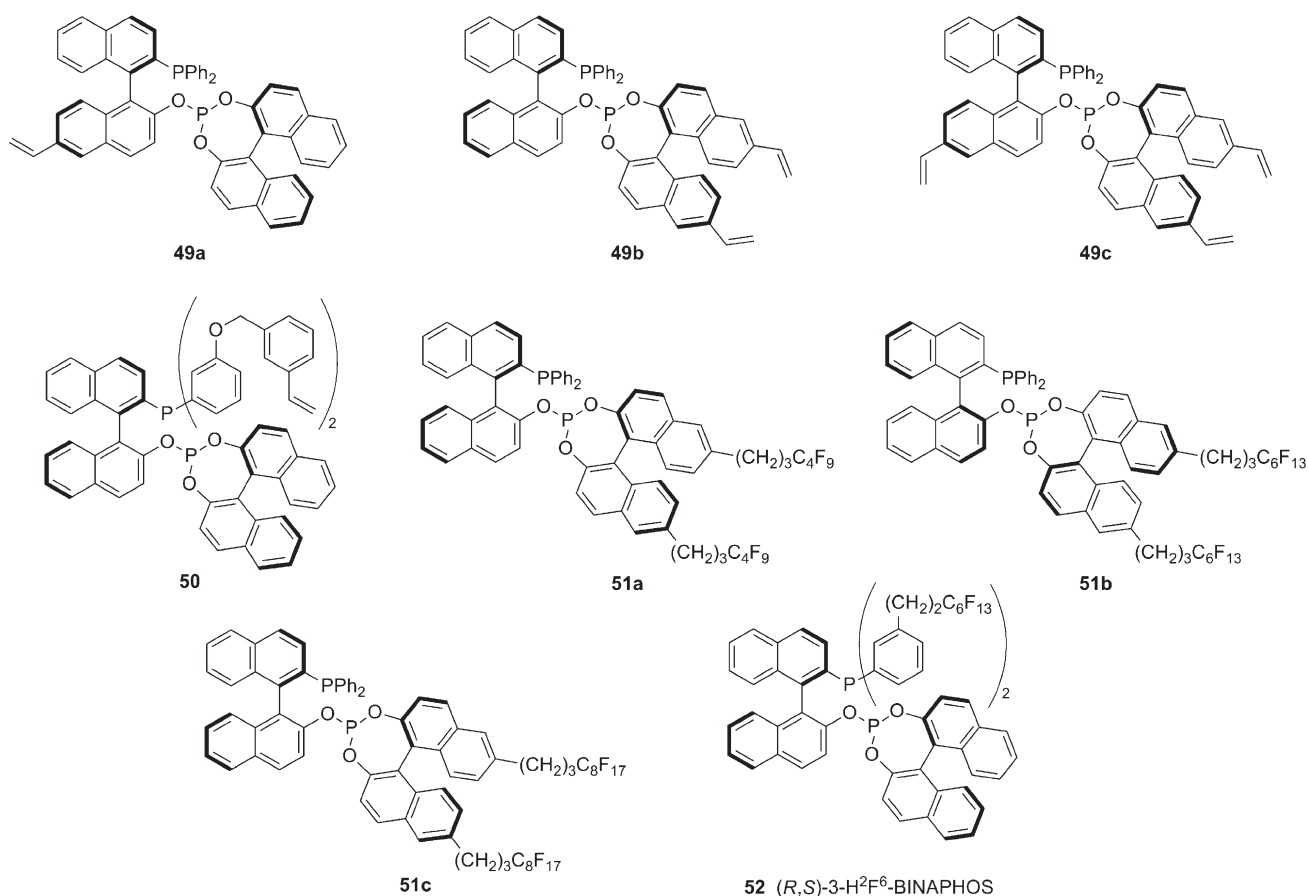
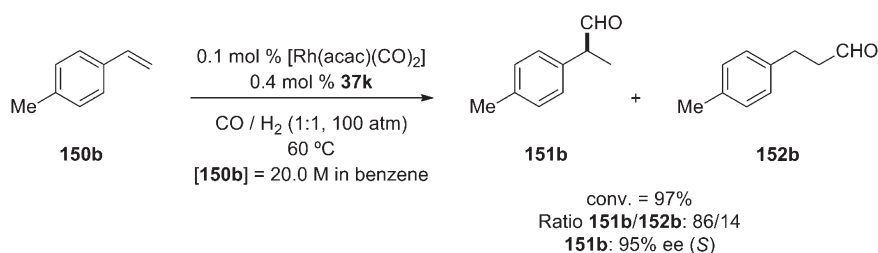
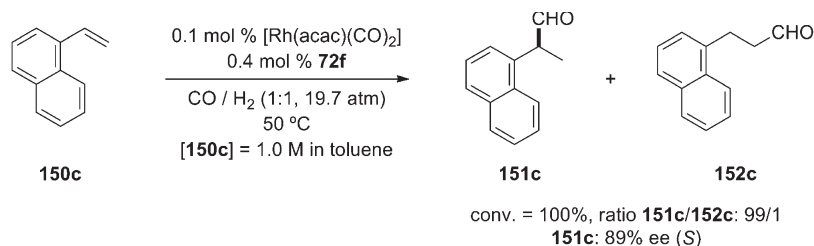


Figure 23. Phosphine–phosphite ligands used in hydroformylation reactions with improved catalyst recycling, catalyst reuse, or product separation.

Scheme 26. Hydroformylation of *p*-Methylstyrene **150b** with a Rhodium Complex of BINAPHOS



Scheme 27. Hydroformylation of 1-Vinyl Naphthalene Catalyzed by the Rhodium Complex of Ligand **72f**

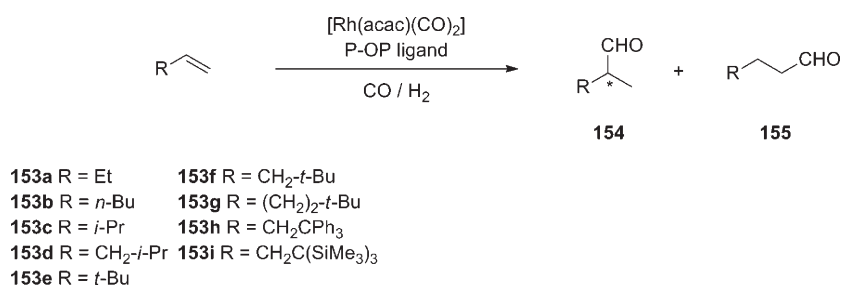


Nozaki et al. applied these catalysts to the hydroformylation of the conjugated dienes **161** (Table 13, Scheme 30).¹⁰³

Hydroformylation of **161a–c** afforded the desired optically active β,γ -unsaturated aldehydes **162a–c** with high regio- and

Table 11. Asymmetric Hydroformylation of Styrene 150a Catalyzed by Polymer-Supported Rhodium Complexes of BINAPHOS

entry	reaction conditions	ratio of 151a to 152a	% ee of 151a (config.)
1	0.05 mol % PS ^a -[Rh(acac)(49a)], 60 °C, 20 atm CO/H ₂ (1/1), 17.7 M in benzene ^{34a}	85/15	90 (R)
2	0.05 mol % PS ^a -[Rh(acac)(49b)], 60 °C, 20 atm CO/H ₂ (1/1), 17.7 M in benzene ^{34a}	90/10	87 (R)
3	0.05 mol % PS ^a -[Rh(acac)(49c)], 60 °C, 20 atm CO/H ₂ (1/1), 17.7 M in benzene ^{34a}	87/13	85 (R)
4	0.05 mol % PS ^a -[Rh(acac)(50)], 60 °C, 20 atm CO/H ₂ (1/1), 17.7 M in benzene ^{34d}	85/15	92 (R)

^a PS = polymer supported.**Scheme 28. Hydroformylation of Terminal Aliphatic Alkenes Catalyzed by Rhodium Complexes of P–OP Ligands****Table 12. Rhodium-Mediated Enantioselective Hydroformylation of Terminal Aliphatic Alkenes 153a–i**

entry	sub- strate	ligand	reaction conditions	conv. (%)	ratio of 154 to 155	% ee of 154 (config.)
1	153a	37a ³⁰	0.1 mol % [Rh(acac)(CO) ₂], 0.4 mol % 37a, 30 °C, 100 atm CO/H ₂ (1/1), 20.0 M in benzene		21/79	83 (R)
2	153b	37a ⁶	0.1 mol % [Rh(acac)(CO) ₂], 0.4 mol % 37a, 30 °C, 100 atm CO/H ₂ (1/1), 20.0 M in benzene	90	24/76	75 (R)
3	153b	37c ²⁵	0.1 mol % [Rh(acac)(CO) ₂], 0.4 mol % 37c, 30 °C, 19.7 atm CO/H ₂ (1/1), 20.0 M in benzene	66	30/70	90 (R)
4	153b	44a ³¹	0.1 mol % [Rh(acac)(CO) ₂], 0.4 mol % 44a, 30 °C, 100 atm CO/H ₂ (1/1), 20.0 M in benzene	51	23/77	85 (S)
5	153c	37a ³⁰	0.1 mol % [Rh(acac)(CO) ₂], 0.4 mol % 37a, 30 °C, 100 atm CO/H ₂ (1/1), 20.0 M in benzene	90	8/92	83 (R)
6	153d	37a ¹⁰¹	0.2 mol % [Rh(acac)(CO) ₂], 0.8 mol % 37a, 50 °C, 100 atm CO/H ₂ (1/1), 5.0 M in benzene	54	26/74	83 (nd)
7	153e	37a ¹⁰¹	0.2 mol % [Rh(acac)(CO) ₂], 0.8 mol % 37a, 50 °C, 100 atm CO/H ₂ (1/1), 5.0 M in benzene	71	0/100	
8	153f	37a ¹⁰¹	0.2 mol % [Rh(acac)(CO) ₂], 0.8 mol % 37a, 50 °C, 100 atm CO/H ₂ (1/1), 5.0 M in benzene	94	43/57	92 (nd)
9	153g	37a ¹⁰¹	0.4 mol % [Rh(acac)(CO) ₂], 1.6 mol % 37a, 50 °C, 100 atm CO/H ₂ (1/1), 5.0 M in benzene	90	26/74	77 (nd)
10	153h	37a ¹⁰¹	0.4 mol % [Rh(acac)(CO) ₂], 1.6 mol % 37a, 50 °C, 100 atm CO/H ₂ (1/1), 5.0 M in benzene	>99	60/40	>99 (nd)
11	153i	37a ¹⁰¹	0.4 mol % [Rh(acac)(CO) ₂], 1.6 mol % 37a, 60 °C, 100 atm CO/H ₂ (1/1), 5.0 M in benzene	51	7/93	nd

enantioselectivities (entries 1–3 in Table 13, respectively), in which careful control of the reaction conditions (e.g., syngas pressure, reaction time, and stirring rate) during the *in situ* formation of the catalyst was essential. Simple conjugated dienes **161d** and **161e** gave poor enantioselectivities (entries 4–5 in Table 13, respectively), indicating that stereodiscrimination in this transformation is dictated by the substituents at C₃– and C₄– (R¹–R³).

Literature reports on enantioselective hydroformylation in target-oriented synthesis are, to the best of our knowledge, scarce; nevertheless, there is one example that clearly highlights the uniqueness of BINAPHOS ligand for use in hydroformylation. Jacobsen et al. have elegantly reported the total synthesis of (+)-ambruticin, whose C₁₅ stereocenter they efficiently generated via asymmetric hydroformylation of the adequate conjugated diene **165** using a rhodium complex of (*S,R*)-BINAPHOS **37k** (Scheme 31).¹⁰⁴ Carbonylation provided the desired branched aldehyde **166** with high regio- and diastereoselectivity (Scheme 31).

Nozaki's group recently expanded the substrate scope of asymmetric hydroformylation to include the vinyl heteroarenes **167**: using a rhodium complex of (*R,S*)-3-MeO-BINAPHOS **37c**, they

obtained the desired branched aldehydes with excellent regio- and enantioselectivities (Scheme 32).¹⁰⁵ Further oxidation of the enantiopure aldehyde **168** yielded the corresponding α-heteroarylpropanoic acids **169** without loss of optical purity.

3.2.4. Asymmetric Hydroformylations of Heteroatom-Substituted Olefins or Alkenes That Contain Substituents with Functional Groups

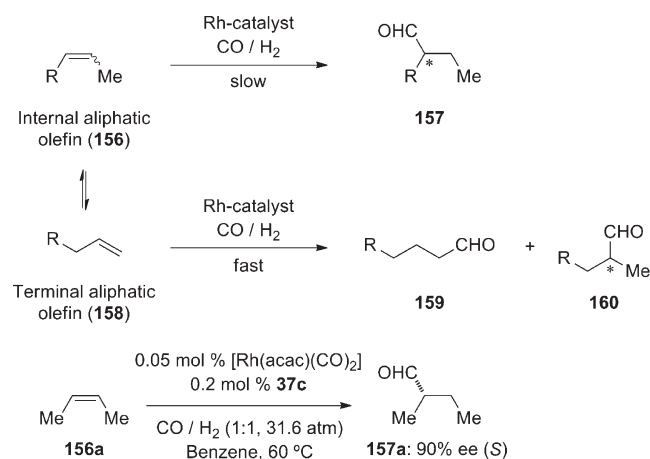
3.2.4.1. Oxygen-Containing Alkenes. Rhodium(I) complexes of enantiomerically pure phosphine–phosphites have also been applied in the asymmetric hydroformylation of diverse heteroatom-substituted alkenes, which is usually more difficult than that of vinyl arenes. The low conversions and low chemo- and regioselectivities observed for bidentate C₂-symmetric diphosphines are due to poor substrate reactivity or undesired reaction pathways.¹⁰⁶ The most representative example presented in this section is the enantioselective hydroformylation of vinyl acetate **170** (Scheme 33), which has been explored with rhodium complexes of different phosphine–phosphite ligands, chiefly, BINAPHOS analogs (see Table 14 for the catalysis results and Figures 22 and 23 for the ligand structures).

Remarkably, the BINAPHOS analogs performed quite well, affording high conversions and excellent regio- and enantioselectivities (up

to 92% ee for (*R,S*)-BINAPHOS **37a**, entry 1 in Table 14). To the best of our knowledge, this was the first example of highly efficient catalysts for asymmetric hydroformylation of vinyl acetate **170**. Moreover, corresponding polymer-supported versions of the catalysts afforded equally good results (compare entries 1–5 with entries 6–9 in Table 14). Hydroformylation of other vinyl carboxylates, spanning a wide range of substituents (EtCOO, *t*-BuCOO, BzO, and Me(CH₂)₆COO instead of the AcO group) also proceeded with high regioselectivity (branched to linear product ratios from 85/15 to 91/9) and enantioselectivities (from 80% ee to 98% ee), demonstrating the unique catalytic properties of Rh–BINAPHOS derived catalytic systems.³⁰

Börner's phosphine–phosphite ligands **53** and **54**³⁷ (see Figure 7 in section 2.1.2) have been evaluated in the rhodium-mediated hydroformylation of allyl acetate **173** (Scheme 34), in which **54a** (Figure 24) provided the best results (up to 44% ee).³⁷ The results depended on the bulk of the aromatic groups and on the relative stereochemistry of the two phosphorus functionalities;

Scheme 29. Hydroformylation with Concomitant Isomerization



thus, the highest ratio of branched to linear isomer and the highest enantioselectivity were obtained with the combination of the *trans* arrangement of substituents and the (*S*)-configuration for the binaphthyl unit.

Cinnamyl alcohol **176** has also been evaluated in enantioselective hydroformylations, as an interesting oxygen-functionalized substrate.¹⁰⁸ A series of two rhodium complexes of P–OP ligands were tested (see Table 15 for catalysis results and Figure 24 for the ligand structures).

As observed in Scheme 35, hydroformylation of **176** yielded the lactol **177** with total regioselectivity (the linear product **178** was not detected by ¹H NMR spectroscopy). The crude lactol **177** was then converted to the corresponding lactone **179** by oxidation with Ag₂CO₃ in high isolated yields (entries 1 and 2 in Table 15). (*R,S*)-BINAPHOS (**37a**) provided the best enantioselectivity (entry 1 in Table 15), whereas its phosphine–phosphinite counterpart **3b** gave relatively low enantioselectivity.

Scheme 31. Asymmetric Hydroformylation Used to Prepare a Key Precursor of (+)-Ambruticin

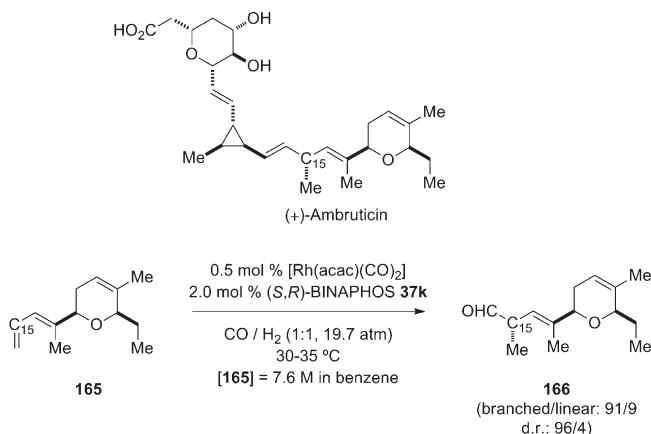
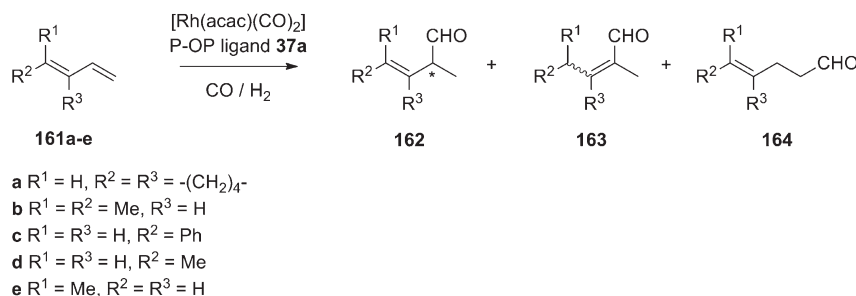


Table 13. Asymmetric Hydroformylation of Conjugated Dienes Catalyzed by Rhodium Complexes of BINAPHOS

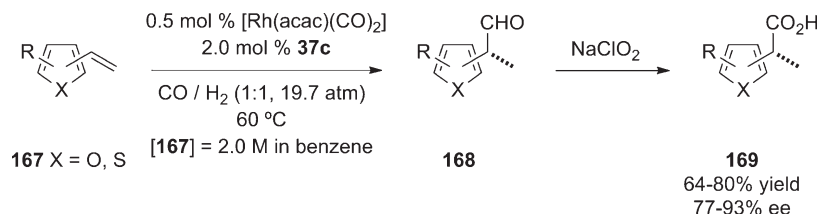
entry	substrate	reaction conditions	conv. (%)	ratio of 162 to (163 + 164)	% ee of 162 (config.)
1	161a ^{103a}	0.5 mol % [Rh(acac)(CO) ₂], 2.0 mol % 37a , 60 °C, 100 atm CO/H ₂ (1/1), 8.0 M in benzene	85	86/(0 + 14)	96 (R)
2	161b ^{103b}	0.5 mol % [Rh(acac)(CO) ₂], 2.0 mol % 37a , 60 °C, 100 atm CO/H ₂ (1/1), 8.0 M in benzene	92	78/(0 + 22)	80 (R)
3	161c ^{103a}	0.5 mol % [Rh(acac)(CO) ₂], 2.0 mol % 37a , 30 °C, 100 atm CO/H ₂ (1/1), 8.0 M in benzene	62	91/(4 + 5)	89 (R)
4	161d ^{103b}	0.1 mol % [Rh(acac)(CO) ₂], 0.4 mol % 37a , 30 °C, 100 atm CO/H ₂ (1/1), 12.0 M in benzene	4.2 h ^{−1a}	75/(25)	22 (R)
5	161e ^{103b}	0.1 mol % [Rh(acac)(CO) ₂], 0.4 mol % 37a , 30 °C, 100 atm CO/H ₂ (1/1), 12.0 M in benzene	4.9 h ^{−1a}	88/(12)	20 (R)

^a TOF.

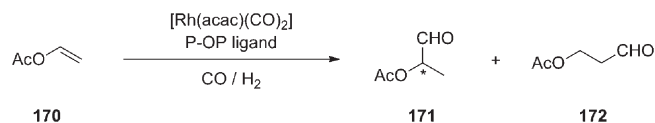
Scheme 30. Asymmetric Hydroformylation of Conjugated Dienes Catalyzed by Rhodium Complexes of BINAPHOS



Scheme 32. Hydroformylation of Vinyl Heteroarenes Catalyzed by Rhodium Complexes of P–OP Ligands



Scheme 33. Asymmetric Hydroformylation of Vinyl Acetate Catalyzed by Rhodium Complexes of P–OP Ligands



The aryl vinyl ethers **180a–e** have been also investigated as substrates for rhodium-mediated asymmetric hydroformylation (Scheme 36), since their resulting branched aldehydes are important subunits for nonracemic agrochemicals. Due to its excellent performance in hydroformylation, (*S,R*)-BINAPHOS **37k** was the obvious choice as ligand.¹⁰⁹ The results are summarized in Table 16.

Under these conditions, the branched to linear product ratios were moderate (from 63/37 to 71/29), whereas the enantioselectivities were high (from 65% to 80% ee). The highest enantiomeric excesses were achieved at roughly 50% conversion. The authors attributed this to a decrease in catalyst stability upon increasing concentration of the branched aldehyde in the reaction mixture, whereby new catalytic species appeared to be involved in the reaction and to lead to worse stereodiscrimination.¹⁰⁹

3.2.4.2. Nitrogen-Containing Alkenes. The hydroformylation of N-containing alkenes is a powerful tool for preparing chiral amino acids or enantiopure amino alcohols. For asymmetric hydroformylation of *N*-vinylphthalimide **183**, rhodium complexes of (*S,R*)-BINAPHOS **37k** provided high chemo-, regio-, and enantioselectivity (Scheme 37).^{6,30}

Enantioselective hydroformylation of allyl cyanide **186** (Scheme 38) can be considered challenging, as it generally leads to the linear aldehyde as major hydroformylation product.¹¹⁰ Remarkably, the use of phosphine–phosphites (*R,S*)-BINAPHOS **37a** and **72e** as ligands in rhodium complexes for catalyzing this transformation enabled switching of the regioselectivity to favor the branched product.^{111,43f} Thus, excellent branched to linear product ratios (up to 93/7) were achieved with **72e** (entry 3 in Table 17), although the enantioselectivities remained moderate for both ligands (Table 17).

Enantioselective hydroformylation has been used as the key step for preparing biologically active compounds, including the 1 β -methylcarbapenem antibiotics **190 β** , which can be stereoselectively synthesized via rhodium-mediated asymmetric hydroformylation of 4-vinyl- β -lactam **189** (Scheme 39). For this chemistry, Takaya, Nozaki, et al. tested several rhodium complexes of the phosphine–phosphite and phosphine–phosphinite ligands shown in Figure 24.²⁰ Their results on catalysis are summarized in Table 18.

In this reaction, the catalyst derived from ligand **42** gave higher regioselectivity but lower diastereoselectivity than did the

catalyst with (*R,S*)-BINAPHOS (**37a**) (compare entries 4 and 5 in Table 18, respectively). Interestingly, the phosphine–phosphinite ligands performed slightly better than did (*R,S*)-BINAPHOS. The best results (in terms of catalytic activity and regio- and diastereoselectivity) were achieved using **3c** (entry 3 in Table 18), which contains an electron-withdrawing fluoro group at the *para* position of both phenyl rings in the phosphinite moiety. This is one of the rare examples of highly efficient asymmetric hydroformylations catalyzed by rhodium complexes of phosphine–phosphinite ligands.

3.2.4.3. Sulfur-Substituted Alkenes. To the best of our knowledge, there are very few publications on the use of P–OP ligands in rhodium-mediated asymmetric hydroformylation of sulfur-containing alkenes. Indeed, only catalysts incorporating (*R,S*)-BINAPHOS **37a** as ligand have been successfully used in the hydroformylation of vinyl sulfides **192a–e**, allyl sulfide **193**, and allyl sulfone **194**, providing branched aldehydes as major products in 65% to 89% ee (Figure 25).¹¹³

The use of bulkier substituents on the sulfur in vinyl substrates enhanced both the regio- and the enantioselectivities (Figure 25).

3.2.4.4. Fluorinated Alkenes. Hydroformylation of fluorinated alkenes is a convenient and relatively unexplored route to enantiomerically enriched organofluorine compounds, which have unique biological and physiological activities. Most of the reported work on enantioselective hydroformylation of fluorinated substrates has employed catalysts in which BINAPHOS was the ligand (Table 19, Scheme 40).^{30,34b}

As illustrated by Table 19, hydroformylation proceeded under mild conditions to give the desired optically enriched aldehydes **196** in high ratios of branched to linear product (ratio of **196** to **197** up to 96/4, entry 1 in Table 19) and with high enantioselectivity (up to 95% ee, entry 2 in Table 19). The authors stated that they had to stop the reaction at moderate levels of conversion to obtain high ee's, probably due to partial racemization of the branched aldehyde (compare entry 1 with entries 2 and 3 in Table 19). Polymer-supported versions of the catalysts offered higher catalytic activity (TOF) and similar selectivities to the corresponding homogeneous conditions (entry 5 in Table 19).

3.2.4.5. Heterocyclic Alkenes. Rhodium complexes of BINAPHOS analogs have also been tested by Nozaki et al. in asymmetric hydroformylations of the five- or seven-membered heterocyclic alkenes **198–200** (Figure 26).²⁷

For most of these substrates, the best results were obtained using **37j** as P–OP ligand (see Figure 24), which contains two methyl groups at the two *ortho* positions of the binaphthyl backbone in the phosphite moiety. Steric bulk around the phosphite fragment improves stereocontrol and catalytic activity and proved to suppress side reactions such as racemization (via β -hydride elimination for **198**) and polymerization or cleavage of the ketal moiety in substrate **200**.

Table 14. Asymmetric Hydroformylation of Vinyl Acetate 170 Catalyzed by Rhodium Complexes of P–OP Ligands

entry	ligand	reaction conditions	conv. (%)	ratio of 171 to 172	% ee of 171 (config.)
1	37a ⁶	0.25 mol % [Rh(acac)(CO) ₂], 1.0 mol % 37a , 60 °C, 100 atm CO/H ₂ (1/1), 20.0 M in benzene	>99	86/14	92 (S)
2	37b ³⁰	0.25 mol % [Rh(acac)(CO) ₂], 1.0 mol % 37b , 60 °C, 100 atm CO/H ₂ (1/1), 20.0 M in benzene	72	85/15	90 (S)
3	37c ¹⁰⁷	0.1 mol % [Rh(acac)(CO) ₂], 0.4 mol % 37c , 60 °C, 20 atm CO/H ₂ (1/1), 7.0 M in benzene	96	94/6	87 (S)
4	37d ¹⁰⁷	0.1 mol % [Rh(acac)(CO) ₂], 0.4 mol % 37d , 60 °C, 20 atm CO/H ₂ (1/1), 7.0 M in benzene	92	84/16	90 (S)
5	44a ³¹	0.1 mol % [Rh(acac)(CO) ₂], 0.4 mol % 44a , 60 °C, 20 atm CO/H ₂ (1/1), 20.0 M in benzene	65	85/15	90 (R)
6	49a ^{34a}	0.2 mol % PS ^a -[Rh(acac)(49a)], 60 °C, 20 atm CO/H ₂ (1/1), 17.7 M in benzene	67	87/13	92 (S)
7	49b ^{34a}	0.2 mol % PS ^a -[Rh(acac)(49b)], 60 °C, 20 atm CO/H ₂ (1/1), 17.7 M in benzene	83	90/10	93 (S)
8	49c ^{34a}	0.2 mol % PS ^a -[Rh(acac)(49c)], 60 °C, 20 atm CO/H ₂ (1/1), 17.7 M in benzene	78	90/10	89 (S)
9	50 ^{34d}	0.2 mol % PS ^a -[Rh(acac)(50)], 60 °C, 80 atm CO/H ₂ (1/1), 17.7 M in benzene	87	84/16	86 (S)

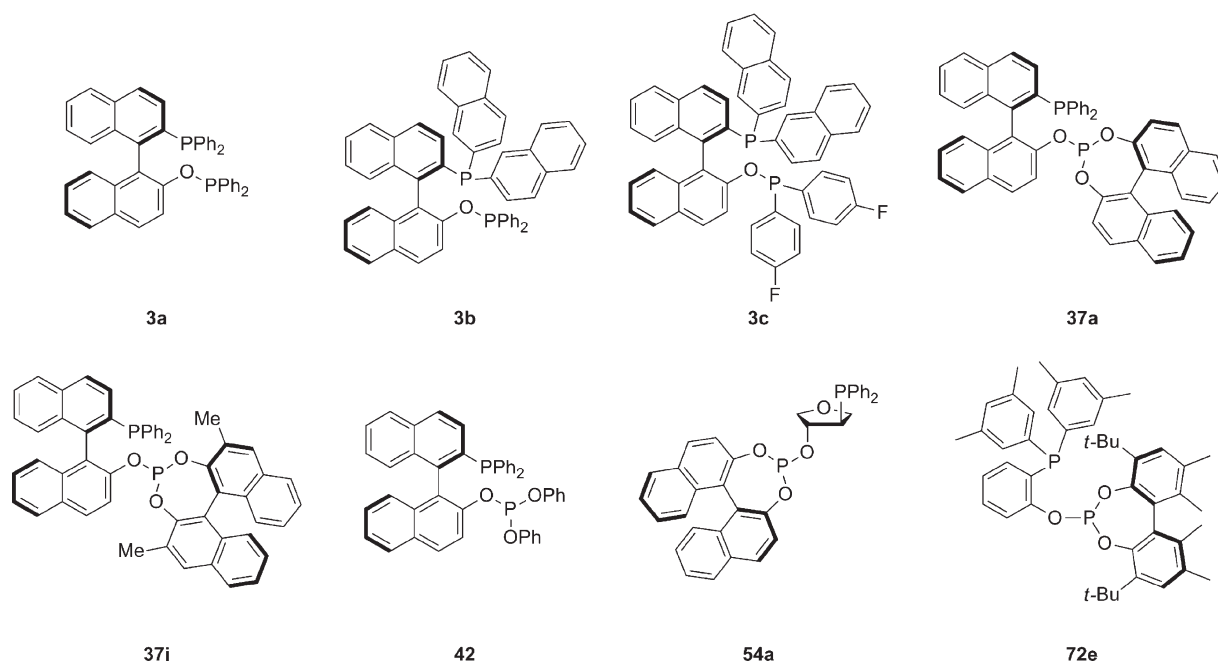
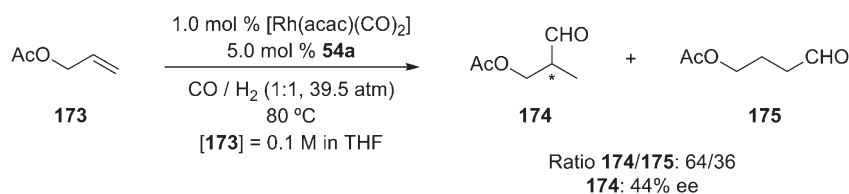
^a PS, polymer supported.

Figure 24. P–OP ligands used in the asymmetric hydroformylation of alkenes substituted with heteroatoms or functional groups.

Scheme 34. Asymmetric Hydroformylation of Allyl Acetate 173 Catalyzed by Rhodium Complexes of P–OP Ligands



3.2.5. Rationalization of the Stereochemical Outcome.

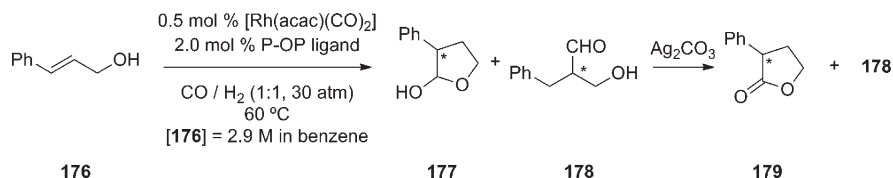
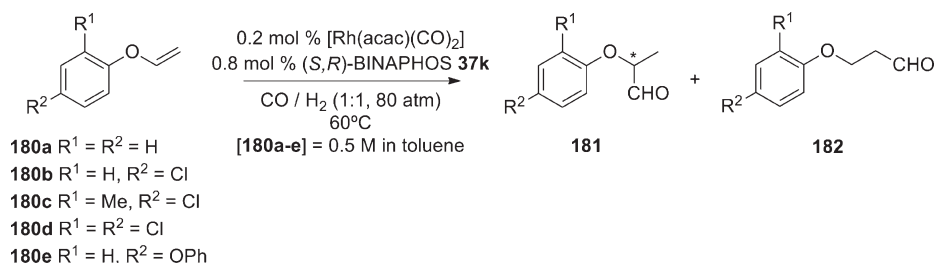
This section of the review has underscored the outstanding catalytic properties of rhodium complexes of (*R,S*)-BINAPHOS for enantioselective hydroformylation of myriad structurally diverse alkenes. Not surprisingly, researchers have endeavored to understand the regio- and enantioselectivity provided by these complexes. The generally accepted dissociative mechanism of the hydroformylation catalyzed by cationic Rh(I) complexes was first proposed by Wilkinson et al.¹¹⁴ It considers five-coordinate di-phosphine rhodium complexes ([RhH(CO)₂(PPh₃)₂]) as key

Table 15. Asymmetric Hydroformylation of Cinnamyl Alcohol 176

entry	ligand	conv. (%)	% yield of 179	% ee of 179 (config.)
1	37a ¹⁰⁸	>99	87	88 (nd)
2	3b ¹⁰⁸	>99	86	5 (nd)

intermediates in the catalytic cycle. Nozaki et al. attributed the superb catalysis results for (*R,S*)-BINAPHOS (**37a**) to the exclusive formation of a single active species, [RhH(CO)(**37a**)] **202**

Scheme 35. Asymmetric Hydroformylation of Cinnamyl Alcohol 176 Catalyzed by Rhodium Complexes of P–OP Ligands

Scheme 36. Asymmetric Hydroformylation of Aryl Vinyl Ethers Catalyzed by a Rhodium Complex of (*S,R*)-BINAPHOS

(Scheme 41), which is formed via decarbonylation from $[\text{RhH}(\text{CO})_2(\text{37a})]$ **201**_{eq,ap} during the catalytic cycle.¹⁰⁷ In this species, the phosphino moiety is preferentially located at the equatorial site, whereas the phosphite fragment occupies the apical position (Scheme 41). The structure of compound **201**_{eq,ap} was determined by *in situ* high-pressure IR and room-temperature NMR studies of a solution of $[\text{Rh}(\text{acac})(\text{37a})]$ in benzene-*d*₆ that had been subjected to a 1:1 mixture of H_2 and CO at atmospheric pressure.^{6,30} It should be noted at this point that other phosphine–phosphite ligands preferentially coordinate in an opposite fashion to the rhodium center (apical–equatorial binding mode, with the phosphite moiety located at the equatorial position).^{39a,43f,50d,97} Very recently,¹¹⁵ ^1H and ^{31}P NMR studies at low temperatures (-90°C) have also allowed the observation in the case of (*R,S*)-BINAPHOS **37a** of the previously undetected minor isomer **201**_{ap,eq} (Scheme 41), with the phosphite moiety located at the equatorial position.

Nozaki et al. performed deuterioformylation reactions, which revealed that the alkene insertion into $[\text{RhH}(\text{CO})(\text{37a})]$ **202** was an irreversible step in the catalytic cycle.^{107,116} These experimental data support the assumption that stereoselection is produced during alkene insertion: the alkene approaches and coordinates to rhodium, thereby minimizing the steric interactions between the ligand and the alkene substituents. Thus, the stereochemical outcome of the reaction can be rationalized according to the quadrant model depicted in Figure 27. The rigid equatorial–apical conformation of $[\text{RhH}(\text{CO})(\text{37a})]$ **202**, in which the phosphite group is *trans* to the hydrido ligand, clearly distinguishes in terms of steric hindrance the bottom left and right quadrants; consequently upon insertion of a monosubstituted alkene, the substituent occupies the bottom right quadrant (Figure 27).^{30,95a} This model can be used to predict the stereochemical outcome of the reaction, not only for monosubstituted alkenes, but also for *cis*-disubstituted alkenes (substituents positioned in the top and bottom right quadrants) and *trans*-disubstituted alkenes (substituents positioned in the top left and bottom right quadrants). However, this model cannot be used to explain the regioselectivity of the hydroformylation (i.e., branched to linear product ratio).

Table 16. Asymmetric Hydroformylation of Aryl Vinyl Ethers Catalyzed by a Rhodium Complex of (*S,R*)-BINAPHOS

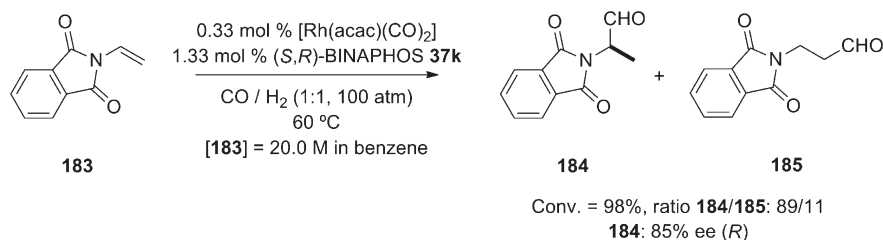
entry	substrate	conv. (%)	ratio of 181 to 182	% ee of 181 , (config.)
1	180a ¹⁰⁹	52	65/35	65 (<i>R</i>)
2	180b ¹⁰⁹	50	70/30	77 (<i>R</i>)
3	180c ¹⁰⁹	56	63/37	80 (<i>R</i>)
4	180d ¹⁰⁹	54	67/33	72 (<i>R</i>)
5	180e ¹⁰⁹	35	71/29	65 (<i>R</i>)

Herrmann et al. have performed computational studies to predict the stereoselectivity of hydroformylations catalyzed by rhodium complexes of BINAPHOS.¹¹⁷ Their findings corroborate the premise that the outstanding properties of (*R,S*)-BINAPHOS as ligand are due to stereoselective coordination of the ligand to the rhodium center as well as to correct relative configuration of the binaphthyl fragments.

3.2.6. Comparative Tables in Hydroformylations. As it has been shown in this part of the review, rhodium complexes of (*R,S*)-BINAPHOS **37a** have proven to be highly efficient in the rhodium-mediated asymmetric hydroformylation of a broad variety of structurally diverse olefins, thus standing out in terms of regio- and enantioselectivity among other P–OP ligands. Tables 20 and 21 provide comparison between the catalytic activity of (*R,S*)-BINAPHOS and several other lead ligands in the rhodium-mediated hydroformylation of benchmark substrates. The aforementioned tables show that results obtained with (*R,S*)-BINAPHOS **37a** compare very favorably to those obtained with rhodium complexes of other chiral ligands that have been successfully applied in this transformation (Figure 28). Therefore, the most convenient ligands for enantioselective hydroformylation appear to be hybrid ligands comprising a phosphino moiety and a phosphite or phosphoramidite group.

3.3. Copper-Mediated Conjugate Additions

Asymmetric 1,4-addition (conjugate addition) of C-nucleophiles to α,β -unsaturated carbonyl compounds and related activated olefins is among the most powerful and reliable methods

Scheme 37. Asymmetric Hydroformylation of *N*-Vinylphthalimides Catalyzed by a Rhodium Complex of (*S,R*)-BINAPHOS

for C–C bond formation with simultaneous introduction of new stereogenic centers in a carbon skeleton. In most of these transformations, enones are used as Michael acceptors and the addition of magnesium, zinc, and aluminum organometallic reagents is mainly catalyzed by chiral copper complexes.¹²⁶

The first application of P–OP ligands in conjugate addition reactions was described in 2000. Diéguez, van Leeuwen, et al. reported the use of a new class of chiral phosphine–phosphite ligands derived from enantiomerically pure epoxides (see ligands **62** and **63** in section 2.1.2, Figure 8)^{39a} in the enantioselective 1,4-addition of triethylaluminum to 2-cyclohexenone **210** (see Scheme 42).¹²⁷ The effects of the absolute configuration of the stereogenic carbon arising from the epoxide and the influence of the chain length between the two phosphorus functionalities were studied. These ligands generally gave low enantioselectivities, except for the (*R_P*,*R_C*)-phosphine–phosphite ligand **63b** (Figure 29), which afforded the best results in asymmetric conjugate addition.¹²⁷ The authors also demonstrated that the configuration of the stereogenic carbon next to the phosphite moiety strongly affected the enantioselectivity: excellent conversion and good enantioselectivity (up to 62% ee in favor of the *S* enantiomer) were obtained with **63b** (entries 1 and 2 in Table 22). Full conversions and excellent selectivities for the 1,4-adduct **211** were obtained at low temperature.

Diéguez et al. also reported the copper-mediated asymmetric 1,4-addition of triethylaluminum to 2-cyclohexenone **210** (see Scheme 42)¹²⁸ by using enantiomerically pure Ruiz and Claver's³⁸ phosphine–phosphite ligands containing a D-(+)-xylose-derived carbohydrate backbone (see ligands **58** in section 2.1.2, Figure 7). Although they obtained excellent reaction rates and selectivities for the 1,4-adduct **211**, the enantioselectivities were poor in all cases (the catalytic activity of the best ligand of the series is summarized in entry 3 of Table 22). The same group also studied addition of diethylzinc to 2-cyclohexenone **210** catalyzed by copper complexes of ligands **58**.¹²⁸ They obtained similar rates of conversion and selectivities for the 1,4-adduct as those with triethylaluminum but observed slightly higher enantioselectivity. Surprisingly, the stereochemical outcome was reversed; thus, diethylzinc showed the influence of the organometallic reagent in determining enantioselectivity.

The scope of the asymmetric conjugate additions of organometallic reagents catalyzed by copper complexes of P–OP ligands has been remarkably broadened by Schmalz et al., who developed a new family of highly modular phosphine–phosphite ligands derived from the corresponding *o*-bromophenol and a chiral diol (e.g., BINOL or TADDOL).^{50a–c} These ligands enabled the enantioselective copper-mediated 1,4-addition of various Grignard reagents to 2-cyclohexenone **210** (Scheme 43).¹²⁹ The enantiomerically pure TADDOL-derived ligands **111a** and **112a**

Scheme 38. Asymmetric Hydroformylation of Allyl Cyanide Catalyzed by a Rhodium Complex of P–OP Ligands 37a or 72e

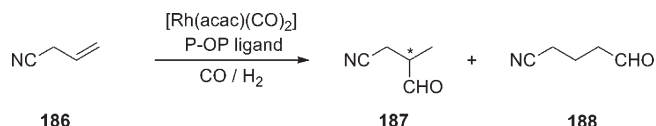


(Figure 29) gave the highest enantioselectivities with a wide range of magnesium organometallic reagents. The reaction conditions were optimized by varying the reaction parameters that affect the ratio of 1,4 to 1,2 product and enantioselectivities (e.g., copper source, solvent, and reaction temperature). The choice of solvent had an extraordinary influence on enantioselectivity; a nonpolar, weakly coordinating ether such as 2-methyltetrahydrofuran (Me-THF) was essential for attaining high enantioselectivity. Moreover, lowering the reaction temperature to –78 °C provided the best enantioselectivities and the use of CuBr·DMS as the copper source gave higher ee values at low temperatures, probably because it was more soluble than CuCl. Table 23 shows the results obtained under optimized conditions for the copper-mediated asymmetric 1,4-addition of different Grignard reagents to 2-cyclohexenone **210** catalyzed by copper complexes of either P–OP ligand **111a** or ligand **112a**.

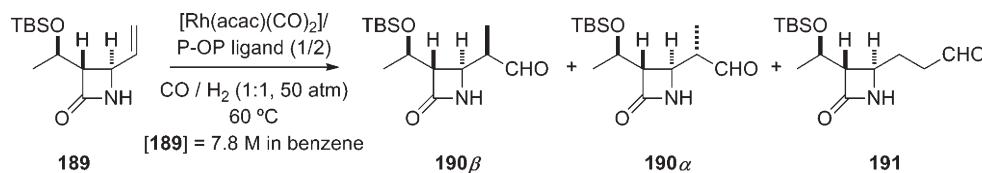
As previously mentioned, Me-THF was found to be a superior solvent in most cases; however, there were exceptions. For instance, the highest ee value for 3-butenylmagnesium bromide was achieved in neat Et₂O (entry 2 in Table 23). In the case of *i*-PrMgBr, optimal results were obtained when Et₂O was used to dissolve the substrate and the catalyst and Me-THF was used to prepare and dissolve the Grignard reagent (entries 3 and 4 in Table 23). When EtMgBr was used, the corresponding 3-alkyl cyclohexanone **211** was obtained with the opposite configuration (entry 1 in Table 23), owing to addition of the nucleophile to the *Si* face of 2-cyclohexenone. Also noteworthy was the fact that at –78 °C, ligand **111a** proved to be better for both branched Grignard reagents (cf. entries 3 and 4 in Table 23) and arylmagnesium reagent (cf. entries 6 and 7 in Table 23), whereas **112a** offered superior results for linear Grignard reagents (entries 1 and 2 in Table 23). In summary, Schmalz's ligands afforded straightforward access to various 3-substituted cyclohexanones **211–215** in high preparative yields (up to 88%) and with high enantioselectivities (from 82% to 92% ee).

3.3.1. Comparative Tables in Conjugate Additions.

The use of chiral P–OP ligands in Cu-mediated asymmetric conjugate addition reactions is not very extended and has been limited to 2-cyclohexenone as substrate with different organometallic

Table 17. Asymmetric Hydroformylation of Allyl Cyanide 186 Catalyzed by a Rhodium Complex of P–OP Ligands 37a or 72e

entry	ligand	reaction conditions	conv. (%)	ratio of 187 to 188	% ee of 187 (config.)
1	37a ¹¹¹	0.2 mol % [Rh(acac)(CO) ₂], 0.8 mol % 37a, 50 °C, 29.6 atm CO/H ₂ (1/1), 2.5 M in toluene	73	72/28	66 (nd)
2	37a ¹¹²	0.05 mol % [Rh(acac)(CO) ₂], 0.06 mol % 37a, 35 °C, 10.2 atm CO/H ₂ (1/1), 1.8 M in toluene	64	74/26	75 (S)
3	72e ^{43f}	0.1 mol % [Rh(acac)(CO) ₂], 0.4 mol % 72e, 50 °C, 19.7 atm CO/H ₂ (1/1), 1.1 M in toluene	75	93/7	53 (S)

Scheme 39. Asymmetric Hydroformylation of 4-Vinyl- β -lactam Catalyzed by Rhodium Complexes of P–OP LigandsTable 18. Asymmetric Hydroformylation of 4-Vinyl- β -lactam 189

entry	ligand	precatalyst (mol %)	% yield of 190 + 191	ratio of 190 to 191	% de of 190 β
1	3a ²⁰	0.2	58	64/36	90
2	3b ²⁰	0.2	76	74/26	90
3	3c ²⁰	0.2	95	74/26	92
4	37a ²⁰	0.1	95	55/45	86
5	42 ²⁰	0.5	92	71/29	20

derivatives. Tables 24 and 25 provide comparison between the catalytic activity of the best performing P–OP ligands and relevant lead ligands (Figure 30) in the Cu-mediated asymmetric conjugate addition of organometallic species to 2-cyclohexenone. Schmalz's phosphine–phosphite ligand **112a**¹²⁹ compares very favorably to the best chiral ligands reported for this concrete enantioselective conjugate addition reaction, among them Pfaltz's oxazoline–phosphite ligand¹³⁰ **216**, Alexakis's TADDOL-derived phosphite ligand¹³¹ **217**, Zhang's P,N ligand¹³² **218**, the chiral aryl diphosphite¹³³ **219**, and the chiral ferrocenyl diphosphine TANIAPHOS¹³⁴ **220**. Regarding P–OP ligands **58c**¹²⁸ and **63b**,¹²⁷ selectivities toward the 1,4-addition product were very high, while enantioselectivities remained low.

3.4. Polymerizations of Alkenes with CO

Polymerization of alkenes and carbon monoxide should be considered *a priori* a very complex transformation in terms of the structure of the final products, as there are nearly infinite ways to connect alkene and CO units in a polymer chain. Furthermore, the number of possible outcomes increases dramatically when stereochemical considerations are introduced. Completely alternating copolymerization of carbon monoxide with ethene was already developed in the early 1950s,¹³⁵ thereby paving the way to the preparation of stereoregular polyketone copolymers. When monosubstituted alkenes are used in place of ethene in this transformation,¹³⁶ three more factors must be controlled in order to obtain stereoregular alternating copolymers: *regioselectivity*, *tacticity*, and *enantioselectivity*. First, the insertion direction of the substituted alkene along the polymerization process must be always the same. Thus, head-to-tail polymers (Figure 31) are obtained when all monomers insert with the same regioselectivity. Second, when the alkene insertion in the catalytic cycle

occurs on the same enantiotopic alkene face during chain propagation (alkene insertion on either the *Re*- or *Si*-face), an *isotactic* polymer is generated: the stereogenic carbons in the polymer chain will have the same configuration (either SSSS... or RRRR..., Figure 31). Contrariwise, if the catalyst used for copolymerization selects the enantioface of the alkene alternately for every growing polymer chain then a *syndiotactic* polymer is obtained: the stereogenic carbons in every chain have alternating configurations (either SRSR... as indicated in Figure 31 or RSRS...). Third, the catalyst can effect the highest degree of stereocontrol during the polymerization by selecting the same alkene enantioface for every growing polymer chain, leading to catalytic *enantioselective* synthesis of an isotactic CO/alkene copolymer (chiral polyketone).¹³⁷

Both aliphatic 1-alkenes and vinyl arenes (styrenes) have been studied in this asymmetric transformation. In the following sections, the levels of stereocontrol that metal complexes derived from enantiomerically pure P–OP ligands have provided in the alternating copolymerization of monoalkyl and monoaryl alkenes with CO are described. Indeed, completely alternating, isotactic, and enantioselective copolymerizations¹³⁸ have been efficiently catalyzed by cationic Pd(II) complexes of (*R,S*)-BINAPHOS⁶ (**37a**) or related phosphine–phosphite ligands (see Figure 5 in section 2.1.2). In section 3.4.4, a few literature examples on asymmetric terpolymerization of aliphatic alkenes or arenes with CO are reviewed.

3.4.1. Alternating Copolymerizations of CO with Propene. In 1995, Takaya, Nozaki, et al. reported the first highly enantioselective alternating copolymerization of propene **221a** and CO catalyzed by a chiral Pd(II) complex of (*R,S*)-BINAPHOS (**37a**)¹³⁹ (Scheme 44).

Very high molecular weights ($M_w = 104\,400$) and optical rotations ($[\Phi]_D = +40$; $c = 0.51$ in HFIP) for poly(propene-*alt*-CO) **222a** were accomplished by using [Pd(Me)(MeCN)(**37a**)]-[BAR₄] (Ar = 3,5-bis(trifluoromethyl)phenyl) as enantioselective catalyst. The simplicity of the ¹³C NMR spectrum of the polyketone **222a** demonstrated that the tacticity control was almost complete (>97% isotactic diad). Moreover, the extremely high molar optical rotation indicated that a highly isotactic polyketone was obtained in high enantioselectivity. Enantiomeric excess was roughly estimated from the alkylpalladium species **225** generated in the first propene insertion. The palladium–carbon bond in this compound was cleaved by treatment with CO in methanol to give

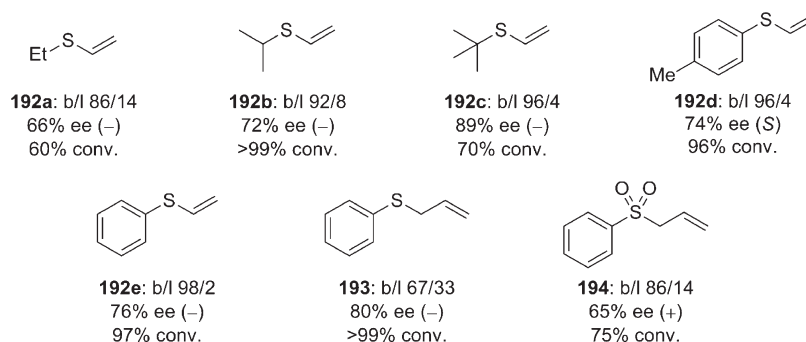


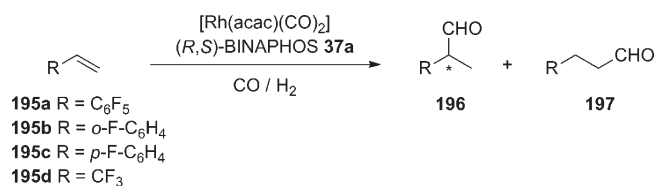
Figure 25. Asymmetric hydroformylation of sulfur-containing alkenes catalyzed by a rhodium complex of (*R,S*)-BINAPHOS.

Table 19. Asymmetric Hydroformylation of the Fluorinated Alkenes 195a–d Catalyzed by a Rhodium Complex of (*R,S*)-BINAPHOS

entry	substrate	reaction conditions	conv. (%)	ratio of 196 to 197	% ee of 196 (config.)
1	195a ³⁰	0.1 mol % [Rh(acac)(CO) ₂], 0.4 mol % 37a , 35 °C, 100 atm CO/H ₂ (1/1), 20.0 M in benzene	>99	96/4	87 (R)
2	195b ³⁰	0.05 mol % [Rh(acac)(CO) ₂], 0.2 mol % 37a , 40 °C, 100 atm CO/H ₂ (1/1), 20.0 M in benzene	52	91/9	95 (nd)
3	195c ³⁰	0.05 mol % [Rh(acac)(CO) ₂], 0.2 mol % 37a , 40 °C, 100 atm CO/H ₂ (1/1), 20.0 M in benzene	43	89/11	92 (nd)
4	195d ³⁰	<0.05 mol % [Rh(acac)(CO) ₂], 0.2 mol % 37a , 40 °C, 100 atm CO/H ₂ (1/1), 20.0 M in benzene	8.26 h ^{−1} ^a	95/5	93 (S)
5	195d ^{34b}	PS ^b -[Rh(acac)(49a)], 60 °C, 20 atm CO/H ₂ (1/1), 17.7 M in benzene	351 h ^{−1} ^a	91/9	84 (S)

^a TOF. ^b PS, polymer supported.

Scheme 40. Asymmetric Hydroformylation of the Fluorinated Alkenes 195a–d Catalyzed by a Rhodium Complex of (*R,S*)-BINAPHOS



methyl (*S*)-3-methyl-4-oxopentanoate (**226**) in 68% overall yield. The results of this experiment indicated that the enantiofacial selection for the propene insertion had proceeded with at least 95% ee in favor of the *S* enantiomer (Scheme 45).¹⁴⁰

The mechanistic aspects of this catalytic transformation were thoroughly explored with the aid of theoretical calculations¹⁴⁰ and by employing high-pressure NMR techniques.¹⁴¹ The alternating copolymerization process included two of the most representative reactions in palladium chemistry: CO insertion into a palladium–alkyl bond and alkene insertion into a palladium–acyl bond. The CO insertion was the key step in determining the reactivity of the alternating copolymerization.¹⁴² Mechanistic studies have revealed that propene coordination for palladium attachment to the terminal propene carbon (1,2-insertion) is favored with respect to a 2,1-insertion (Scheme 46 for 1,2-insertion) and occurs at the *cis* position of the phosphino group in the Pd–(*R,S*)-BINAPHOS catalytic species. Contrariwise, the C=O insertion occurs at the *trans* position of the phosphino group (Scheme 46). Remarkably, each of the two possible coordination sites in the catalytically active Pd–(*R,S*)-BINAPHOS complexes are used by the two monomers (CO and propene) for their coordination and subsequent insertion.^{138c} The different *trans*-influences of

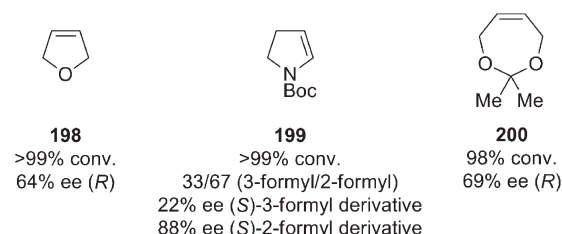
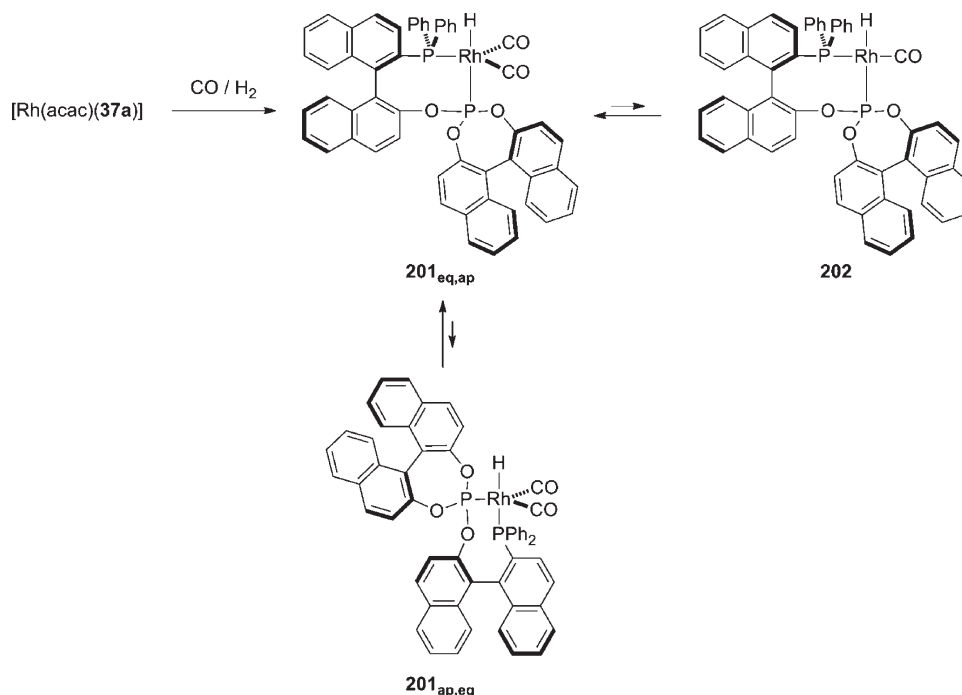


Figure 26. Hydroformylation of Heterocyclic Alkenes.

the phosphino and phosphite groups toward the metal center in Pd–(*R,S*)-BINAPHOS complexes are thus crucial for obtaining high regioselectivity (>99% head-to-tail). Density functional (DFT) and *ab initio* MO calculations provided geometric and energy evidence to corroborate the aforementioned stabilization influence.

In addition to (*R,S*)-BINAPHOS **37a**, Nozaki et al. also prepared the related chiral phosphine–phosphite ligands **37b**, **37h**, **37i**, and **40** (Figure 32), which they assessed in Pd(II) complexes for catalyzing asymmetric alternating copolymerization of propene with CO.²⁶

The chiral cationic Pd(II) complexes of (*R,S*)-BINAPHOS derivatives **37b**, **37h**, **37i**, and **40** were all active, providing completely alternating copolymers (Table 26). (*R,S*)-(3,5-Me₂C₆H₃)₂-BINAPHOS (**37b**) and (*R,S*)-(c-Pen)₂-BINAPHOS (**37h**) (entries 2 and 3 in Table 26, respectively) afforded highly isotactic polyketones analogously to **37a** (entry 1 in Table 26). However, **37i** (entry 4 in Table 26) gave a polyketone with lower regioselectivity. Comparison of the results obtained with **37h** and **37i** suggested that the different steric demands in the phosphino site substantially affect the regioselectivity. Among the BINAPHOS derivatives, (*R,S*)-H₈-BINAPHOS **40** gave the product in the highest yield and with the highest molecular weight (entry 5 in Table 26), revealing that the Pd(II) complex of ligand **40** was a

Scheme 41. Active Species in (*R,S*)-BINAPHOS-Mediated Asymmetric Hydroformylation

more active catalyst than that of (*R,S*)-BINAPHOS 37a for the alternating copolymerization of propene with CO.

Circular dichroism (CD) measurements on the polyketones obtained with palladium complexes derived from ligands 37a, 37b, 37h, 37i, and 40 suggested that the enantiomeric homogeneity of the polymers was essentially equal. The copolymers produced with 37b and 40 were estimated to have almost complete enantiomeric purity, in concordance with the previously determined¹⁴⁰ enantioselectivity of the propene–CO copolymer obtained with 37a (at least 95% ee (*S*)). Interestingly, (*R,S*)-(*c*-Pen)₂-BINAPHOS 37h gave a polyketone whose CD absorption sign was opposite to that of the products obtained with BINAPHOS derivatives containing diarylphosphino groups. Therefore, the enantiofacial selection for propene strongly depended on the structure and the electronic properties of the phosphino site.

In conclusion, small changes of the ligand substituents caused drastic changes in the stereoregularity of the polyketone, revealing that not only the electronic bias of (*R,S*)-BINAPHOS but also its steric demand are essential to produce completely isotactic copolymer from propene and CO with high enantioselectivity.

3.4.2. Alternating Copolymerizations of CO with Higher Aliphatic 1-Alkenes. Asymmetric alternating copolymerization between CO and 1-alkenes with a longer alkyl chain (153b, 153e, and 221a–f) was also studied by Nozaki et al., for which they employed a chiral cationic Pd(II) complex of (*R,S*)-BINAPHOS (37a) as an efficient catalyst (Scheme 47).¹⁴³ Their results are summarized in Table 27.

Completely alternating copolymerization proceeded with 1-hexene 153b (entry 3 in Table 27), dodecene 221b (entry 4 in Table 27), and 1-eicocene 221c (entry 5 in Table 27) with a reaction rate comparable to that of propene 221a (entry 2 in Table 27). The ¹³C NMR spectra of the products indicated almost complete head-to-tail and isotactic selectivities. The molar optical rotation ([Φ]_D) of the copolymers increased with the length of

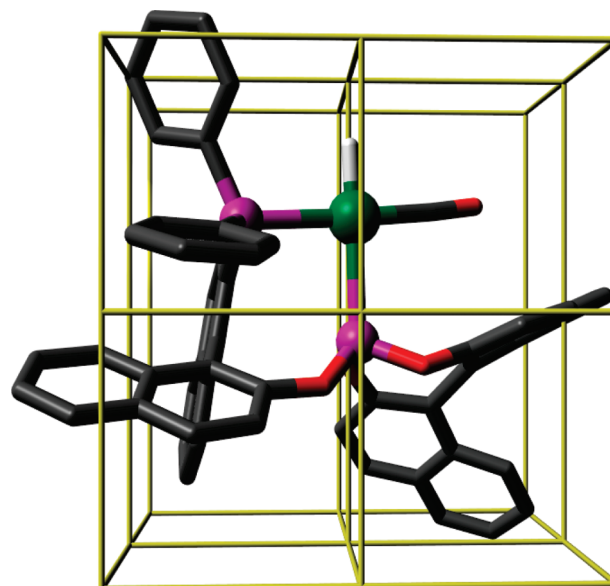


Figure 27. Quadrant diagram for complex 202. (Its structure has been generated with CAChe.)

the alkyl chain. Although completely alternating copolymerization occurred with alkene 153e, which has a large substituent (*tert*-butyl group) attached to the C=C double bond, the reaction rate was much slower (entry 6 in Table 27). The presence of a trimethylsilyl group separated from the C=C double bond by at least two methylene groups (alkenes 221d and 221e in entries 7 and 8, respectively, in Table 27) did not affect the catalyst reactivity in the copolymerization; however, vinylsilane and allylsilane were both inert (data not listed in the table). A trialkoxysilyl substituent, which potentially enabled the attachment of the polymer to silica

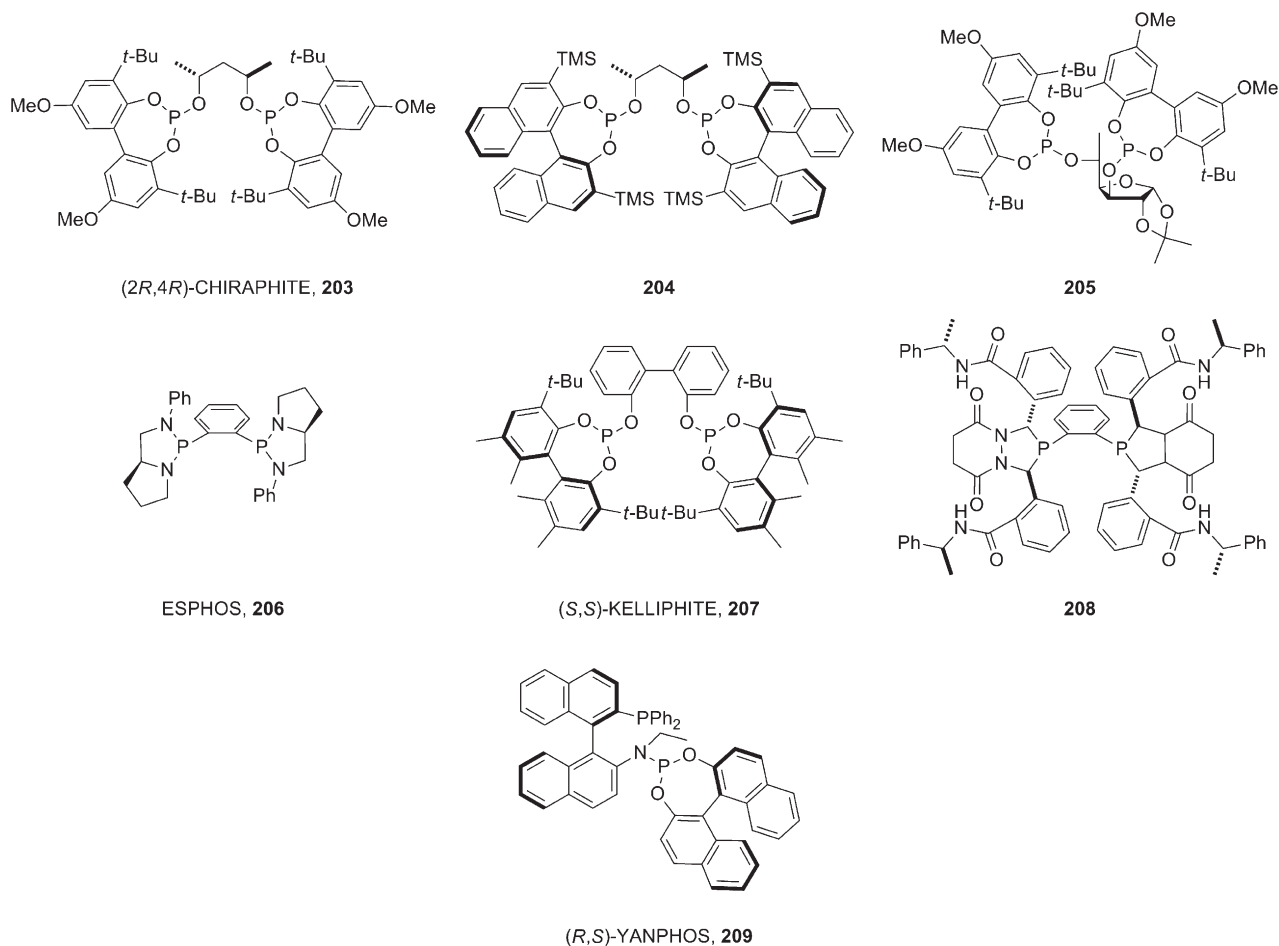
Table 20. Comparison of the Enantioselectivities (% ee) Obtained with the Lead P–OP Ligand 37a to Those Obtained with Ligands 203–209 in Rhodium-Mediated Asymmetric Hydroformylation of Structurally Diverse Olefins

substrate	ligands							
	203	204	205	206	207	208	209	37a
150a	90 (S) ¹¹⁸	86 (S) ¹¹⁹	90 (S) ¹²⁰	<i>rac</i> ¹²¹	18 (R) ¹²²	82 (R) ¹²³	99 (R) ⁹⁹	92 (R) ³⁰
170	50 (S) ¹¹⁸		73 (R) ¹²⁴	90 (S) ¹²¹	88 (S) ¹²²	96 (S) ¹²³	96 (S) ¹²⁵	92 (S) ³⁰
186	15 (R) ¹¹²				78 (S) ¹¹²	87 (R) ¹²³	96 (R) ¹²⁵	75 (S) ¹¹²

Table 21. Comparison of the Regioselectivities (b/l)^a Obtained with the Lead P–OP Ligand 37a to Those Obtained with Ligands 203–209 in Rhodium-Mediated Asymmetric Hydroformylation of Structurally Diverse Olefins

substrate	ligands							
	203	204	205	206	207	208	209	37a
150a	98/2 ¹¹⁸	92/6 ^{119b}	99/1 ¹²⁰	78/22 ¹²¹	98/2 ¹²²	87/13 ¹²³	89/11 ⁹⁹	88/12 ³⁰
170	99/1 ¹¹⁸		99/1 ¹²⁴	94/6 ¹²¹	99/1 ¹²²	97/3 ¹²³	94/6 ¹²⁵	86/14 ³⁰
186	86/14 ¹¹²				94/6 ¹¹²	81/19 ¹²³	80/20 ¹²⁵	74/26 ¹¹²

^ab/l = ratio of branched to linear product. ^bVery small amounts of hydrogenated product (ethyl benzene) were obtained.

**Figure 28.** Structures of representative examples of successful ligands in asymmetric hydroformylation.

gel, was also incorporated into the substrate **221f** (entry 9 in Table 27).

3.4.3. Alternating Copolymerizations of CO with Vinyl Arenes. The first asymmetric alternating copolymerization of CO with a vinyl arene catalyzed by a metal complex of a chiral

P–OP ligand was reported in 1997 by Nozaki et al., who used a cationic palladium complex of (*R*,*S*)-BINAPHOS (**37a**) as catalyst and 4-*tert*-butylstyrene **229a** as substrate¹⁴⁰ (Scheme 48). The corresponding alternating copolymer **230a** was obtained in almost complete isotacticity, with a

molecular weight (M_n) of 5600 and a molar optical rotation ($[\Phi]_D$) of -492 .

The substrate scope of asymmetric alternating copolymerization of CO with vinyl arenes catalyzed by a palladium complex of **37a** was later explored by employing styrene **150a** and different *para*-substituted derivatives (**150b** and **229a–c**) as alkenes¹⁴³ (Scheme 49). As shown in Table 28, alternating copolymers were obtained with styrene **150a** (entry 1 in Table 28), *para*-alkyl-substituted styrenes **150b** and **229a** (entries 2–6 in Table 28), and *para*-chlorostyrene **229b** (entry 7 in Table 28). Styrene **229c**, which contains an electron-donating methoxy group, gave an atactic homopolymer (entry 8 in Table 28). In contrast, the styrenes with an electron-withdrawing substituent (e.g., nitro or trifluoromethyl group) did not react (data not listed in the table).

The regioselectivity of styrene insertion to a palladium–acyl bond in the palladium-mediated alternating copolymerization with CO catalyzed by **37a** was investigated in detail by *ex situ* NMR spectroscopy (under 1 atm of CO) and by computational studies.¹⁴⁴ The authors found evidence supporting 1,2-insertion of styrene into the palladium–acyl bonds for chain propagation and 2,1-insertion for chain termination. Theoretical calculations suggested that the 1,2-insertion stemmed from the steric demand of (*R,S*)-BINAPHOS rather than from electronic demand. This steric requirement apparently increased as the polymer chain grew. Iggo and Nozaki later performed *in situ* high-pressure

NMR studies to reveal the catalytic pathway in the asymmetric copolymerization of styrene and CO catalyzed by a Pd-(*R,S*)-BINAPHOS complex.¹⁴⁵ *In situ* ³¹P NMR spectroscopy enabled direct observation of potential catalytic intermediates under real copolymerization conditions. The formation of Pd–alkyl complexes via 1,2-insertion of styrene into palladium–acyl complexes was confirmed to be the most active catalytic pathway. The 2,1-insertion complexes were found to be inactive to further insertion at high pressure and inert toward β -hydride elimination, although it had been previously proposed that rapid β -hydride elimination from 2,1-complexes occurs at low pressures.¹⁴⁴

In addition to asymmetric alternating copolymerization of CO with propene (see section 3.4.1), monosubstituted alkyl-alkenes (see section 3.4.2), and monosubstituted aryl-alkenes (see section 3.4.3), this transformation has been used to convert suitably modified alkenes into enantiomerically enriched materials with interesting properties (e.g., liquid crystalline polymers,¹⁴⁶ photo-responsive polyketones,¹⁴⁷ and fluorinated polymers¹⁴⁸). Details on the alternating CO copolymerization and on the properties of the resulting materials have already been fully reviewed.^{137a,c,138b,149}

3.4.4. Terpolymerizations of Aliphatic Alkenes, Vinyl Arenes, and CO. Far less effort has been devoted to terpolymer synthesis than to copolymer synthesis; nevertheless, several interesting examples of this asymmetric transformation have been reported. For example, by exploiting the fact that the Pd(II)–(*R,S*)-BINAPHOS catalysts are applicable to both aliphatic 1-alkenes and vinyl arenes, researchers have performed asymmetric terpolymerization of propene (**221a**), 4-*tert*-butylstyrene (**229a**), and CO (Scheme 50).¹⁵⁰ A mixture of **221a** and **229a** was treated with an excess amount of CO in the presence of complex [Pd(Me)(MeCN)(**37a**)] [Ar₄] (Ar = 3,5-bis(trifluoromethyl)phenyl), affording the terpolymer **231**, which encompasses two units: [propene-*alt*-CO] (unit A) and [4-*tert*-butylstyrene-*alt*-CO] (unit B). Units A and B were randomly distributed in the chains: the ratio of A to B varied from 0.8 to 24, depending on the monomer ratio (see Table 29). Prolonging the reaction time, gave a higher total yield of **231**, but the molecular weight remained roughly 8000–10000 (cf. entries 1, 6, 7, and 8 in Table 29). Although the alternating copolymerization of propene–CO with the same catalyst occurred in living mode, the terpolymerization did not. Chain termination was accelerated at higher initial

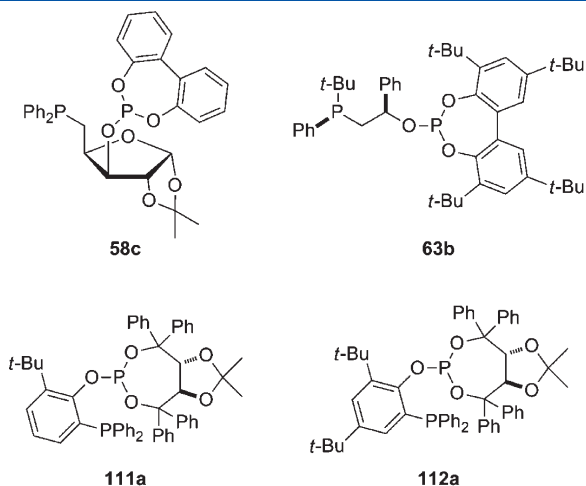
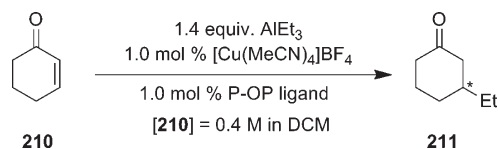


Figure 29. P–OP ligands used for conjugate addition of organometallic species to 2-cyclohexenone.

Scheme 42. Conjugate Addition of AlEt_3 to 2-Cyclohexenone Catalyzed by a Copper Complex of a P–OP Ligand



Scheme 43. Asymmetric Conjugate Addition of an Organo-magnesium Species to 2-Cyclohexenone Catalyzed by Copper Complexes of P–OP Ligands

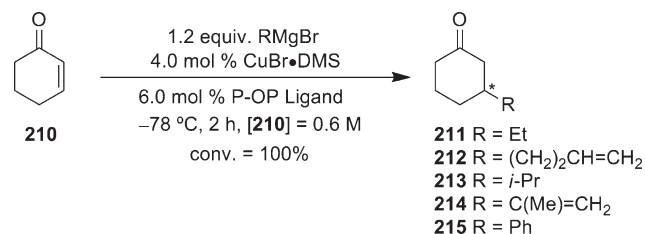


Table 22. Asymmetric Conjugate Addition of AlEt_3 to 2-Cyclohexenone Catalyzed by a Copper Complex of a P–OP Ligand

entry	ligand	<i>T</i> (°C)	TOF ^a	conv. (%) ^b	ratio of 1,4 to 1,2 product	% ee of 211 (config.)
1	63b ¹²⁷	0	1164	100	99/1	59 (S)
2	63b ¹²⁷	–20	1200	100 ^c	98/2	62 (S)
3	58c ¹²⁸	–20	504	42	100/0	12 (R)

^a TOF in mol product · mol Cu^{–1} · h^{–1} determined after 5 min reaction time. ^b Conversion determined after 5 min. ^c Conversion determined after 30 min.

Table 23. Asymmetric Conjugate Addition of Alkyl, Alkenyl, and Aryl Magnesium Reagents to 2-Cyclohexenone Catalyzed by Copper Complexes of P–OP Ligands

entry	ligand	product	solvent	ratio of 1,4 to 1,2 product	yield (%)	% ee of 211–215 (config.)
1	112a ¹²⁹	211	Me-THF	89/11	60	90 (S)
2	112a ¹²⁹	212	Et ₂ O	91/9	71	91 (R)
3	112a ¹²⁹	213	Et ₂ O ^a	98/2	<i>b</i>	67 (R)
4	111a ¹²⁹	213	Et ₂ O ^a	99/1	88	82 (R)
5	111a ¹²⁹	214	Me-THF	91/9	49	92 (R)
6	112a ¹²⁹	215	Me-THF	60/40	<i>b</i>	74 (R)
7	111a ¹²⁹	215	Me-THF	91/9	50	92 (R)

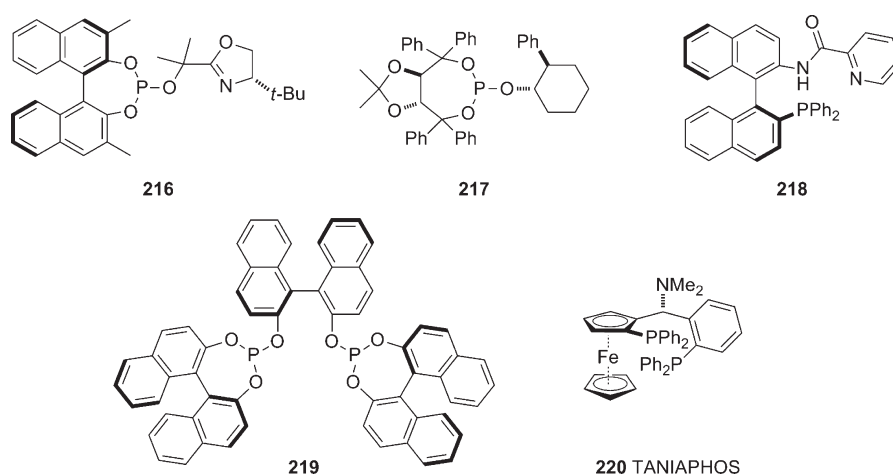
^a A solution of the Grignard reagent in Me-THF was used. ^b Full conversion after 2 h.

Table 24. Comparison of the Enantioselectivities (% ee) Obtained with the Lead P–OP Ligands to Those Obtained with Ligands 216–220 in the Cu-Mediated Asymmetric Conjugate Addition to 2-Cyclohexenone Using Two Different Substituted Organometallic Reagents

products	ligands							
	216	217	218	219	220	58c	63b	112a
211	90 (R) ¹³⁰	96 (S) ¹³¹	91 (S) ¹³²	90 (S) ¹³³	96 (R) ¹³⁴	12 (R) ¹²⁸	62 (S) ¹²⁷	90 (S) ¹²⁹
215					40 (nd) ¹³⁴			74 (R) ¹²⁹

Table 25. Comparison of the Selectivities (Ratio of 1,4 to 1,2 Product) Obtained with the Lead P–OP Ligands to Those Obtained with Ligands 216–220 in the Cu-Mediated Asymmetric Conjugate Addition to 2-Cyclohexenone Using Two Different Substituted Organometallic Reagents

products	ligands							
	216	217	218	219	220	58c	63b	112a
211	100/0 ¹³⁰	100/0 ¹³¹	100/0 ¹³²	100/0 ¹³³	95/5 ¹³⁴	100/0 ¹²⁸	98/2 ¹²⁷	89/11 ¹²⁹
215					50/50 ¹³⁴			60/40 ¹²⁹

**Figure 30.** High performing ligands used for Cu-mediated asymmetric conjugate addition of ethyl-containing organometallic reagents to 2-cyclohexenone.

concentrations of 4-*tert*-butylstyrene relative to propene, leading to lower molecular weights and higher M_w/M_n ratios.

During terpolymerization, the alkenes were incorporated in a head-to-tail and isotactic fashion. The enantioface of each alkene was selected by the catalyst at its incorporation step, regardless of the kind of the preceding alkenes, with similar enantiocontrol to that observed in the copolymerization of propene–CO and of

4-*tert*-butylstyrene–CO.¹⁴⁰ The [4-*tert*-butylstyrene–CO] unit was incorporated into the terpolymer to a much lower degree than the [propene–CO] unit was.

The same authors also tested 1-hexene (153b) as aliphatic 1-alkene monomer, using the same catalyst based on (*R,S*)-BINAPHOS (37a)¹⁵¹ (Scheme 51). Thus, reaction of 1-hexene (153b), 4-*tert*-butylstyrene (229a), and CO afforded the terpolymer

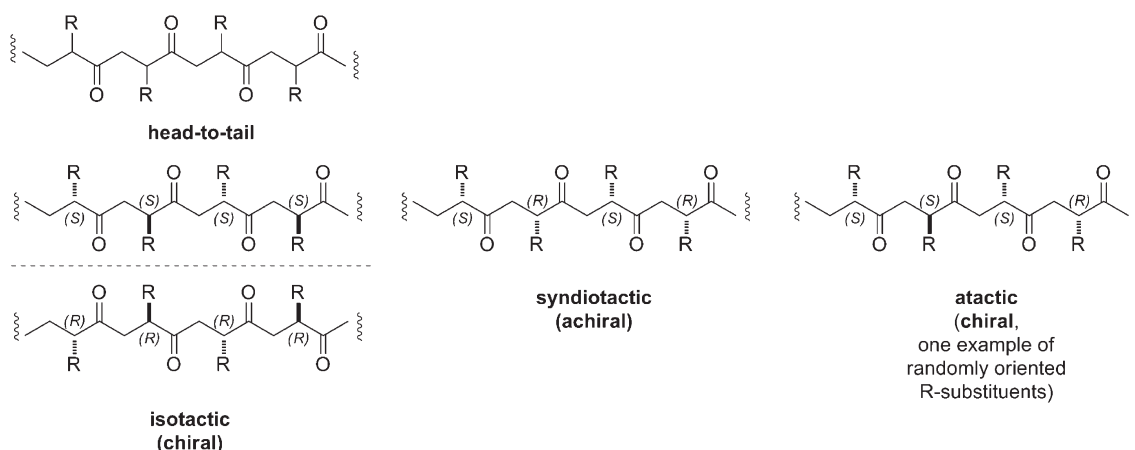
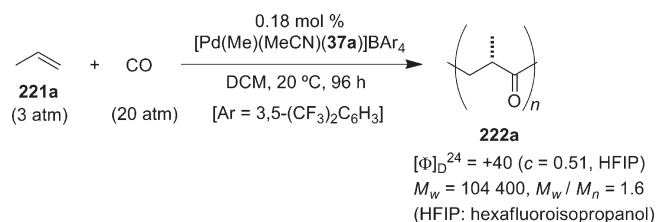


Figure 31. Stereoregularity in alternating CO/alkene copolymers.

Scheme 44. Asymmetric Alternating Copolymerization of Propene with CO Catalyzed by a Pd(II)-(R,S)-BINAPHOS Complex



222, which also comprises two units: [4-*tert*-butylstyrene-*alt*-CO] (unit B) and [1-hexene-*alt*-CO] (unit C). The ratio of C to B was 6.22. Units B and C were also randomly distributed. Based on the measured molar optical rotation ($[\Phi]_D$), the enantioselectivity of each alkene insertion was as high as in the copolymerization of 1-hexene-CO and 4-*tert*-butylstyrene-CO.

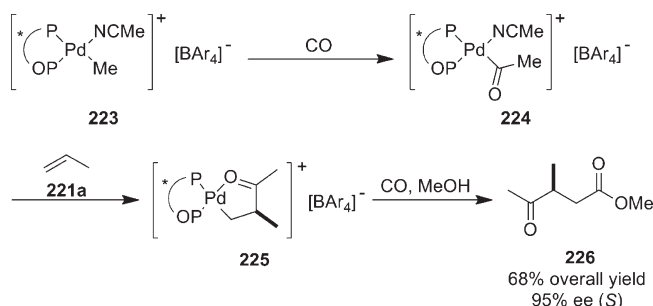
In summary, the terpolymers synthesized using a Pd(II)-(R,S)-BINAPHOS catalyst contained a higher content in 1-alkene than in vinyl arene. Although the rate of the aryl-substituted alkene insertion was higher than for the alkyl-substituted analog,¹⁴⁴ the 4-*tert*-butylstyrene unit was incorporated into the terpolymer to a lower extent. This apparent contradiction may be attributed to a possible deceleration in the insertion of the aryl-substituted alkene into the palladium-acyl bond as the polymer chain grows.

3.5. Palladium-Mediated Allylic Substitutions

Considering that metal-mediated allylic substitutions have been thoroughly investigated for more than four decades and that they have become benchmark reactions for evaluating new chiral ligands,^{5a,152} it is quite surprising that only a few studies concerning the use of P-OP ligands in these transformations have been published. These have focused mainly on the assessment of new chiral ligands in one or two model reactions, namely, the palladium-mediated allylic substitution of racemic 1,3-diphenylallyl acetate 233 with dimethyl malonate (DMM) or benzylamine (BZA) (Scheme 52).^{39b,40,42a,52,53a,c,58c}

Only two palladium complexes derived from phosphine-phosphinite ligands (15a and 15b in Figure 33) have been tested in the allylic alkylation of racemic 1,3-diphenylallyl acetate 233 with DMM (Scheme 52). Although full conversions were achieved, the

Scheme 45. Enantiomeric Excess in the Asymmetric Alternating Copolymerization of Propene with CO Catalyzed by a Pd(II)-(R,S)-BINAPHOS Complex



enantioselectivities were low (16% and 21% ee, respectively; entries 1 and 2 in Table 30). In contrast, far more palladium complexes derived from phosphine-phosphites (see structures in Figure 33) were evaluated, and these provided better results. For the reactions indicated in Scheme 52, moderate to full conversions (from 37% to 100%) were obtained, with a broad range of ee's (from 6% to 83%). By comparison of the catalytic results obtained with these phosphine-phosphite ligands, several conclusions could be drawn. First, it appeared that linking two oxygen atoms of the phosphite moiety with an alkyl chain rather than a biaryl group was detrimental to both activity and enantioselectivity (cf. entries 3 and 4 in Table 30).

For the ligands containing a chiral biarylphosphite fragment, the influence of the biaryl group proved crucial to selectivity. Indeed, the absolute configuration of the biaryl was shown to be more influential than the structure of the ligand backbone in terms of dictating the stereochemical outcome of the reaction and therefore in determining the direction of stereoselection (cf. entries 5 and 6 and 7 and 8 in Table 30). However, in the case of ligands 64a and 64b, the combination of a P-stereogenic phosphine donor and a chiral backbone appeared to be more influential (see entries 9 and 10 in Table 30 and Figure 33 for the ligand structures). Thus, significant matched/mismatched effects were observed. Additionally, upon evaluating structural variations in ligands 62–64 (see Figure 8 in section 2.1.2 for the ligand structures), van Leeuwen et al. deduced that a substituent at the backbone of the ligands controls the configuration of the biaryl moiety when the latter is capable of interconverting but

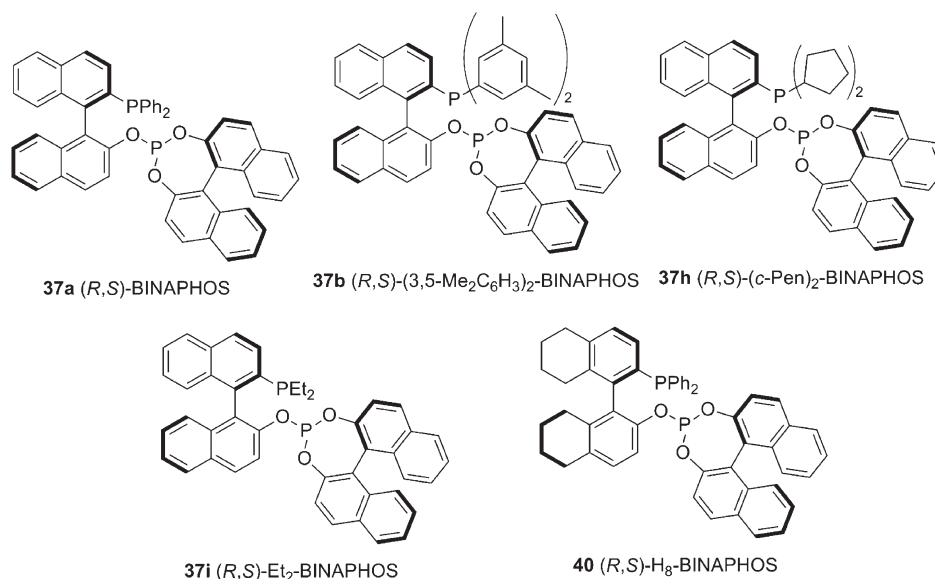
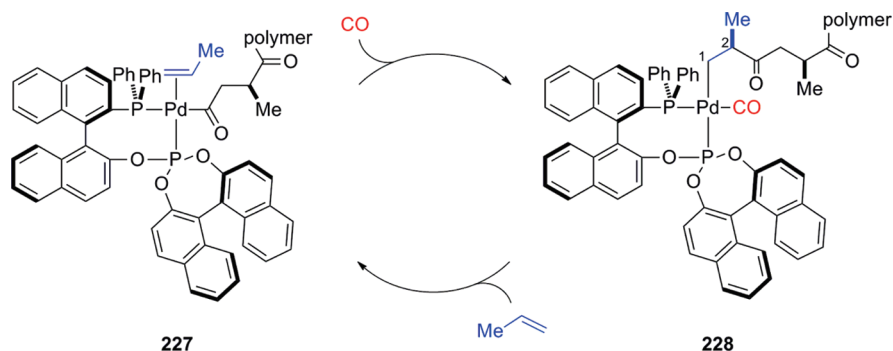


Figure 32. (*R,S*)-BINAPHOS and derivatives used in palladium complexes for catalyzing asymmetric alternating copolymerization of propene with CO.

Scheme 46. Alternating Copolymerization of CO with Propene



also affects the position of the phosphite moiety with respect to the Pd center.^{39b}

The stereochemical outcome of palladium-mediated allylic substitutions is known to depend on many parameters apart from the absolute and relative configurations of the different stereogenic elements of the ligand.¹⁵² For a polydentate ligand, these may include the relative strengths of the *trans* influences of its different binding groups, as well as the size of its chelate or width of its bite angle,¹⁵³ all of which may interplay. Faraone et al. performed two-dimensional NMR experiments on Pd(η^3 -PhCHCHCHPh) complexes of ligands **70a** and **70b**, which contain a single carbon atom in the chain that tethers the phosphine to the phosphite.^{42a} They observed a NOE correlation between one phenyl group of the allyl moiety and a trimethylsilyl substituent of ligand **70b** but did not find a similar interaction for **70a** (Scheme 53). Hence, for nucleophilic attack, they expected a transition state of higher activation energy for **70b** than for **70a**. Since the enantiomeric excesses obtained with the two ligands were not significantly different, they concluded that dimethyl malonate preferentially attacked *trans* to the phosphite (i.e., away from the trimethylsilyl groups). Van Leeuwen et al. observed that the ligands **62a**, **62b**, **62e**, and **62g**, which have in common a stereogenic carbon of

Table 26. Asymmetric Alternating Copolymerization of Propene with CO Catalyzed by Pd(II)–Phosphine–Phosphite Complexes

entry	ligand	time (h)	yield (%)	tacticity	M_n	M_w/M_n
1	37a ²⁶	6	15	isotactic	16 400	1.07
2	37b ²⁶	6	11	isotactic	13 700	1.07
3	37h ²⁶	6	20	isotactic	15 900	1.24
4	37i ²⁶	24	7	atactic ^a	1 300	1.04
5	40 ²⁶	6	29	isotactic	26 600	1.07

^a Regioirregular and atactic polyketone was obtained.

identical configuration, all gave the final product with the same absolute configuration, regardless of the nature of the phosphine substituents and their arrangement around the phosphorus. Thus, they inferred that the nucleophile attacks the allylpalladium complex *trans* to the phosphine (Scheme 53).^{39b}

The electronic distinction between the coordinating groups of a bidentate ligand is often invoked to rationalize the stereochemical outcome of an allylic substitution reaction: regioselective attack occurs *trans* to the donor having the stronger *trans* influence.

Nevertheless, the aforementioned examples suggest that, despite the nearly identical electronic properties of the ligands, the nucleophilic attack is influenced by the length of the carbon tether between the phosphine phosphorus and the closest oxygen of the phosphite (one carbon in **70a** and **70b** and three carbons in **62a**, **62b**, **62e**, and **62g**). Thus, the chelate size seems to overpower the apparently weak difference between the *trans* influences of the phosphino and phosphite moieties.

The relative *trans* influences of the two phosphorus functionalities were further studied by Vidal-Ferran et al. who synthesized the ligands **66b–d**, whose phosphino groups possess variable electronic richness (see Table 30 for results on catalysis and Figure 33 for the ligand structures).⁴⁰ Since phosphines are better σ -donors and worst π -acceptors than phosphites,¹⁵⁴ an enhancement in differentiation between the *trans* influences of the two coordinating groups and, therefore, an increase in stereoselectivity were anticipated in the order CF₃, H, and OMe (Table 31). This expected trend was indeed observed, with enantiomeric excesses of 64%, 80%, and 80% for the *p*-CF₃, *p*-H, and *p*-MeO substituted phosphino groups, respectively, in the allylic alkylation of **233** with dimethyl malonate (see entries 1, 2, and 3 in Table 31 for results on catalysis and Figure 33 for the ligand structures), and 46%, 61%, and 81% ee, respectively, in the allylic amination of **233** with benzylamine for the same ligand series (entries 4, 5, and 6 in Table 31).

To gain further insight into the bases of the stereodirecting mechanisms, Vidal-Ferran et al. performed ground-state calculations on $[\text{Pd}(\eta^3\text{-PhCHCHCHPh})(\mathbf{66b})]^+$ (complex **235**), which may exist in solution as the following six most probable diastereoisomers: *endo-anti-syn*, *endo-syn-anti*, *endo-syn-syn*, *exo-anti-syn*, *exo-syn-anti*, and *exo-syn-syn*.¹⁵⁵ Calculations

Scheme 47. Alternating Copolymerization of Higher Aliphatic 1-Alkenes with CO Catalyzed by a Pd(II)-(R,S)-BINAPHOS Complex

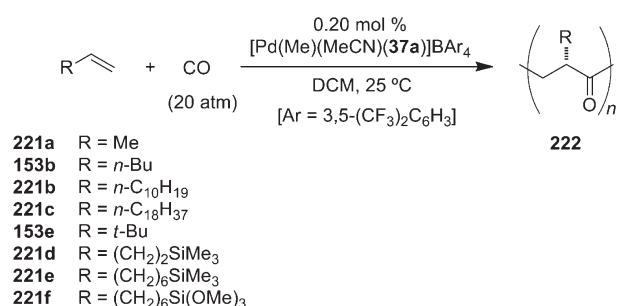
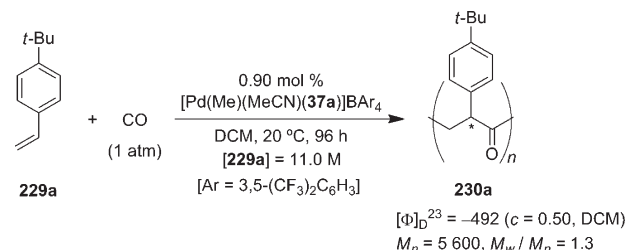


Table 27. Alternating Copolymerization of Higher Aliphatic 1-Alkenes with CO Catalyzed by a Pd(II)-(R,S)-BINAPHOS Complex

entry	substrate	[substrate] (M)	time (h)	g of polymer/mol of Pd	M_n (M_w/M_n)	$[\Phi]_D^a$
1	221a ¹⁴³	1.2 (3 atm)	24	12 600	43 000 (1.1)	−43.99
2	221a ¹⁴³	2.5	24 ^b	23 300	20 000 (1.7)	−43.91
3	153b ¹⁴³	2.5	24 ^b	44 100	15 000 (1.8)	−45.95
4	221b ¹⁴³	2.5	24 ^b	59 600	14 000 (2.0)	−63.49
5	221c ¹⁴³	2.5	24 ^b	40 900	16 000 (1.8)	−73.22
6	153e ¹⁴³	1.7	120	2 500	6 900 (1.3)	−40.02
7	221d ¹⁴³	1.8	24	8 900	nd ^c	nd ^c
8	221e ¹⁴³	2.5	24	38 900	11 000 (1.6)	−89.51
9	221f ¹⁴³	1.1	18	13 400	35 000 (1.5)	nd ^d

^a Measured at $c = 0.49$ to 0.51 in CHCl₃ at 26.8 °C. ^b At 40 °C. ^c No polymeric material was obtained. ^d Not determined due to the poor solubility of the polymer obtained. Formation of the polyketone was confirmed by IR. An inorganic polymer was gradually formed.

Scheme 48. Asymmetric Alternating Copolymerization of 4-*tert*-Butylstyrene with CO Catalyzed by a Pd(II)-(R,S)-BINAPHOS Complex



Scheme 49. Alternating Copolymerization of Styrene and Its Derivatives with CO Catalyzed by a Pd(II)-(R,S)-BINAPHOS Complex

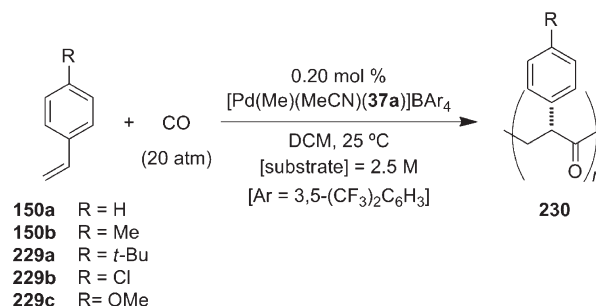


Table 28. Alternating Copolymerization of Styrene and Its Derivatives with CO Catalyzed by a Pd(II)-(R,S)-BINAPHOS Complex

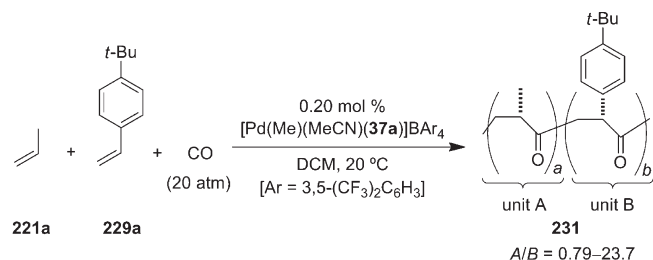
entry	substrate	time (h)	g of polymer/mol of Pd	M_n (M_w/M_n)	$[\Phi]_D^a$
1	150a ¹⁴³	24	5 940	3 900 (1.8)	−451.54
2	150b ¹⁴³	24	7 440	4 200 (1.8)	−318.35
3	229a ¹⁴³	3	2 870	4 900 (1.3)	−373.64
4	229a ¹⁴³	6	2 010	4 500 (1.4)	−418.24
5	229a ¹⁴³	12	3 450	3 200 (1.8)	−432.02
6	229a ¹⁴³	24	5 580	3 900 (1.5)	−446.75
7	229b ¹⁴³	24	2 050	3 100 (1.5)	−403.56 ^b
8	229c ¹⁴³	24	^c	^c	^c

^a Measured at $c = 0.30$ – 0.50 in CHCl₃ at 25 to 27 °C, unless otherwise stated. ^b Measured at $c = 0.045$ due to a low solubility of the polymer. ^c An atactic homopolymer was obtained.

revealed that an analysis of the stereochemical outcome of the reaction based merely on the differentiation of the allyl unit due to the *trans* influences of the phosphino and phosphite groups failed to provide a full understanding of the stereochemical outcome. Moreover, this work showed that the orientation of the allyl moiety relative to the P–Pd–PO coordination plane may be more influential than the electronic effects in terms of the stereodiscriminating mechanisms. When two vicinal allylic carbons tend to be aligned with that plane in the starting palladium–allyl complex, nucleophilic attack takes place preferably at the allylic terminus, which is furthest out of the plane (carbons marked pro-(*R*) in **235-endo-syn-syn and pro-(*S*) in **235-endo-anti-syn** in Figure 34).⁴⁰ Thus, a subtle interplay between electronic and steric effects in the $[\text{Pd}(\eta^3\text{-PhCHCHCHPh})(\mathbf{66b})]^+$ complexes appears to be determinant for stereochemical induction.**

As summarized in section 2.3, Reek, van Leeuwen, et al. employed noncovalent interactions to prepare supramolecular

Scheme 50. Terpolymerization of Propene, 4-*tert*-Butylstyrene, and CO Catalyzed by a Pd(II)-(*R,S*)-BINAPHOS Complex



phosphine–phosphite ligands (Figure 35), which they tested in asymmetric palladium-mediated allylic substitutions.^{52,53a} The most representative catalysis results are summarized in Table 32. The importance of the bridge length between the phosphino and phosphite fragments was also demonstrated in this case: minor variations in the chelate size led to different results in terms of the enantiomeric excess and the sense of enantioinduction (Table 32, Scheme 54).

For instance, whereas palladium complex derived from **124b,u**, which contains a *meta*-diphenylphosphinopyridine unit, gave 47% ee, its isomer **124c,u**, whose phosphino group is in the *para* position and, therefore, whose bridge between the phosphino and phosphite moieties is longer, gave no enantioinduction (entries 1 and 2 in Table 32). In contrast, the presence of an additional carbon atom between the phosphino group and the pyridine ring in **124e,u** completely reversed the enantioselectivity (compare entries 1 and 3 in Table 32). The position of the phosphite was also important: when the phosphite was in the *meta*- rather than the *ortho*-position of the aryl-substituted porphyrin ring, a reversal and an increase in enantiomeric excess was observed (ligands **124b,u** and **124b,w**, entries 1 and 4 in Table 32, respectively). Running the

Scheme 52. Palladium-Mediated Allylic Substitution of Racemic 1,3-Diphenylallyl Acetate in the Presence of P–OP Ligands

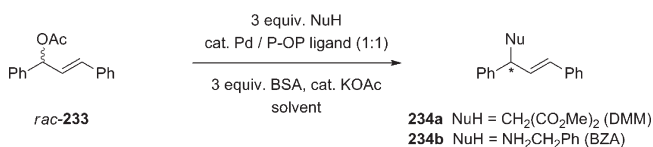
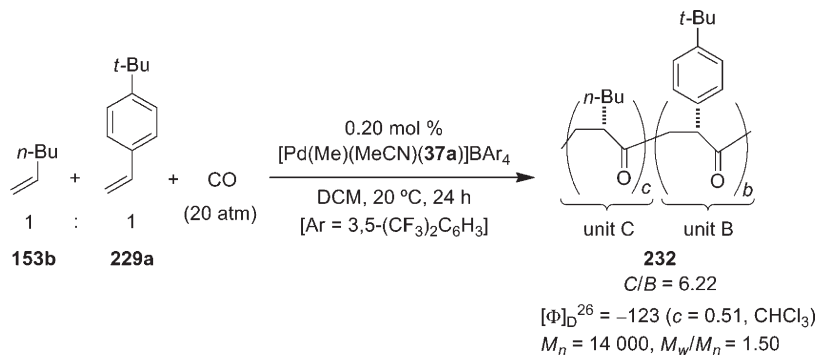


Table 29. Terpolymerization of Propene, 4-*tert*-Butylstyrene, and CO Catalyzed by a Pd(II)-(*R,S*)-BINAPHOS Complex

entry	221a (atm)	229a (M)	time (h)	ratio of A to B	yield (%)		M_n (M_w/M_n)	$[\alpha]_D^a$	$[\Phi]_D^b$
					221a	229a			
1	1	1.02^{150}	24	1.85	31.4	5.6	8 100 (1.5)	−220	−249
2	3	1.02^{150}	24	11.0	31.0	3.1	28 000 (1.2)	−125	−115
3	6	1.02^{150}	24	23.7	23.3	2.0	30 200 (1.3)	−98	−81
4	1	0.51^{150}	24	3.38	34.2	6.7	14 800 (1.3)	−191	−198
5	1	2.04^{150}	24	0.79	16.0	3.4	8 500 (1.4)	−206	−283
6	1	1.02^{150}	3	1.67	7.5	1.5	8 400 (1.2)	−200	−239
7	1	1.02^{150}	6	1.47	11.6	2.6	9 400 (1.3)	−201	−246
8	1	1.02^{150}	12	1.50	15.1	3.4	10 500 (1.3)	−220	−269

^a Measured at $c = 0.49\text{--}0.57$ in CHCl_3 at $25.6\text{--}26.8$ °C. ^b $[\Phi]_D = [\alpha]_D \cdot M/100$, where M is the average molecular weight per unit.

Scheme 51. Terpolymerization of 1-Hexene, 4-*tert*-Butylstyrene, and CO Catalyzed by a Pd(II)-(*R,S*)-BINAPHOS Complex



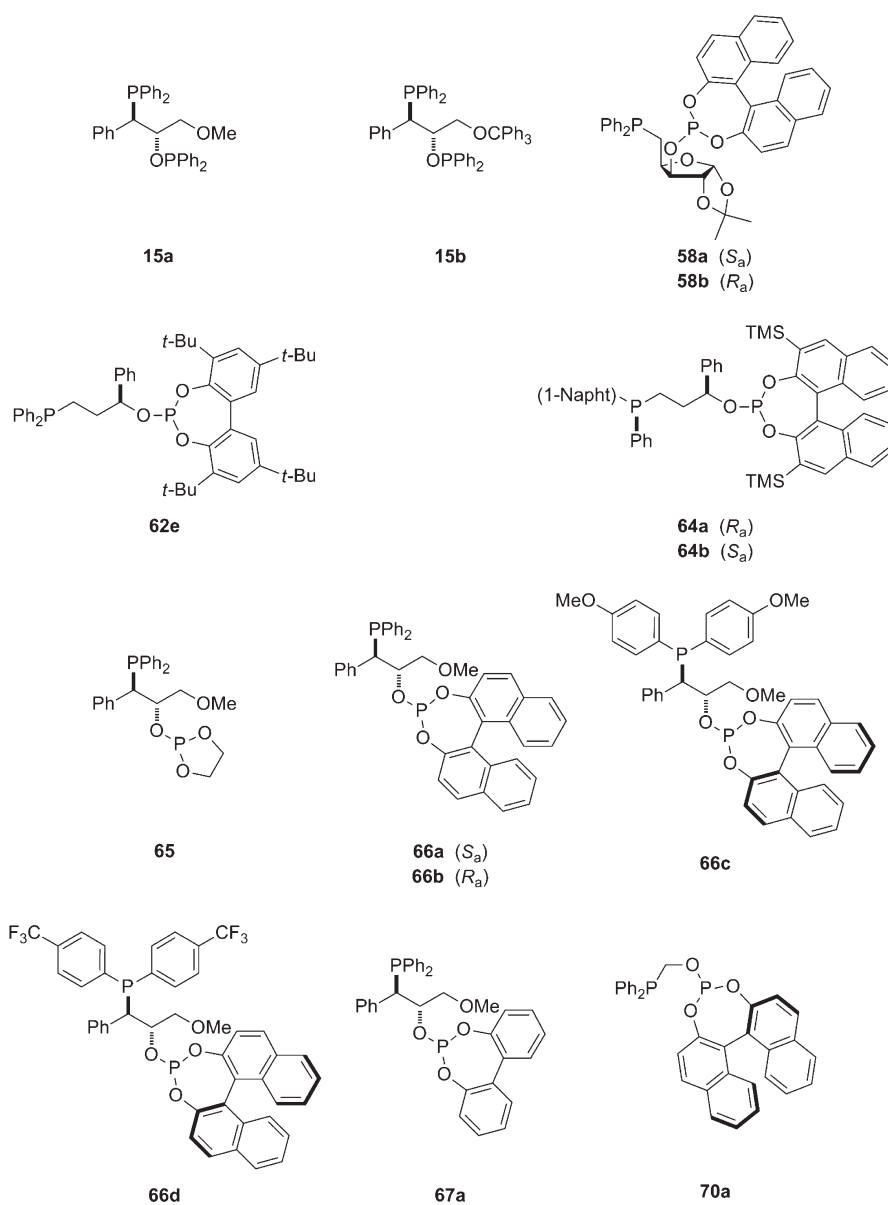


Figure 33. Selected P–OP ligands tested in palladium-mediated allylic substitution of 1,3-diphenylallyl acetate.

Table 30. Palladium-Mediated Allylic Substitution of Racemic 1,3-Diphenylallyl Acetate with Dimethyl Malonate in the Presence of P–OP Ligands

entry	ligand	reaction conditions	conv. (%)	% ee of 234a (config.)
1	15a ⁴⁰	2.5 mol % catalyst, 0.2 M in DCM, rt, 2.5 h	>95	16 (<i>R</i>)
2	15b ⁴⁰	2.5 mol % catalyst, 0.2 M in DCM, rt, 2.5 h	>95	21 (<i>R</i>)
3	65 ⁴⁰	2.5 mol % catalyst, 0.2 M in DCM, rt, 24 h	37	14 (<i>R</i>)
4	67a ⁴⁰	2.5 mol % catalyst, 0.2 M in DCM, rt, 5 h	>95	40 (<i>R</i>)
5	58a ^{58c}	1 mol % catalyst, 0.4 M in DCM, rt, 22 h	100	20 (<i>S</i>)
6	58b ^{58c}	1 mol % catalyst, 0.4 M in DCM, rt, 22 h	100	6 (<i>R</i>)
7	66a ⁴⁰	2.5 mol % catalyst, 0.2 M in DCM, rt, 24 h	56	56 (<i>S</i>)
8	66b ⁴⁰	2.5 mol % catalyst, 0.2 M in DCM, rt, 1 h	>95	80 (<i>R</i>)
9	64a ^{39b}	1 mol % catalyst, 0.4 M in DCM, rt, 1.25 h	61	21 (<i>S</i>)
10	64b ^{39b}	1 mol % catalyst, 0.4 M in DCM, rt, 1.25 h	74	79 (<i>S</i>)

reactions at $-20\text{ }^{\circ}\text{C}$ instead of room temperature gave higher enantiomeric excesses (entries 5–7 in Table 32).

Reek, van Leeuwen, et al. obtained remarkable results when applying their library of *SUPRAPHos* ligands to allylic

Scheme 53. Influence of Chelate Size on the Regioselectivity of the Nucleophilic Attack in Allylic Substitutions Catalyzed by Palladium Complexes of P–OP Ligands

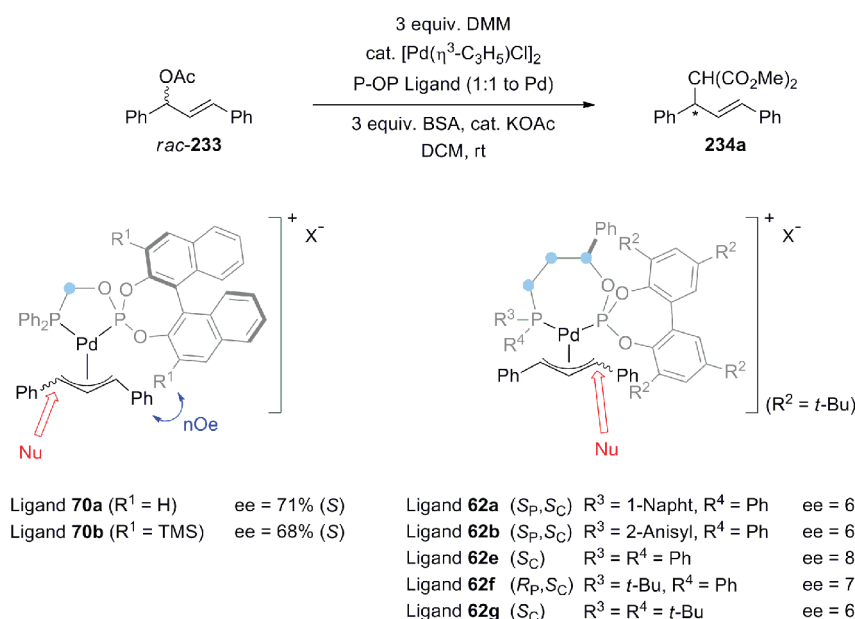


Table 31. Effect of Varying the *para* Substituent in Ligands 66b–d on the Enantioselectivity of the Reaction

entry	ligand	NuH	reaction conditions	conv. (%)	% ee of 234 (config.)
1	66d ⁴⁰	CH ₂ (COOMe) ₂	2.5 mol % catalyst, 0.2 M in DCM, rt, 1 h	>95	64 (R)
2	66b ⁴⁰	CH ₂ (COOMe) ₂	2.5 mol % catalyst, 0.2 M in DCM, rt, 1 h	>95	80 (R)
3	66c ⁴⁰	CH ₂ (COOMe) ₂	2.5 mol % catalyst, 0.2 M in DCM, rt, 1 h	>95	80 (R)
4	66d ⁴⁰	PhCH ₂ NH ₂	2.5 mol % catalyst, 0.2 M in DCM, rt, 24 h	3	46 (S)
5	66b ⁴⁰	PhCH ₂ NH ₂	2.5 mol % catalyst, 0.2 M in DCM, rt, 72 h	3	61 (S)
6	66c ⁴⁰	PhCH ₂ NH ₂	2.5 mol % catalyst, 0.2 M in DCM, rt, 24 h	9	81 (S)

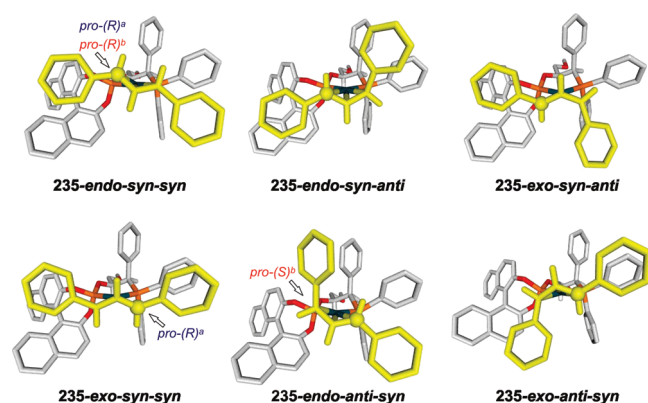


Figure 34. Calculated geometries for the diastereomeric Pd(η^3 -PhCHCHCHPh) complexes derived from ligand 66b. Positions in the allyl units, the nucleophile attack of which is favored due to bond elongation, are marked with a yellow sphere. ^aAttack at the *trans* influence-favored C_{allyl} leads to (R)-234a with DMM. ^bAttacks with DMM at the C_{allyl} that are furthest out of the plane lead to (R)- or (S)-234a as indicated.

substitution-mediated kinetic resolution.^{53c} They studied the resolution of racemic cyclohexenyl acetate (236) in the presence of malonate nucleophiles, evaluating 28 supramolecular P–OP ligands 124 in the reaction with dimethyl malonate (Scheme 55).

Most of the ligands gave modest results, except for those with *ortho*-pyridyl-functionalized phosphino moieties, which yielded highly enantioenriched (99% ee) (S)-cyclohexenyl acetate 236 plus the substituted product (R)-237 (from 12% ee to 32% ee) in conversions from 69% to 84% (Table 33). The authors attributed these notable results to the supramolecular nature of the ligand: they envisioned that decoordination of the phosphine–pyridine from zinc during certain stages of the catalytic cycle would enable changes in the palladium coordination sphere.

In conclusion, rather few studies on palladium-mediated allylic substitutions using P–OP ligands have been published. Clearly, even the best of the P–OP ligands tested to date, which gave a maximum enantiomeric excess of 83% in the allylic alkylation of racemic 1,3-diphenylallyl acetate with dimethyl malonate,^{39b} did not perform as well as myriad other ligands in this reaction.¹⁵² A biaryl group (either a configurationally stable biaryl fragment or an achiral one, whose configuration is determined by a proximal stereocenter) has proven to be a better stereogenic relay than the centrochiral aliphatic backbones of P–OP ligands in terms of affording high enantioselectivities (compare the results of Faraone et al., van Leeuwen et al., Claver et al., and Vidal-Ferran et al.).^{39b,40,42a,52,53a,53c,58c} Hence, the aforementioned backbone structures have not yet been optimized for this transformation. Notably, such an optimization seems critical, insofar as the influence on enantioselectivity of the electronic differentiation

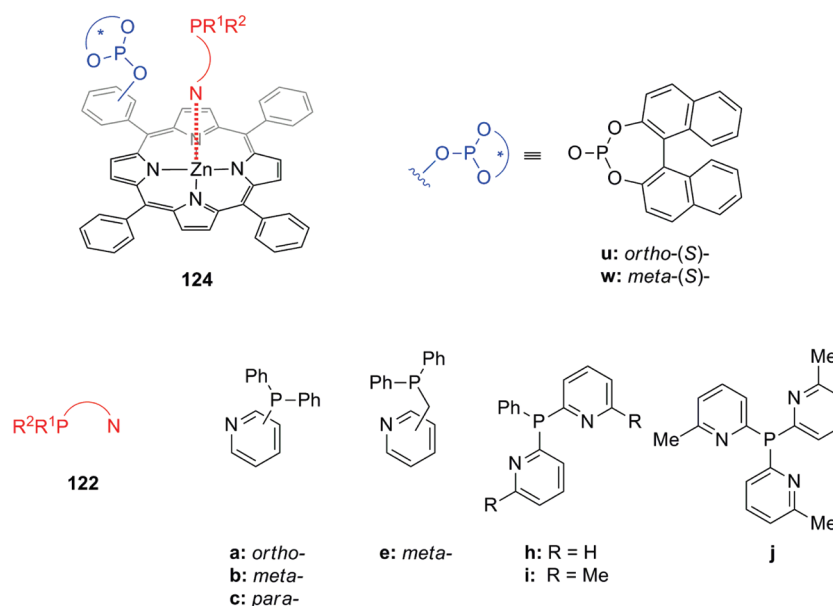
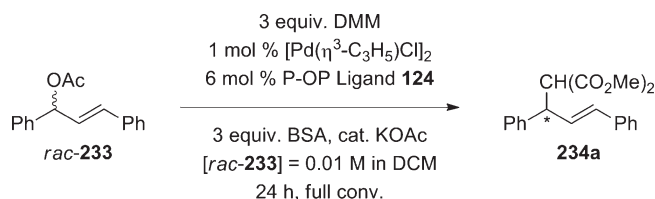


Figure 35. The most representative supramolecular phosphine-phosphite ligands tested in palladium-mediated allylic substitutions.

Table 32. Influence of the Bridge Length between the Phosphine and Phosphite Moieties of SUPRAPHos Ligands on the Stereochemical Outcome of the Reaction

entry	ligand	T (°C)	% ee of 234a (config.)
1	124b,u ⁵²	25	47 (R)
2	124c,u ⁵²	25	rac
3	124e,u ⁵²	25	40 (S)
4	124b,w ⁵²	25	59 (S)
5	124b,u ^{53a}	−20	60 (R)
6	124e,u ^{53a}	−20	44 (S)
7	124b,w ^{53a}	−20	70 (S)

Scheme 54. Influence of the Bridge Length between the Phosphine and Phosphite Moieties of SUPRAPHos Ligands on the Stereochemical Outcome of the Reaction



between the phosphino and phosphite coordinating groups appears rather unpredictable in comparison with other, more successful chiral bidentate nonsymmetrical ligands (e.g., phosphino-oxazolines or phosphito-oxazolines). The nonsymmetrical nature of P-OP remains underexplored in Pd-mediated allylic substitutions: the two distinct donor groups of the ligand could be of great advantage in the reaction of nonsymmetrical allyl moieties, which still remains to be studied. Nonetheless, supramolecular P-OP ligands have exhibited intriguing behavior in allylic alkylation-induced kinetic resolution and deserve further attention in this context.

3.5.1. Comparative Table in Allylic Substitutions. The use of chiral P-OP ligands in palladium-mediated asymmetric

Scheme 55. Palladium-Mediated Kinetic Resolution of *rac*-Cyclohexenyl Acetate Using SUPRAPHos Ligands

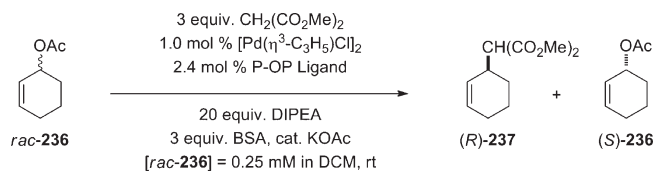


Table 33. Palladium-Mediated Kinetic Resolution of Racemic Cyclohexenyl Acetate Using SUPRAPHos Ligands

entry	ligand	conv. into 237 (%)	t (h)	% ee of <i>(R)</i> - 237	% ee of <i>(S)</i> - 236	s ^a
1	124a,u ^{53c}	81	0.6	13	99	6.4
2	124h,u ^{53c}	69	0.5	32	99	11.9
3	124i,u ^{53c}	81	0.5	17	99	6.4
4	124j,u ^{53c}	84	0.5	12	99	5.6

^a Selectivity factor (s) calculated according to Kagan et al. first-order model.¹⁵⁶

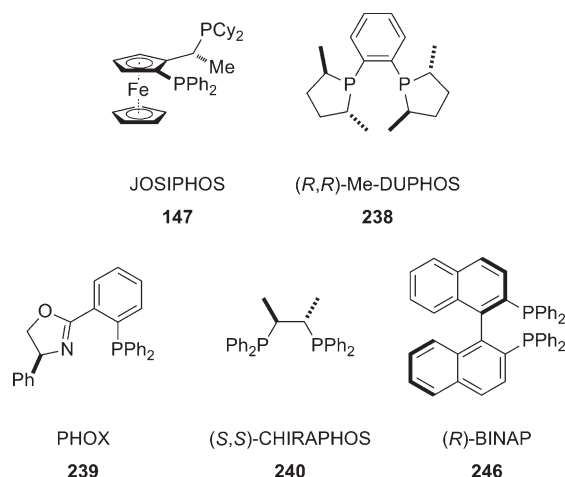
allylic substitution is not very extended, and Table 34 provides comparison of the catalytic activity between the best performing P-OP ligands and several other lead ligands (Figure 36) in the palladium-mediated asymmetric allylic substitution on racemic 1,3-diphenylallyl acetate **233** with C- and N-nucleophiles.¹⁵⁷ This transformation is a clear example in which the P-OP ligands do not fulfill the steric and electronic requirements around the palladium center to achieve the same level of enantioselectivity that many structurally different lead ligands in this transformation¹⁵² give.

3.6. Rhodium-Mediated Hydroborations of Alkenes

Hydroboration of alkenes is a very appealing transformation to synthetic chemists owing to the versatility of alkylboron compounds, which can be converted into alcohols or amines, or be used as partners in Suzuki-Miyaura-Heck coupling reactions. Enantioselective metal-mediated hydroborations of olefins have

Table 34. Comparison of the Enantioselectivities (% ee) Obtained with the P–OP Ligands to Those Obtained with Selected Ligands in Palladium-Mediated Asymmetric Allylic Substitutions of 1,3-Diphenylallyl Acetate

products	ligands									
	147	246	238	239	240	58d	62e	66c	70a	124b,w
234a	93 (S) ⁸¹	99 (S) ¹⁵⁸	97 (S) ¹⁵⁹	99 (S) ¹⁶⁰	90 (R) ¹⁶¹	42 (S) ^{58c}	83 (S) ^{39b}	80 (R) ⁴⁰	71 (S) ^{42a}	59 (S) ⁵²
234b		93 (R) ¹⁶²				66 (R) ^{58c}		81 (S) ⁴⁰		

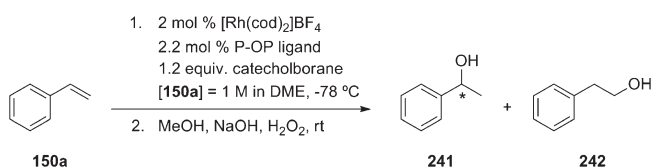
**Figure 36.** Milestone ligands for palladium-mediated asymmetric allylic substitutions of racemic 1,3-diphenylallyl acetate.

garnered particular interest, because they give the products under milder conditions and with different chemo-, regio-, and stereo-selectivities than in non-metal-mediated processes.¹⁶³ Rhodium as metal catalyst provides excellent enantioselectivities in the hydroboration of styrene derivatives in the presence of commercially available ligands such as BINAP and QUINAP or their analogs.^{163b}

Schmalz et al. have tested several enantiopure phosphine–phosphite ligands in this asymmetric transformation. They employed a modular synthetic approach to prepare a vast library of enantioenriched ligands, in which the chirality was provided solely by the phosphite moiety (see Figure 14, section 2.2).^{50b,c,164} They then assessed 12 of these ligands in a model reaction: the rhodium-mediated hydroboration of styrene **150a** with catecholborane (Scheme 56) followed by oxidation to the corresponding alcohol(s) (see Table 35 for the results obtained with selected P–OP ligands and Figure 37 for the ligand structures).^{50b}

The enantiomeric excesses attained using rhodium complexes derived from ligands with a nonbiaryl chiral moiety were much higher for this reaction than in other asymmetric transformations (compare the TADDOL-derived ligands **100a** and **100b** in entries 1 and 2 with the BINOL-derived ligands **100d** and **100e** in entries 3 and 4, Table 35). Very good enantioselectivity (91% ee) and regioselectivity (95/5) were achieved using ligand **103a**, albeit with a nonoptimal yield (63%) (entry 6 in Table 35). This high level of enantioselectivity is almost competitive with the levels reached using either BINAP (from 93% to 96% ee)¹⁶⁵ or Togni's planar chiral phosphine–pyrazoline ligand (>98% ee).¹⁶⁶

In addition to the model hydroboration of styrene, Schmalz et al. employed one of their P–OP ligands (ligand **107a**) to prepare an anti-infective agent, which was also used as a precursor for the total synthesis of marine diterpenes.¹⁶⁴ In fact, ligand **107a** performed better than the traditionally used BINAP

Scheme 56. Rhodium-Mediated Hydroboration of Styrene in the Presence of P–OP Ligands Developed by Schmalz et al.**Table 35.** Rhodium-Mediated Hydroboration of Styrene in the Presence of P–OP Ligands Developed by Schmalz et al.

entry	ligand	time (h)	ratio of 241 to 242	% yield of 241	% ee of 241 (config.)
1	100a ^{50b}	2.5	95/5	81	77 (R)
2	100b ^{50b}	2.5	94/6	24	87 (R)
3	100d ^{50b}	2.5	95/5	80	13 (R)
4	100e ^{50b}	2.5	89/11	75	17 (S)
5	101b ^{50b}	2.5	95/5	25	38 (S)
6	103a ^{50b}	3.5	95/5	63	91 (R)

in the hydroboration of the synthetic intermediate **243**, furnishing the borylated product **244** in 80% yield and with the rather high enantiomeric excess of 93% (Scheme 57). Compound **244** was then converted to the desired precursor **245** after double homologation, Suzuki–Miyaura–Heck coupling, and cyclization.

In conclusion, although prediction of the stereochemical outcome of the reaction in function of ligand structure remains difficult, the modular nature of phosphine–phosphites has proven invaluable for identifying efficient catalyst structures, enabling very good results for cases in which classical ligands fail.

3.6.1. Comparative Table in Hydroborations. The contribution of chiral P–OP ligands in rhodium-mediated hydroboration of alkenes is also scarce. Nevertheless, Table 36 shows that the highest performing rhodium complex derived from P–OP ligand **103a** in the hydroboration of styrene **150a** afforded similar levels of enantio- and regioselectivity to the ones attained with several other lead ligands (structures **246**–**248** in Figure 38).

3.7. Palladium-Mediated Hydrophosphorylations of Vinyl Arenes

Following the pioneering examples of palladium-mediated hydrophosphorylation of alkenes by Tanaka et al.,¹⁶⁸ the groups of Beletskaya and Leitner jointly reported on the first asymmetric version of this reaction.^{23a} They screened several known mono- and bidentate ligands, including Pringle's phosphine–phosphite **38** (see Figure 39 for the ligand structure) in the hydrophosphorylation of styrene **150a**, identifying (R,S)-BINAPHOS (**37a**) as the best (Scheme 58). At 70 °C, the products were obtained with full conversion, a branched to linear ratio of 93/7, and an enantiomeric excess for the branched product of 56%

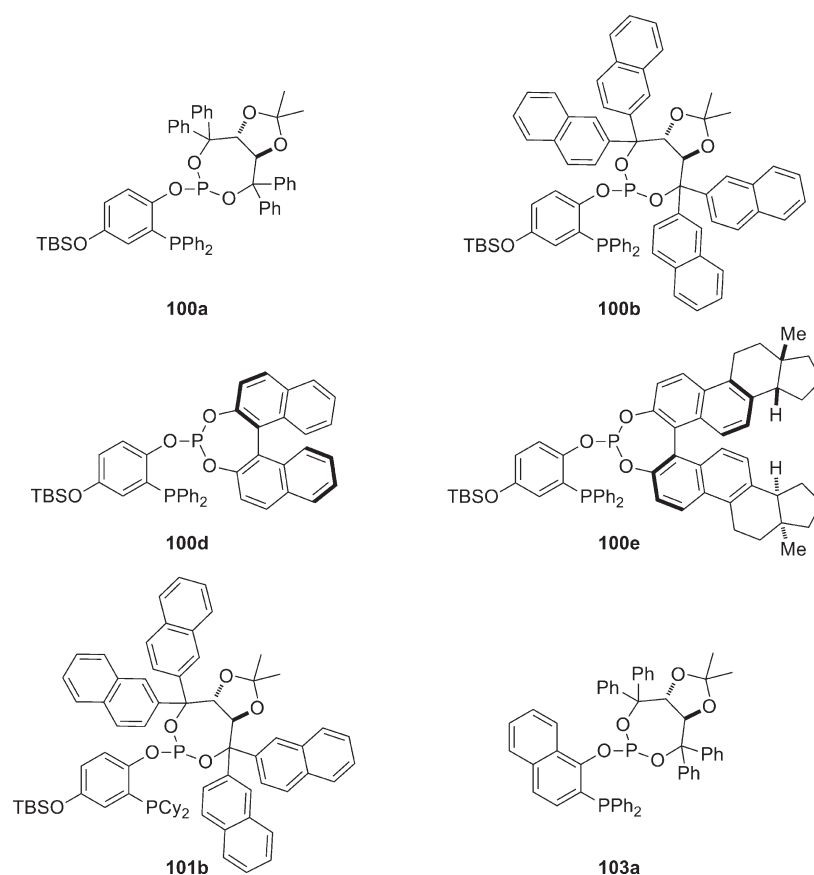
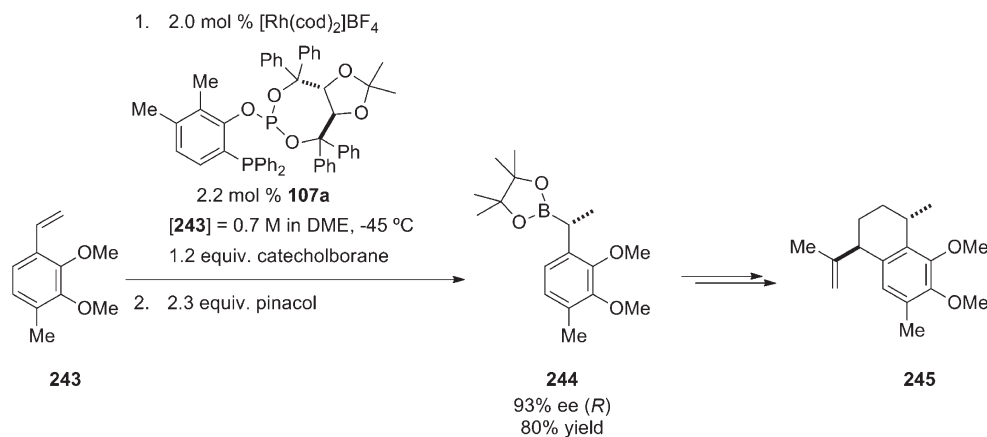


Figure 37. Selected P–OP ligands in the rhodium-mediated hydroboration of vinyl arenes.

Scheme 57. Use of P–OP Ligand 107a in the Rhodium-Mediated Hydroboration of a Useful Synthetic Intermediate



(entry 1 in Table 37). Increasing the temperature to 100 °C allowed halving the reaction time, although a drop in enantioselectivity was observed; and changing for a 2:1 ligand to metal ratio appeared detrimental to regioselectivity, albeit with a small increase in enantioselectivity (compare entries 1–3 in Table 37). Other substrates than styrene led to rather similar levels of conversion and regio- and stereoselectivity (entries 4–6 in Table 37).

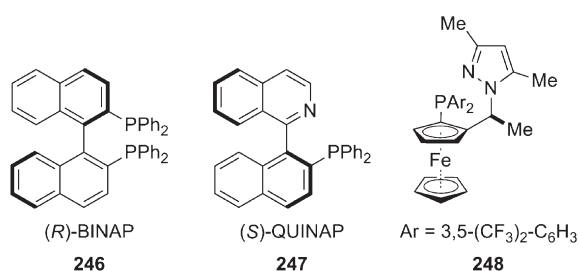
The groups of Leitner and Lloyd-Jones later extended this study by evaluating their library of sulfonylated analogs of BINAPHOS 39a–k (see Table 38 for the catalysis results and

Figure 39 for ligand structures).²⁸ The palladium precatalyst $[\text{Pd}(\text{allyl})(\text{CH}_3\text{CN})_2]\text{OTf}$ performed better in terms of conversion than $[\text{Pd}(\text{allyl})\text{Cp}]$ for the sulfonylated analogs of BINAPHOS 39 (compare entries 1 and 2 in Table 38). The introduction of a sulfonyl group was shown to strongly influence the reaction outcome. The nature of the substituent at the sulfur atom (R^3) barely affected regioselectivity but did dramatically influence catalyst activity and enantioinduction, despite the remoteness of this substituent to both phosphorus atoms. In particular, when R^3 was an alkyl group instead of a perfluoroalkyl one, conversion and

Table 36. Comparison of the Regio- (b/l) and Enantioselectivities (% ee) Obtained with the P–OP Ligand 103a to Those Obtained with Selected Ligands 246–248 in Rhodium-Mediated Asymmetric Hydroboration of Styrene 150a

	ligands							
	246		247		248		103a	
	% ee	b/l ^a	% ee	b/l ^a	% ee	b/l ^a	% ee	b/l ^a
150a	96 (R) ¹⁶⁵	>99/1 ¹⁶⁵	88 (S) ¹⁶⁷	97/3 ¹⁶⁷	99 (S) ¹⁶⁶	nd ¹⁶⁶	91 (R) ^{50b}	95/5 ^{50b}

^a b/l = ratio of branched to linear product.

**Figure 38.** Structures of representative examples of successful ligands in asymmetric hydroboration.

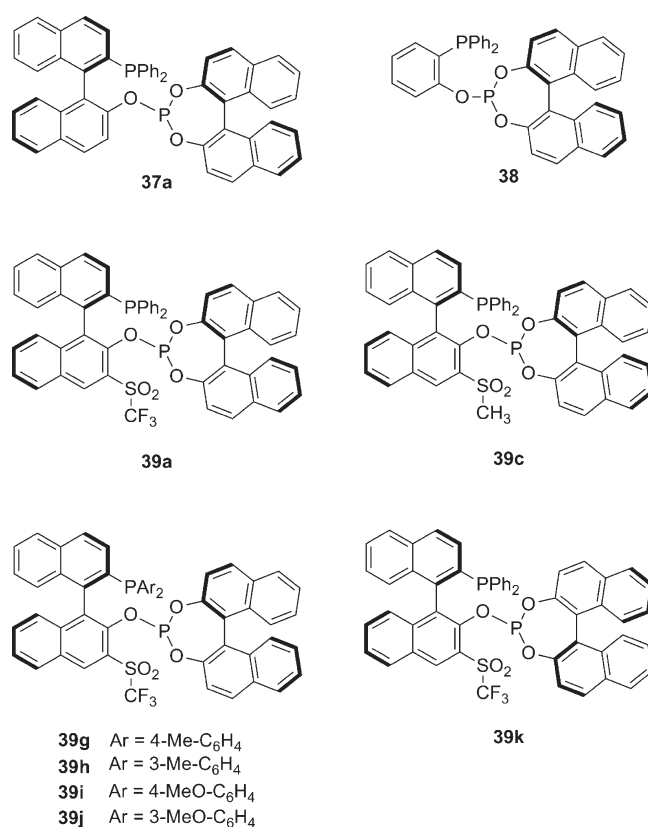
enantioselectivity diminished (entry 4 in Table 38). The authors studied other features of the ligand, showing that the (*R,R*)-diastereomer **39k** provided equivalent conversion and regioselectivity but a higher enantioselectivity than the (*R,S*)-diastereoisomer **39a** (entry 9 in Table 38). The absolute configuration of the product **251** was unchanged, demonstrating that the main stereo-directing element in the structure of these ligands is the binaphthylphosphino fragment, and not the binaphthylphosphite. The same conclusion could be reached upon comparing the enantiomeric excesses obtained with Pringle's ligand **38** (0% ee) and (*R,S*)-BINAPHOS **37a** (56% ee). Variations on the phenyl groups of the phosphino moiety (achieved by introducing electron-donating or electron-withdrawing substituents at the *meta* or *para* positions) gave comparable results, with some improvement of enantioinduction, offering the highest enantiomeric excess (74%) in hydrophosphorylation of styrene reported to date (entry 7 in Table 38).

In conclusion, BINAPHOS-based phosphine–phosphites performed better than several other kinds of ligands in the still understudied asymmetric palladium-mediated hydrophosphorylation of vinyl arenes, providing the best enantioselectivity reported to date for this transformation. Although higher enantiomeric excesses were attained in the parent reaction of norbornene derivatives using a JOSIPHOS-type ligand,¹⁶⁹ BINAPHOS and related ligands should soon give optimal results for a broad array of substrates, namely, through synergy between the ligand's stereogenic elements and its steric and electronic properties.

3.8. Miscellaneous Reactions

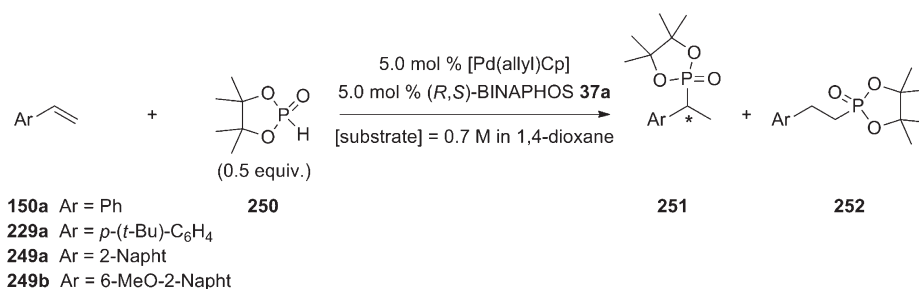
Encouraged by the success of enantiopure P–OP ligands in enantioselective processes like hydroformylation or hydrogenation, various groups have tried to extend the use of phosphine–phosphinites or phosphine–phosphites to other asymmetric transformations. However, these studies remain as singular examples, as none of them have since been pursued.

Nozaki, Takaya, et al. assessed BINAPHOS in the relatively understudied nickel- or palladium-mediated hydrocyanation of norbornene (Scheme 59).¹⁷⁰ Although they obtained a range of activities (from 4% to 69% yield) and modest enantioselectivities

**Figure 39.** Selected P–OP ligands in the rhodium-mediated hydrophosphorylation of alkenes.

(from 17% ee to 48% ee), they did glean valuable information from complexation experiments with nickel or palladium, namely, on the importance of the BINAPHOS to metal ratio and on the influence of other suitable ligands in solution. The highest enantiomeric excess in this study (48% ee) was in the same range as those obtained by other groups that had used Pd/diphosphine (31% and 40% ee)¹⁷¹ or Ni/diphosphite (38% and 55% ee)¹⁷² catalysts.

Nozaki, Takaya, et al. also studied the hydroesterification (alkoxycarbonylation) of styrene **150a** with heterogenized palladium/BINAPHOS catalysts (Scheme 60).¹⁷³ The homogeneous system alone, in which the catalyst was formed by mixing Pd-(dba)₂ with 5 equiv of (*R,S*)-BINAPHOS **37a**, showed almost no activity in the methoxycarbonylation of styrene **150a**, even under 45 atm pressure of carbon monoxide; moreover, the regio- and stereoselectivities were either null or very low. Contrariwise, the same system immobilized onto a montmorillonite clay afforded the expected products **256** and **257** with a combined conversion of 52%, a branched to linear product ratio of 86/14, and a very

Scheme 58. Hydrophosphorylation of Vinyl Arenes Catalyzed by a Pd–[(*R,S*)-BINAPHOS]] ComplexTable 37. Hydrophosphorylation of Vinyl Arenes Catalyzed by a Pd–(*R,S*)-BINAPHOS Complex

entry	substrate	<i>T</i> (°C)	<i>t</i> (h)	conv. (yield) (%)	ratio of 251 to 252	% ee of 251
1	150a ^{23a}	70	70	>99	93/7	56
2	150a ^{23a}	100	35	>99 (85)	89/11	42
3 ^a	150a ^{23a}	100	35	>99	67/33	50
4	229a ^{23a}	100	35	>99 (65)	91/9	54
5	249a ^{23a}	100	35	>99 (80)	96/4	39
6	249b ^{23a}	100	35	>99 (85)	91/9	29

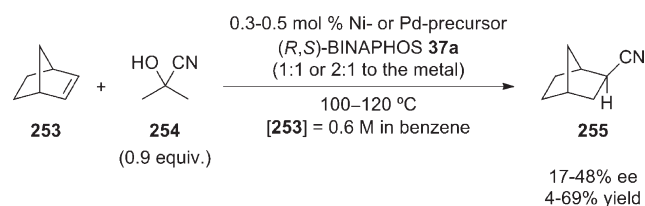
^a Reaction carried out with a 2/1 ligand to metal ratio.Table 38. Palladium-Mediated Hydrophosphorylation of Styrene Using Ligands **39a,c,g–k**

entry	ligand	reaction conditions	conv. (%)	ratio of 251 to 252	% ee of 251
1	39a ²⁸	5.0 mol % [Pd(allyl)Cp], 5.0 mol % 39a , 100 °C, 35 h, 0.7 M in 1,4-dioxane	87	88/12	63
2	39a ²⁸	5.0 mol % [Pd(allyl)(CH ₃ CN) ₂]OTf, 5.0 mol % 39a , 5.0 mol % [NaCH(CO ₂ Me) ₂], 100 °C, 18 h, 0.7 M in 1,4-dioxane	94	84/16	61
3	39a ²⁸	5.0 mol % [Pd(allyl)(CH ₃ CN) ₂]OTf, 5.0 mol % 39a , 5.0 mol % [NaCH(CO ₂ Me) ₂], 70 °C, 48 h, 0.7 M in 1,4-dioxane	10	82/18	68
4	39c ²⁸	5.0 mol % [Pd(allyl)Cp], 5.0 mol % 39c , 100 °C, 35 h, 0.7 M in 1,4-dioxane	42	86/14	42
5	39g ²⁸	5.0 mol % [Pd(allyl)(CH ₃ CN) ₂]OTf, 5.0 mol % 39g , 5.0 mol % [NaCH(CO ₂ Me) ₂], 100 °C, 18 h, 0.7 M in 1,4-dioxane	98	80/20	71
6	39h ²⁸	5.0 mol % [Pd(allyl)(CH ₃ CN) ₂]OTf, 5.0 mol % 39h , 5.0 mol % [NaCH(CO ₂ Me) ₂], 100 °C, 18 h, 0.7 M in 1,4-dioxane	99	89/11	72
7	39i ²⁸	5.0 mol % [Pd(allyl)(CH ₃ CN) ₂]OTf, 5.0 mol % 39i , 5.0 mol % [NaCH(CO ₂ Me) ₂], 100 °C, 18 h, 0.7 M in 1,4-dioxane	99	76/24	74
8	39j ²⁸	5.0 mol % [Pd(allyl)(CH ₃ CN) ₂]OTf, 5.0 mol % 39j , 5.0 mol % [NaCH(CO ₂ Me) ₂], 100 °C, 18 h, 0.7 M in 1,4-dioxane	99	81/19	63
9	39k ²⁸	5.0 mol % [Pd(allyl)(CH ₃ CN) ₂]OTf, 5.0 mol % 39k , 5.0 mol % [NaCH(CO ₂ Me) ₂], 100 °C, 18 h, 0.7 M in 1,4-dioxane	99	82/18	72

low enantiomeric excess (6% ee) for **256**. The lack of activity of the homogeneous catalyst raised the question of whether BINAPHOS operates as a monodentate instead of a bidentate ligand, owing to possible hydrolysis of the phosphite moiety in the acidic reaction medium (benzene/methanol/concentrated hydrochloric acid, 100/2.4/1). The poor enantioselectivity, in comparison with the >99% enantiomeric excess obtained with a PdCl₂/CuCl₂/diphosphine system,¹⁷⁴ may explain why P–OP ligands were not further tested in this reaction.

Murahashi et al. reported a process similar to the one described above: the alkoxycarbonylation of the allylic phosphate *cis*-**258** with a palladium–[(*R,S*)-BINAPHOS] catalyst (Scheme 61).¹⁷⁵ The product *trans*-**259** was obtained via inversion of configuration at the allyl carbon in 52% yield and with an enantiomeric excess of 25%. The authors noted that (*R,S*)-BINAPHOS surprisingly showed comparable activity and enantioselectivity to chiral monodentate phosphorus ligands; contrariwise, chiral diphosphines ((*R*)-BINAP, (*R,R*)-DIOP, and (*S,S*)-CHIRAPHOS) appeared unsuited to this reaction, since the formation of a chelate with palladium saturated the coordination sites of the palladium–allyl complex, preventing coordination of carbon monoxide. Addition-

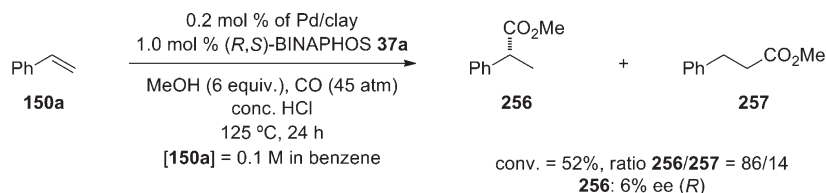
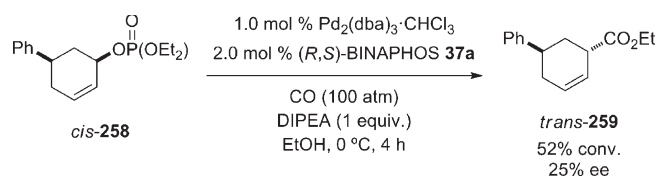
Scheme 59. Hydrocyanation of Norbornene Mediated by BINAPHOS-Based Nickel or Palladium Catalysts



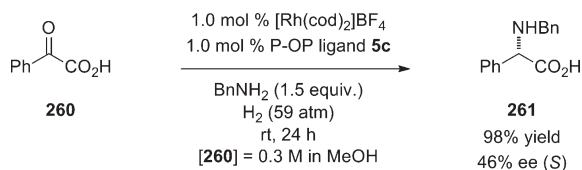
ally, the authors remarked that the absolute configuration of product **259** was determined by the binaphthylphosphino moiety, not the phosphite one. These observations may be again indicating that in the reaction conditions (*R,S*)-BINAPHOS acts as a monodentate ligand, due to cleavage of the phosphite unit.

Lastly, the phosphine–phosphinite ligand **5c** was evaluated in the rhodium-mediated asymmetric reductive amination of phenylpyruvic acid **260** with benzylamine.^{48d} A catalyst based on P–OP ligand **5c** showed high activity and a moderate

Scheme 60. Hydroesterification of Styrene Employing a Pd/BINAPHOS Catalytic System Immobilized onto Clay

Scheme 61. Palladium/(*R,S*)-BINAPHOS-Catalyzed Ethoxycarbonylation of Allylic Phosphate **258**

Scheme 62. Reductive Amination of Phenylpyruvic Acid Catalyzed by a Rh/(P–OP Ligand) System



enantioselectivity in favor of the (*S*)-enantiomer of the product **261** (Scheme 62). However, the superior results attained with the C₂-symmetric diphosphines ((*R,R*)-NORPHOS, (*R,R*)-DEGUPHOS, and (*S,S*)-CHIRAPHOS) demonstrated that **5c** was not an optimal ligand for this reaction.

3.9. Most Recent Progress

In last stages of the preparation of this manuscript, the group of Schmalz published a study on copper-mediated allylic alkylation of cinnamyl chlorides with Grignard reagents in the presence of P–OP ligands.¹⁷⁶ The phosphine–phosphite ligands used (**104a**, **105a**, **108a–114a**, **103d**, **106d**, **107d**, **109d**, and **113d**), and more precisely TADDOL-derived ligands **109a** and **113a**, led from good to excellent results in terms of yields (up to 99%) and regio- and enantioselectivities (up to 99/1 ratio in favor of the branched adducts with up to >99% ee). The catalytic system allowed for efficient and selective transformation of a broad range of functionalized substrates and variation on the nature of the Grignard reagent.

In addition, the groups of Clarke and Pizzano recently reported the hydroformylation of dimethylacrylamide mediated by rhodium complexes derived from phosphine–phosphite ligands **72a**, **72c**, **72e**, and **74a** with very high ratios of branched to linear products, but with low reactivity (up to 67% conversion) and moderate enantioselectivity (up to 46% ee).¹⁷⁷ New P–OP ligands derived from the ring-opening of epoxides have recently been reported by Pizzano et al.¹⁷⁸ The performance of these new ligands in the Rh-catalyzed enantioselective hydrogenation and

hydroformylation of several representative olefins has been analyzed.

Very recently, van Leeuwen et al. have synthesized novel isostructural BINOL-derived enantiopure phosphine–phosphite ligands by condensation of chiral 3,3′-bis(trialkylsilyl)-2,2′-bisnaphthol phosphorochloridites and phosphino phenol derivatives.¹⁷⁹ These P–OP ligands were tested in the rhodium-mediated asymmetric hydroformylation of vinyl acetate and several styrene derivatives. The highest recorded enantioselectivity (78% ee) was achieved with vinyl acetate.

Lastly, Pizzano et al. have reported the use of several phosphine–phosphite ligands in the iridium-mediated hydrogenation of 2-methylquinoline (up to 73% ee).¹⁸⁰ Furthermore, the groups of Schmalz and Reek have screened a reduced library of ligands **100–114** (see Figure 14) in the rhodium-mediated enantioselective hydrogenation of functionalized alkenes (up to 92% ee).¹⁸¹

4. CONCLUSIONS AND OUTLOOK

Numerous phosphine–phosphinite and phosphine–phosphite ligands are known in the literature. These have typically been synthesized by preparation and subsequent O-phosphorylation of the corresponding phosphino alcohols or their phenolic analogs. Highly efficient synthetic transformations have enabled introduction of the phosphino and the phosphinite or phosphite functionalities into many hydrocarbon skeletons. Complementarily, noncovalent and metal–ligand interactions have been used for constructing the catalyst's chiral backbone with unprecedented ease via supramolecular-guided attachment of building blocks that contain the phosphino and phosphite groups required for catalysis as well as motifs necessary for the supramolecular assembly. The repertoire of ligand scaffolds and molecular chirality in P–OP ligands has expanded remarkably since the seminal work of the Brunner,⁸ Pringle,⁷ and Takaya⁶ groups.

Phosphine–phosphinites and phosphine–phosphites are intrinsically modular ligands: they contain two independent phosphorus coordination groups with electronic dissimilarity. In addition to these P-binding groups, the ligand's remaining molecular fragments and stereogenic elements (*modules*) have enabled the development of efficient catalytic systems for various asymmetric transformations (e.g., hydrogenation, hydroformylation, conjugate addition, polymerization of alkenes with CO, allylic substitution, and hydroboration) through steric and electronic modification of the modules.

Compared with phosphine–phosphites, far fewer phosphine–phosphinite ligands have been reported and evaluated in asymmetric catalysis. However, high-performing enantiopure phosphine–phosphinite ligands have been developed for particular cases (e.g., hydrogenation).

Asymmetric hydrogenation of functionalized alkenes is undoubtedly among the best-studied asymmetric transformations and one for which myriad highly efficient metal catalysts have been developed. Even in this highly competitive arena, P–OP ligands have made a niche, rivaling so-called *milestone ligands* (e.g., DIPAMP, DUPHOS, TCFP, JOSIPHOS) in terms of conversion and enantioselectivity. The P–OP ligands studied in asymmetric hydrogenation encompass diverse carbon backbones and stereogenic elements as well as different distances between the two phosphorus functionalities, and many of them provide a highly stereodifferentiating environment around the catalytic rhodium metal center. Various structurally diverse functionalized alkenes have been hydrogenated by rhodium complexes of P–OP ligands with high enantioselectivities and low catalyst loadings. In contrast, studies on asymmetric hydrogenation of imines and heteroaromatic compounds catalyzed by iridium complexes of P–OP ligands are still in their infancy. The enantiomeric excesses achieved to date have been good, but the modular design of P–OP ligands should enable further enhancements.

Highly efficient metal complexes of P–OP ligands have been developed for hydroformylations and for polymerizations of alkenes with CO. Despite the wide structural diversity of highly efficient P–OP ligands for asymmetric hydrogenation, to date, only BINAPHOS-type ligands have provided high enantioselectivities in hydroformylations and in polymerizations of alkenes with CO. Rhodium complexes of BINAPHOS-related ligands catalyze hydroformylations of a vast array of alkenes with high ratios of branched to linear product and with high enantioselectivities. Analogously, palladium complexes of BINAPHOS analogs offer excellent stereoregularity for alternating copolymers of alkenes with CO.

The modular nature of P–OP ligands has facilitated their optimization and a gain in the understanding of copper-mediated conjugate additions, palladium-mediated allylic substitutions, rhodium-mediated hydroborations, and palladium-mediated hydrophosphorylations. Pioneering results have been obtained in the last case, and will certainly be followed by others. Moreover, in the other asymmetric transformations, P–OP ligands are sometimes better ligands than the more traditional bidentate or monodentate phosphorus compounds.

Encouraged by the success of P–OP ligands in the aforementioned processes, and particularly in hydroformylations and hydrogenations, various groups have tried to extend the use of P–OP ligands to other transformations, including hydrocyanations, hydroesterifications, ethoxycarbonylations, and reductive aminations. However, work in these areas has yielded only moderate enantioselectivities so far, and the studies remain as singular examples.

Enantiopure phosphine–phosphinites and phosphine–phosphites have gained an important role in asymmetric catalysis. Given the wide repertoire of ligand scaffolds, and the ever-increasing reports of their applications, one can only imagine that the near future will witness several new examples of successful application of this highly versatile ligands.

AUTHOR INFORMATION

Corresponding Author

*E-mail: avidal@iciq.es.

BIOGRAPHIES



Héctor Fernández-Pérez was born in Valladolid (Spain) in 1977. He graduated in Chemistry at the University of Valladolid in 2003 and started his research career in the same university obtaining his Diploma in Advanced Studies in 2004 in the field of organometallic synthesis with a work on intramolecular cyclization reactions for the preparation of cycloheptanone derivatives under the supervision of Profs. F. J. Pulido and A. Barbero. In October 2004, he moved to the Institute of Chemical Research of Catalonia (Tarragona, Spain) where he started his doctoral studies under the supervision of Prof. Anton Vidal-Ferran working on covalent and supramolecular approaches to asymmetric catalysis. In 2009, he obtained his Ph.D. (Ph.D. Thesis Award) with a research thesis about highly efficient chiral phosphorus ligands for asymmetric hydrogenations. Nowadays he continues developing his research interest in Prof. Vidal's group to discover new catalysts for asymmetric transformations in still challenging fields.



Pablo Etayo was born in Pamplona, Spain, in 1980. He graduated in Chemistry with Honors from the University of Zaragoza in 2003. In 2008, he received his Ph.D. (Ph.D. Thesis Award) from the same university under the supervision of Drs. María D. Díaz de Villegas and José A. Gálvez. During his Ph.D., he worked on the field of asymmetric synthesis and applications of biologically relevant piperidine derivatives. Then, belonging to the same research group at the University of Zaragoza, he spent around one year as a postdoctoral fellow of the University Institute of Research in Homogeneous Catalysis (IUCH) working in enantioselective organocatalysis. In October 2009, he was appointed to his present position at the Institute of Chemical Research of Catalonia (ICIQ) in Tarragona, Spain, where he

joined Prof. Anton Vidal's group as a postdoctoral researcher under contract awarded by Navarra's Government. His research interests focus on asymmetric metal-assisted catalysis and its applications.



Armen Panossian was born in Sèvres (France) in 1980. He graduated in Chemical Engineering from the "Ecole Nationale Supérieure de Chimie de Paris" (Paris, France) in 2004 and in 2005 obtained a research master degree in Fundamental and Applied Chemistry in the specialty of Organic and Bioorganic Chemistry from the Université Pierre et Marie Curie (Paris, France). In 2008, he obtained his Ph.D. in organic chemistry supervised by Prof. Angela Marinetti from the "Institut de Chimie des Substances Naturelles" (Gif-sur-Yvette, France) in the field of enantioselective organocatalysis. During his studies, he carried out short stays in AstraZeneca Research Centre (Reims, France), the Royal Institute of Technology (Prof. Kristina Moberg, Stockholm, Sweden), and the Laboratory of Organic Chemistry of the Université Pierre et Marie Curie (Dr. Pierre Mangeney, Paris, France). In January 2009, he joined Prof. Anton Vidal's Research Group in the Institute of Chemical Research of Catalonia (Tarragona, Spain) where he is working in the area of asymmetric catalysis.



Anton Vidal graduated in Chemical Engineering at the "Institut Químic de Sarrià" in 1987 and completed his Ph.D. on the synthesis of new heterocycles at the same institution in 1992 with Prof. P. Victory. Throughout the two postdoctoral appointments that followed (at the University of Cambridge 1993–1994 with Prof. J. K. M. Sanders and the University of Barcelona 1995–1999 with Prof. M. A. Pericàs), he studied topical and diverse areas of chemistry such as Molecular Recognition, Supramolecular Chemistry, and aspects of Enantioselective

Catalysis. He had the opportunity to complement his academic background with the industrial experience gained during his tenure in a number of research departments at Bayer-AG (Leverkusen 1999–2003). Following the appointment as ICREA Research Professor (Catalan Institution for Research and Advanced Studies), he started his independent research activities as a Group Leader at the Institute of Chemical Research of Catalonia (ICIQ) in Tarragona, Spain, in September 2003. The ultimate aim of his research activities is the design and development of efficient and sustainable catalytic tools in asymmetric synthesis. The strategy to achieve these goals combines a modular design of the catalytic systems, the study of the molecular recognition processes that govern the catalytic event and the use of computational methods.

ACKNOWLEDGMENT

We thank MICINN (Grant CTQ2008-00950/BQU), DURSI (Grant 2009GR623), Consolider Ingenio 2010 (Grant CSD2006-0003), and ICIQ Foundation for financial support. H.F.-P. gratefully acknowledges the "Programa Torres Quevedo" for financial support, and P.E. thanks the "Educational Department of Navarra's Government" for a postdoctoral contract.

REFERENCES

- (1) See, for example: (a) *Comprehensive Asymmetric Catalysis*, 1st ed.; Jacobsen, E. N., Pfaltz, A., Yamamoto, H., Eds.; Springer-Verlag: Heidelberg, 1999; Vols. I–III. (b) *Comprehensive Asymmetric Catalysis: Supplement I*, 1st ed.; Jacobsen, E. N., Pfaltz, A., Yamamoto, H., Eds.; Springer-Verlag: Heidelberg, 2004. (c) *Comprehensive Asymmetric Catalysis: Supplement II*, 1st ed.; Jacobsen, E. N., Pfaltz, A., Yamamoto, H., Eds.; Springer-Verlag: Heidelberg, 2004.
- (2) Kagan, H. B.; Dang, T. P. *J. Chem. Soc., Chem. Commun.* **1971**, 481.
- (3) Whitesell, J. K. *Chem. Rev.* **1989**, 89, 1581.
- (4) (a) Gleich, D.; Herrmann, W. A. *Organometallics* **1999**, 18, 4354. (b) Pavlov, V. A. *Russ. Chem. Rev.* **2004**, 73, 1173. (c) Pavlov, V. A. *Tetrahedron* **2008**, 64, 1147.
- (5) See, for example: (a) Consiglio, G.; Waymouth, R. M. *Chem. Rev.* **1989**, 89, 257. (b) Diéguez, M.; Pàmies, O.; Ruiz, A.; Díaz, Y.; Castellón, S.; Claver, C. *Coord. Chem. Rev.* **2004**, 248, 2165. (c) Grushin, V. V. *Chem. Rev.* **2004**, 104, 1629.
- (6) Sakai, N.; Mano, S.; Nozaki, K.; Takaya, H. *J. Am. Chem. Soc.* **1993**, 115, 7033.
- (7) Baker, M. J.; Pringle, P. G. *J. Chem. Soc., Chem. Commun.* **1993**, 314.
- (8) Brunner, H.; Pieronczyk, W. *J. Chem. Res., Synop.* **1980**, 74.
- (9) See, for example, ref 5b and (a) Diéguez, M.; Pàmies, O.; Claver, C. *Chem. Rev.* **2004**, 104, 3189. (b) Pàmies, O.; Diéguez, M.; Ruiz, A.; Claver, C. *Chim. Oggi* **2004**, 22, 12. (c) Castellón, S.; Claver, C.; Díaz, Y. *Chem. Soc. Rev.* **2005**, 34, 702. (d) Woodward, S.; Diéguez, M.; Pàmies, O. *Coord. Chem. Rev.* **2010**, 254, 2007.
- (10) See, for example: (a) Diéguez, M.; Pàmies, O.; Claver, C. *Tetrahedron: Asymmetry* **2004**, 15, 2113. (b) Claver, C.; Diéguez, M.; Pàmies, O.; Castellón, S. *Top. Organomet. Chem.* **2006**, 18, 35. (c) Gual, A.; Godard, C.; Castellón, S.; Claver, C. *Tetrahedron: Asymmetry* **2010**, 21, 1135.
- (11) See for example: (a) Grabulosa, A.; Granell, J.; Muller, G. *Coord. Chem. Rev.* **2007**, 251, 25. (b) Boaz, N. W.; Ponasik, J. A., Jr. In *Phosphorus Ligands in Asymmetric Catalysis*; Börner, A., Ed.; Wiley-VCH: Weinheim, 2008; Vol. II, p 453. (c) Goudriaan, P. E.; van Leeuwen, P. W. N. M.; Birkholz, M.-N.; Reek, J. N. H. *Eur. J. Inorg. Chem.* **2008**, 2939. (d) Allen, D. W. *Organophosphorus Chem.* **2010**, 39, 1. (e) Kollar, L.; Keglevich, G. *Chem. Rev.* **2010**, 110, 4257.
- (12) Yamashita, M.; Hiramatsu, K.; Yamada, M.; Suzuki, N.; Inokawa, S. *Bull. Chem. Soc. Jpn.* **1982**, 55, 2917.

- (13) Ohe, K.; Morioka, K.; Yonehara, K.; Uemura, S. *Tetrahedron: Asymmetry* **2002**, *13*, 2155.
- (14) (a) Sell, T.; Laschat, S.; Dix, I.; Jones, P. G. *Eur. J. Org. Chem.* **2000**, 4119. (b) Monsees, A.; Laschat, S. *Synlett* **2002**, 1011.
- (15) Boyer, N.; Léauté, M.; Jubault, P.; Pannecoucke, X.; Quirion, J.-C. *Tetrahedron: Asymmetry* **2005**, *16*, 2455.
- (16) See, for example, the following references and those cited therein: (a) Brunner, H.; Sicheneder, A. *Angew. Chem., Int. Ed. Engl.* **1988**, *100*, 718. (b) Gorla, F.; Togni, A.; Venanzi, L. M.; Albinati, A.; Lianza, F. *Organometallics* **1994**, *13*, 1607.
- (17) Jiang, R.; He, W.; Wang, P.-a.; Li, X.-y.; Zhang, S.-y. *Fenzi Cuihua* **2006**, *20*, 207.
- (18) Fernández-Pérez, H.; Pericàs, M. A.; Vidal-Ferran, A. *Adv. Synth. Catal.* **2008**, *350*, 1984.
- (19) Fernández-Pérez, H.; Donald, S. M. A.; Munslow, I. J.; Benet-Buchholz, J.; Maseras, F.; Vidal-Ferran, A. *Chem.—Eur. J.* **2010**, *16*, 6495.
- (20) Nozaki, K.; Li, W.-G.; Horiuchi, T.; Takaya, H.; Saito, T.; Yoshida, A.; Matsumura, K.; Kato, Y.; Imai, T.; Miura, T.; Kumobayashi, H. *J. Org. Chem.* **1996**, *61*, 7658.
- (21) Yan, Y.; Chi, Y.; Zhang, X. *Tetrahedron: Asymmetry* **2004**, *15*, 2173.
- (22) Erre, G.; Enthaler, S.; Junge, K.; Gladiali, S.; Beller, M. *J. Mol. Catal. A: Chem.* **2008**, *280*, 148.
- (23) (a) Shulyupin, M. O.; Franciò, G.; Beletskaya, I. P.; Leitner, W. *Adv. Synth. Catal.* **2005**, *347*, 667. (b) Li, Y.; Dong, L.; Yan, M. *Zhongshan Daxue Xuebao, Ziran Kexueban* **2006**, *45*, 58.
- (24) Yoon, T. P.; Jacobsen, E. N. *Science* **2003**, *299*, 1691.
- (25) Nozaki, K.; Matsuo, T.; Shibahara, F.; Hiyama, T. *Adv. Synth. Catal.* **2001**, *343*, 61.
- (26) Nozaki, K.; Yasutomi, M.; Nakamoto, K.; Hiyama, T. *Polyhedron* **1998**, *17*, 1159.
- (27) Horiuchi, T.; Ohta, T.; Shirakawa, E.; Nozaki, K.; Takaya, H. *J. Org. Chem.* **1997**, *62*, 4285.
- (28) Barta, K.; Franciò, G.; Leitner, W.; Lloyd-Jones, G. C.; Shepperson, I. R. *Adv. Synth. Catal.* **2008**, *350*, 2013.
- (29) (a) Matsumura, K.; Saito, T.; Sayo, N.; Kumobayashi, H.; Takaya, H. European Patent EP 0614902, 1994. (b) Saito, T.; Matsumura, K.; Kato, Y.; Sayo, N.; Kumobayashi, H. European Patent EP 0614903, 1994.
- (30) Nozaki, K.; Sakai, N.; Nanno, T.; Higashijima, T.; Mano, S.; Horiuchi, T.; Takaya, H. *J. Am. Chem. Soc.* **1997**, *119*, 4413.
- (31) Higashijima, T.; Sakai, N.; Nozaki, K.; Takaya, H. *Tetrahedron Lett.* **1994**, *35*, 2023.
- (32) Despite the absence of substituents on positions 6 and 6' of the biphenyl moiety in ligands **44b**/**44d**, the latter were obtained as an inseparable 55:45 mixture of diastereomers (**44b** to **44d**) rather than a single enantiomer (see ref 31).
- (33) Dyke, A. M.; Gill, D. M.; Harvey, J. N.; Hester, A. J.; Lloyd-Jones, G. C.; Muñoz, M. P.; Shepperson, I. R. *Angew. Chem., Int. Ed.* **2008**, *47*, S067.
- (34) (a) Nozaki, K.; Itoi, Y.; Shibahara, F.; Shirakawa, E.; Ohta, T.; Takaya, H.; Hiyama, T. *J. Am. Chem. Soc.* **1998**, *120*, 4051. (b) Nozaki, K.; Shibahara, F.; Itoi, Y.; Shirakawa, E.; Ohta, T.; Takaya, H.; Hiyama, T. *Bull. Chem. Soc. Jpn.* **1999**, *72*, 1911. (c) Nozaki, K.; Shibahara, F.; Hiyama, T. *Chem. Lett.* **2000**, 694. (d) Shibahara, F.; Nozaki, K.; Matsuo, T.; Hiyama, T. *Bioorg. Med. Chem. Lett.* **2002**, *12*, 1825. (e) Shibahara, F.; Nozaki, K.; Hiyama, T. *J. Am. Chem. Soc.* **2003**, *125*, 8555. (f) Kinoshita, S.; Shibahara, F.; Nozaki, K. *Green Chem.* **2005**, *7*, 256.
- (35) Bonafoux, D.; Hua, Z.; Wang, B.; Ojima, I. *J. Fluorine Chem.* **2001**, *112*, 101.
- (36) (a) Franciò, G.; Leitner, W. *Chem. Commun.* **1999**, 1663. (b) Franciò, G.; Wittmann, K.; Leitner, W. *J. Organomet. Chem.* **2001**, *621*, 130.
- (37) Kless, A.; Holz, J.; Heller, D.; Kadyrov, R.; Selke, R.; Fischer, C.; Börner, A. *Tetrahedron: Asymmetry* **1996**, *7*, 33.
- (38) Pàmies, O.; Diéguez, M.; Net, G.; Ruiz, A.; Claver, C. *Chem. Commun.* **2000**, 2383.
- (39) (a) Deerenberg, S.; Kamer, P. C. J.; van Leeuwen, P. W. N. M. *Organometallics* **2000**, *19*, 2065. (b) Deerenberg, S.; Schrekker, H. S.; van Strijdonck, G. P. F.; Kamer, P. C. J.; van Leeuwen, P. W. N. M.; Fraanje, J.; Goubitz, K. *J. Org. Chem.* **2000**, *65*, 4810.
- (40) Panossian, A.; Fernández-Pérez, H.; Popa, D.; Vidal-Ferran, A. *Tetrahedron: Asymmetry* **2010**, *21*, 2281.
- (41) Hegedüs, C.; Gulyás, H.; Szöllosy, A.; Bakos, J. *Inorg. Chim. Acta* **2009**, *362*, 1650.
- (42) (a) Arena, C. G.; Drommi, D.; Faraone, F. *Tetrahedron: Asymmetry* **2000**, *11*, 2765. (b) Beghetto, V.; Scrivanti, A.; Matteoli, U. *Catal. Commun.* **2001**, *2*, 139.
- (43) (a) Suárez, A.; Pizzano, A. *Tetrahedron: Asymmetry* **2001**, *12*, 2501. (b) Suárez, A.; Méndez-Rojas, M. A.; Pizzano, A. *Organometallics* **2002**, *21*, 4611. (c) Vargas, S.; Rubio, M.; Suárez, A.; Pizzano, A. *Tetrahedron Lett.* **2005**, *46*, 2049. (d) Rubio, M.; Suárez, A.; Álvarez, E.; Pizzano, A. *Chem. Commun.* **2005**, 628. (e) Vargas, S.; Rubio, M.; Suárez, A.; del Río, D.; Álvarez, E.; Pizzano, A. *Organometallics* **2006**, *25*, 961. (f) Rubio, M.; Suárez, A.; Álvarez, E.; Bianchini, C.; Oberhauser, W.; Peruzzini, M.; Pizzano, A. *Organometallics* **2007**, *26*, 6428. (g) Rubio, M.; Vargas, S.; Suárez, A.; Álvarez, E.; Pizzano, A. *Chem.—Eur. J.* **2007**, *13*, 1821. (h) Vargas, S.; Suárez, A.; Álvarez, E.; Pizzano, A. *Chem.—Eur. J.* **2008**, *14*, 9856.
- (44) (a) Müller, C.; Lopez, L. G.; Kooijman, H.; Spek, A. L.; Vogt, D. *Tetrahedron Lett.* **2006**, *47*, 2017. (b) Müller, C.; Vogt, D. *Dalton Trans.* **2007**, 5505.
- (45) Breit, B.; Fuchs, E. *Synthesis* **2006**, 2121.
- (46) See, for example: (a) Brunel, J.-M.; Constantieux, T.; Legrand, O.; Buono, G. *Tetrahedron Lett.* **1998**, *39*, 2961. (b) Legrand, O.; Brunel, J.-M.; Buono, G. *Tetrahedron Lett.* **1998**, *39*, 9419. (c) Buono, G.; Chiodi, O.; Wills, M. *Synlett* **1999**, 377. (d) Legrand, O.; Brunel, J.-M.; Buono, G. *Tetrahedron Lett.* **2000**, *41*, 2105.
- (47) Moulin, D.; Bago, S.; Bauduin, C.; Darcel, C.; Jugé, S. *Tetrahedron: Asymmetry* **2000**, *11*, 3939.
- (48) (a) Bosch, B. E.; Trauthwein, H.; Riermeier, T.; Dingerdissen, U.; Monsees, A.; Bosch, B. International Patent WO 200064914, 1999. (b) Bosch, B. E.; Monsees, A.; Dingerdissen, U.; Knochel, P.; Hupe, E. International Patent WO 014330, 2002. (c) Bosch, B. E.; Trauthwein, H.; Riermeier, T.; Dingerdissen, U.; Monsees, A. U.S. Patent 6,573,389, 2003. (d) Kadyrov, R.; Riermeier, T. H.; Dingerdissen, U.; Tararov, V.; Börner, A. *J. Org. Chem.* **2003**, *68*, 4067.
- (49) Jia, X.; Li, X.; Lam, W. S.; Kok, S. H. L.; Xu, L.; Lu, G.; Yeung, C.-H.; Chan, A. S. C. *Tetrahedron: Asymmetry* **2004**, *15*, 2273.
- (50) (a) Kranich, R.; Eis, K.; Geis, O.; Mühle, S.; Bats, J. W.; Schmalz, H.-G. *Chem.—Eur. J.* **2000**, *6*, 2874. (b) Blume, F.; Zemolka, S.; Fey, T.; Kranich, R.; Schmalz, H.-G. *Adv. Synth. Catal.* **2002**, *344*, 868. (c) Velder, J.; Robert, T.; Weidner, I.; Neudörfl, J.-M.; Lex, J.; Schmalz, H.-G. *Adv. Synth. Catal.* **2008**, *350*, 1309. (d) Robert, T.; Abiri, Z.; Wassenaar, J.; Sandee, A. J.; Romanski, S.; Neudörfl, J.-M.; Schmalz, H.-G.; Reek, J. N. H. *Organometallics* **2010**, *29*, 478.
- (51) Heinicke, J.; Kadyrov, R.; Kindermann, M. K.; Koesling, M.; Jones, P. G. *Chem. Ber.* **1996**, *129*, 1547.
- (52) Slagt, V. F.; Röder, M.; Kamer, P. C. J.; van Leeuwen, P. W. N. M.; Reek, J. N. H. *J. Am. Chem. Soc.* **2004**, *126*, 4056.
- (53) (a) Reek, J. N. H.; Röder, M.; Goudriaan, P. E.; Kamer, P. C. J.; van Leeuwen, P. W. N. M.; Slagt, V. F. *J. Organomet. Chem.* **2005**, *690*, 4505. (b) Jiang, X.-B.; Lefort, L.; Goudriaan, P. E.; de Vries, A. H. M.; van Leeuwen, P. W. N. M.; de Vries, J. G.; Reek, J. N. H. *Angew. Chem., Int. Ed.* **2006**, *45*, 1223. (c) Jiang, X.-B.; van Leeuwen, P. W. N. M.; Reek, J. N. H. *Chem. Commun.* **2007**, 2287.
- (54) Hattori, G.; Hori, T.; Miyake, Y.; Nishibayashi, Y. *J. Am. Chem. Soc.* **2007**, *129*, 12930.
- (55) The two diastereoisomers arise from bonding the phosphite group to each of the two possible meta positions to the oxygens from the pyrocatechol unit.
- (56) Li, Y.; Feng, Y.; He, Y.-M.; Chen, F.; Pan, J.; Fan, Q.-H. *Tetrahedron Lett.* **2008**, *49*, 2878.
- (57) (a) Vidal-Ferran, A.; Moyano, A.; Pericàs, M. A.; Riera, A. *J. Org. Chem.* **1997**, *62*, 4970. (b) Vidal-Ferran, A.; Bampas, N.; Moyano, A.;

- Pericàs, M. A.; Riera, A.; Sanders, J. K. M. *J. Org. Chem.* **1998**, *63*, 6309.
- (c) Jimeno, C.; Vidal-Ferran, A.; Moyano, A.; Pericàs, M. A.; Riera, A. *Tetrahedron Lett.* **1999**, *40*, 777. (d) Puigjaner, C.; Vidal-Ferran, A.; Moyano, A.; Pericàs, M. A.; Riera, A. *J. Org. Chem.* **1999**, *64*, 7902. (e) Pericàs, M. A.; Puigjaner, C.; Riera, A.; Vidal-Ferran, A.; Gómez, M.; Jiménez, F.; Muller, G.; Rocamora, M. *Chem.—Eur. J.* **2002**, *8*, 4164. (f) Popa, D.; Puigjaner, C.; Gómez, M.; Benet-Buchholz, J.; Vidal-Ferran, A.; Pericàs, M. A. *Adv. Synth. Catal.* **2007**, *349*, 2265. (g) Popa, D.; Marcos, R.; Sayalero, S.; Vidal-Ferran, A.; Pericàs, M. A. *Adv. Synth. Catal.* **2009**, *351*, 1539.
- (58) See, for example: (a) Trost, B. M.; Van Vranken, D. L.; Bingel, C. J. *Am. Chem. Soc.* **1992**, *114*, 9327. (b) Rajanbabu, T. V.; Casalnuovo, A. L.; Ayers, T. A. *Adv. Catal. Processes* **1997**, *2*, 1. (c) Pàmies, O.; van Strijdonck, G. P. F.; Diéguez, M.; Deerenberg, S.; Net, G.; Ruiz, A.; Claver, C.; Kamer, P. C. J.; van Leeuwen, P. W. N. M. *J. Org. Chem.* **2001**, *66*, 8867. (d) Dalko, P. I.; Moisan, L.; Cossy, J. *Angew. Chem., Int. Ed.* **2002**, *41*, 625. (e) Locatelli, M.; Cozzi, P. G. *Angew. Chem., Int. Ed.* **2003**, *42*, 4928. (f) Jensen, J. F.; Sotofte, I.; Sørensen, H. O.; Johannsen, M. *J. Org. Chem.* **2003**, *68*, 1258. (g) Jeulin, S.; De Paule, S. D.; Ratovelomanana-Vidal, V.; Genêt, J.-P.; Champion, N.; Dellis, P. *Proc. Natl. Acad. Sci. U.S.A.* **2004**, *101*, 5799. (h) Goldfuss, B.; Löschmann, T.; Rominger, F. *Chem.—Eur. J.* **2004**, *10*, 5422. (i) Knöpfel, T. F.; Zarotti, P.; Ichikawa, T.; Carreira, E. M. *J. Am. Chem. Soc.* **2005**, *127*, 9682. (j) Miller, J. J.; Sigman, M. S. *J. Am. Chem. Soc.* **2007**, *129*, 2752. (k) Diéguez, M.; Pàmies, O. *Acc. Chem. Res.* **2010**, *43*, 312.
- (59) See, for example: (a) Kagan, H. B. *J. Organomet. Chem.* **1998**, *567*, 3. (b) Traverse, J. F.; Snapper, M. L. *Drug Discovery Today* **2002**, *7*, 1002. (c) Reetz, M. T. *Angew. Chem., Int. Ed.* **2002**, *41*, 1335. (d) Gennari, C.; Piarulli, U. *Chem. Rev.* **2003**, *103*, 3071. (e) Hoveyda, A. H.; Murphy, K. E. In *Comprehensive Asymmetric Catalysis: Supplement I*; Springer-Verlag: 2004; Vol. 1, p 171. (f) Jäkel, C.; Paciello, R. *Chem. Rev.* **2006**, *106*, 2912.
- (60) See, for example: (a) Takacs, J. M.; Reddy, D. S.; Moteki, S. A.; Wu, D.; Palencia, H. J. *Am. Chem. Soc.* **2004**, *126*, 4494. (b) Breit, B. *Angew. Chem., Int. Ed.* **2005**, *44*, 6816. (c) Thomas, C. M.; Ward, T. R. *Chem. Soc. Rev.* **2005**, *34*, 337. (d) Takacs, J. M.; Chaiseeda, K.; Moteki, S. A.; Reddy, D. S.; Wu, D.; Chandra, K. *Pure Appl. Chem.* **2006**, *78*, 501. (e) Pignataro, L.; Carboni, S.; Civera, M.; Colombo, R.; Piarulli, U.; Gennari, C. *Angew. Chem., Int. Ed.* **2010**, *49*, 6633.
- (61) (a) Brown, J. M. In *Comprehensive Asymmetric Catalysis*; Jacobsen, E. N., Pfaltz, A., Yamamoto, H., Eds.; Springer-Verlag: Heidelberg, 1999; Vols. I–III, p 121. (b) Halterman, R. L. In *Comprehensive Asymmetric Catalysis*; Jacobsen, E. N., Pfaltz, A., Yamamoto, H., Eds.; Springer-Verlag: Heidelberg, 1999; Vol. I, p 183. (c) Ohkuma, T.; Noyori, R. In *Comprehensive Asymmetric Catalysis*; Jacobsen, E. N., Pfaltz, A., Yamamoto, H., Eds.; Springer-Verlag: Heidelberg, 1999; Vol. I, p 199. (d) Blaser, H.-U.; Spindler, F. In *Comprehensive Asymmetric Catalysis*; Jacobsen, E. N., Pfaltz, A., Yamamoto, H., Eds.; Springer-Verlag: Heidelberg, 1999; Vol. I, p 247. (e) Noyori, R. *Angew. Chem., Int. Ed.* **2002**, *41*, 2008. (f) Knowles, W. S. *Angew. Chem., Int. Ed.* **2002**, *41*, 1998. (g) Tang, W.; Zhang, X. *Chem. Rev.* **2003**, *103*, 3029. (h) Gridnev, I. D.; Imamoto, T. *Acc. Chem. Res.* **2004**, *37*, 633. (i) Cui, X.; Burgess, K. *Chem. Rev.* **2005**, *105*, 3272. (j) Knowles, W. S.; Noyori, R. *Acc. Chem. Res.* **2007**, *40*, 1238. (k) Minnaard, A. J.; Feringa, B. L.; Lefort, L.; de Vries, J. G. *Acc. Chem. Res.* **2007**, *40*, 1267. (l) Zhang, W.; Chi, Y.; Zhang, X. *Acc. Chem. Res.* **2007**, *40*, 1278. (m) *Phosphorus Ligands in Asymmetric Catalysis*, 1st ed.; Börner, A., Ed.; Wiley-VCH: Weinheim, 2008; Vols. I–III.
- (62) (a) *Asymmetric Catalysis on Industrial Scale: Challenges, Approaches and Solutions*, 1st ed.; Blaser, H. U.; Schmidt, E., Eds.; Wiley VCH: Weinheim, 2004. (b) Blaser, H.-U.; Pugin, B.; Spindler, F.; Thommen, M. *Acc. Chem. Res.* **2007**, *40*, 1240. (c) Johnson, N. B.; Lennon, I. C.; Moran, P. H.; Ramsden, J. A. *Acc. Chem. Res.* **2007**, *40*, 1291. (d) Shultz, C. S.; Krska, S. W. *Acc. Chem. Res.* **2007**, *40*, 1320. (e) Klingler, F. D. *Acc. Chem. Res.* **2007**, *40*, 1367. (f) Shimizu, H.; Nagasaki, I.; Matsumura, K.; Sayo, N.; Saito, T. *Acc. Chem. Res.* **2007**, *40*, 1385.
- (63) Halpern, J.; Riley, D. P.; Chan, A. S. C.; Pluth, J. J. *J. Am. Chem. Soc.* **1977**, *99*, 8055.
- (64) Deerenberg, S.; Pàmies, O.; Diéguez, M.; Claver, C.; Kamer, P. C. J.; van Leeuwen, P. W. N. M. *J. Org. Chem.* **2001**, *66*, 7626.
- (65) Fernández-Pérez, H.; Etayo, P.; Núñez-Rico, J. L.; Vidal-Ferran, A. *Chim. Oggi* **2010**, *28*, XXVI.
- (66) See, for example: (a) Renaud, J. L.; Dupau, P.; Hay, A. E.; Guingouain, M.; Dixneuf, P. H.; Bruneau, C. *Adv. Synth. Catal.* **2003**, *345*, 230. (b) Sandee, A. J.; van der Burg, A. M.; Reek, J. N. H. *Chem. Commun.* **2007**, 864. (c) Patureau, F. W.; de Boer, S.; Kuil, M.; Meeuwissen, J.; Breuil, P.-A. R.; Siegler, M. A.; Spek, A. L.; Sandee, A. J.; de Bruin, B.; Reek, J. N. H. *J. Am. Chem. Soc.* **2009**, *131*, 6683. (d) Pautigny, C.; Debout, C.; Vayron, P.; Ayad, T.; Ratovelomanana-Vidal, V. *Tetrahedron: Asymmetry* **2010**, *21*, 1382.
- (67) Vargas, S.; Suarez, A.; Alvarez, E.; Pizzano, A. *Chem.—Eur. J.* **2010**, *16*, 9937.
- (68) (a) *Multiphase Homogeneous Catalysis*; Cornils, B., Herrmann, W. A., Horváth, I. T., Leitner, W., Mecking, S., Olivier-Bourbigou, H., Vogt, D., Eds.; Wiley-VCH Verlag GmbH & Co. KGaA: Weinheim, 2005; Vols. 1–2. (b) Lombardo, M.; Quintavalla, A.; Chiarucci, M.; Trombini, C. *Synlett* **2010**, 1746.
- (69) (a) Burgemeister, K.; Franciò, G.; Hugl, H.; Leitner, W. *Chem. Commun.* **2005**, 6026. (b) Burgemeister, K.; Franciò, G.; Gego, V. H.; Greiner, L.; Hugl, H.; Leitner, W. *Chem.—Eur. J.* **2007**, *13*, 2798.
- (70) (a) Bayardon, J.; Holz, J.; Schäffner, B.; Andrushko, V.; Verevkin, S.; Preetz, A.; Börner, A. *Angew. Chem., Int. Ed.* **2007**, *46*, 5971. (b) Schäffner, B.; Schäffner, F.; Verevkin, S. P.; Börner, A. *Chem. Rev.* **2010**, *110*, 4554.
- (71) Fleury-Brégeot, N.; de la Fuente, V.; Castillón, S.; Claver, C. *ChemCatChem* **2010**, *2*, 1346.
- (72) Vargas, S.; Rubio, M.; Suárez, A.; Pizzano, A. *Tetrahedron Lett.* **2006**, *47*, 615.
- (73) Núñez-Rico, J. L.; Fernández-Pérez, H.; Benet-Buchholz, J.; Vidal-Ferran, A. *Organometallics* **2010**, *29*, 6627.
- (74) (a) Chan, A. S. C.; Pluth, J. J.; Halpern, J. J. *Am. Chem. Soc.* **1980**, *102*, 5952. (b) Wilczynski, R.; Fordyce, W. A.; Halpern, J. J. *Am. Chem. Soc.* **1983**, *105*, 2066. (c) Landis, C. R.; Halpern, J. J. *Am. Chem. Soc.* **1987**, *109*, 1746. (d) Brown, J. M. *Chem. Soc. Rev.* **1993**, *22*, 25. (e) Landis, C. R.; Hilfenhaus, P.; Feldgus, S. J. *Am. Chem. Soc.* **1999**, *121*, 8741. (f) Feldgus, S.; Landis, C. R. *J. Am. Chem. Soc.* **2000**, *122*, 12714. (g) Landis, C. R.; Feldgus, S. *Angew. Chem., Int. Ed.* **2000**, *39*, 2863. (h) Feldgus, S.; Landis, C. R. *Organometallics* **2001**, *20*, 2374.
- (75) (a) Donoghue, P. J.; Helquist, P.; Norrby, P. O.; Wiest, O. *J. Chem. Theory Comput.* **2008**, *4*, 1313. (b) Donoghue, P. J.; Helquist, P.; Norrby, P.-O.; Wiest, O. *J. Am. Chem. Soc.* **2009**, *131*, 410.
- (76) Donald, S. M. A.; Vidal-Ferran, A.; Maseras, F. *Can. J. Chem.* **2009**, *87*, 1273.
- (77) Pàmies, O.; Diéguez, M.; Net, G.; Ruiz, A.; Claver, C. *J. Org. Chem.* **2001**, *66*, 8364.
- (78) Table 9 is not intended to provide a detailed comparison of the enantioselectivities obtained with P–OP ligands with those obtained with the many hundreds of efficient ligands that have been developed up until now for this transformation. Due to space limitations, the authors have considered only a very limited set of P-containing derivatives that, in their opinion, have played a key role in the development of the field and that allow comparison with the results reported for P–OP ligands. The reader is referred to more specific reviews on asymmetric hydrogenation for more detailed comparison with many kinds of highly efficient ligands (for example, see ref 61).
- (79) Kagan, H. B.; Dang, T.-P. *J. Am. Chem. Soc.* **1972**, *94*, 6429.
- (80) Vineyard, B. D.; Knowles, W. S.; Sabacky, M. J.; Bachman, G. L.; Weinkauff, D. J. *J. Am. Chem. Soc.* **1977**, *99*, 5946.
- (81) Togni, A.; Breutel, C.; Schnyder, A.; Spindler, F.; Landert, H.; Tijani, A. *J. Am. Chem. Soc.* **1994**, *116*, 4062.
- (82) Miyashita, A.; Yasuda, A.; Takaya, H.; Toriumi, K.; Ito, T.; Souchi, T.; Noyori, R. *J. Am. Chem. Soc.* **1980**, *102*, 7932.
- (83) Gridnev, I. D.; Imamoto, T.; Hoge, G.; Kouchi, M.; Takahashi, H. *J. Am. Chem. Soc.* **2008**, *130*, 2560.
- (84) Kreuzfeld, H. J.; Döbler, C.; Krause, H. W.; Facklam, C. *Tetrahedron: Asymmetry* **1993**, *4*, 2047.
- (85) Burk, M. J. *J. Am. Chem. Soc.* **1991**, *113*, 8518.
- (86) Hopkins, J. M.; Dalrymple, S. A.; Parvez, M.; Keay, B. A. *Org. Lett.* **2005**, *7*, 3765.

- (87) Yan, Y.-Y.; RajanBabu, T. V. *Org. Lett.* **2000**, *2*, 4137.
- (88) Burk, M. J.; Wang, Y. M.; Lee, J. R. *J. Am. Chem. Soc.* **1996**, *118*, 5142.
- (89) Sento, T.; Shimazu, S.; Ichikuni, N.; Uematsu, T. *J. Mol. Catal. A: Chem.* **1999**, *137*, 263.
- (90) Christopf, W. C.; Vineyard, B. D. *J. Am. Chem. Soc.* **1979**, *101*, 4406.
- (91) Burk, M. J.; Bienewald, F.; Harris, M.; Zanotti-Gerosa, A. *Angew. Chem., Int. Ed.* **1998**, *37*, 1931.
- (92) Donate, P. M.; Frederico, D.; da Silva, R.; Constantino, M. G.; Del Ponte, G.; Bonatto, P. S. *Tetrahedron: Asymmetry* **2003**, *14*, 3253.
- (93) (a) Agbossou, F.; Carpentier, J.-F.; Mortreux, A. *Chem. Rev.* **1995**, *95*, 2485. (b) Gladiali, S.; Bayón, J. C.; Claver, C. *Tetrahedron: Asymmetry* **1995**, *6*, 1453. (c) Claver, C.; van Leeuwen, P. W. N. M. In *Catalysis by Metal Complexes*; Bianchini, C., Cole-Hamilton, D. J., van Leeuwen, P. W. N. M., Eds.; Kluwer Academic Publishers: Dordrecht, 2000; Vol. 22, p 107.
- (94) Keulemans, A. I. M.; Kwantes, A.; van Bavel, T. *Recl. Trav. Chim. Pays-Bas* **1948**, *67*, 298.
- (95) (a) Nozaki, K.; Takaya, H.; Hiyama, T. *Top. Catal.* **1997**, *4*, 175. (b) Klosin, J.; Landis, C. R. *Acc. Chem. Res.* **2007**, *40*, 1251.
- (96) Although several examples of rhodium complexes of phosphine–phosphite ligands catalyzing enantioselective hydroformylations have been published, to the best of the author's knowledge, examples on the application of rhodium complexes of phosphine–phosphinites are very scarce in the literature. In this example, the ligand decomposed under the reaction conditions²²
- (97) Pàmies, O.; Net, G.; Ruiz, A.; Claver, C. *Tetrahedron: Asymmetry* **2001**, *12*, 3441.
- (98) Arena, C. G.; Faraone, F.; Graiff, C.; Tiripicchio, A. *Eur. J. Inorg. Chem.* **2002**, 711.
- (99) Yan, Y.; Zhang, X. *J. Am. Chem. Soc.* **2006**, *128*, 7198.
- (100) Hydroformylation of styrene mediated by (R,S)-BINAPHOS **37a** in compressed carbon dioxide has been reported to give appreciable asymmetric induction; however very low ee's were obtained at high CO₂ densities: Kainz, S.; Leitner, W. *Catal. Lett.* **1998**, *55*, 223.
- (101) Nozaki, K.; Nanno, T.; Takaya, H. *J. Organomet. Chem.* **1997**, *527*, 103.
- (102) Sakai, N.; Nozaki, K.; Takaya, H. *J. Chem. Soc., Chem. Commun.* **1994**, 395.
- (103) (a) Horiuchi, T.; Ohta, T.; Nozaki, K.; Takaya, H. *Chem. Commun.* **1996**, 155. (b) Horiuchi, T.; Ohta, T.; Shirakawa, E.; Nozaki, K.; Takaya, H. *Tetrahedron* **1997**, *53*, 7795.
- (104) Liu, P.; Jacobsen, E. N. *J. Am. Chem. Soc.* **2001**, *123*, 10772.
- (105) (a) Nakano, K.; Tanaka, R.; Nozaki, K. *Helv. Chim. Acta* **2006**, *89*, 1681. (b) Tanaka, R.; Nakano, K.; Nozaki, K. *J. Org. Chem.* **2007**, *72*, 8671.
- (106) Hobbs, C. F.; Knowles, W. S. *J. Org. Chem.* **1981**, *46*, 4422.
- (107) Nozaki, K.; Matsuo, T.; Shibahara, F.; Hiyama, T. *Organometallics* **2003**, *22*, 594.
- (108) Nozaki, K.; Li, W.-g.; Horiuchi, T.; Takaya, H. *Tetrahedron Lett.* **1997**, *38*, 4611.
- (109) Solinas, M.; Gladiali, S.; Marchetti, M. *J. Mol. Catal. A: Chem.* **2005**, *226*, 141.
- (110) Botteghi, C.; Paganelli, S. *J. Organomet. Chem.* **1991**, *417*, C41.
- (111) Lambers-Verstappen, M. M. H.; de Vries, J. G. *Adv. Synth. Catal.* **2003**, *345*, 478.
- (112) Cobley, C. J.; Gardner, K.; Klosin, J.; Praquin, C.; Hill, C.; Whiteker, G. T.; Zanotti-Gerosa, A.; Petersen, J. L.; Abboud, K. A. *J. Org. Chem.* **2004**, *69*, 4031.
- (113) Nanno, T.; Sakai, N.; Nozaki, K.; Takaya, H. *Tetrahedron: Asymmetry* **1995**, *6*, 2583.
- (114) (a) Evans, D.; Osborn, J. A.; Wilkinson, G. *J. Chem. Soc. (A)* **1968**, 3133. (b) Yagupsky, G.; Brown, C. K.; Wilkinson, G. *J. Chem. Soc. (A)* **1970**, 1392. (c) Wilkinson, G.; Brown, C. K. *J. Chem. Soc. (A)* **1970**, 2753.
- (115) Castillo Molina, D. A.; Casey, C. P.; Müller, I.; Nozaki, K.; Jäkel, C. *Organometallics* **2010**, *29*, 3362.
- (116) Horiuchi, T.; Shirakawa, E.; Nozaki, K.; Takaya, H. *Organometallics* **1997**, *16*, 2981.
- (117) Gleich, D.; Schmid, R.; Herrmann, W. A. *Organometallics* **1998**, *17*, 2141.
- (118) (a) Babin, J. E.; Whiteker, G. T. International Patent WO 9303839, 1993. (b) Whiteker, G. T.; Briggs, J. R.; Babin, J. E.; Barner, B. A. *Chem. Ind.* **2003**, 89, 359.
- (119) Buisman, G. J. H.; van der Veen, L. A.; Klootwijk, A.; de Lange, W. G. J.; Kamer, P. C. J.; van Leeuwen, P. W. N. M.; Vogt, D. *Organometallics* **1997**, *16*, 2929.
- (120) Diéguez, M.; Pàmies, O.; Ruiz, A.; Castellón, S.; Claver, C. *Chem.—Eur. J.* **2001**, *7*, 3086.
- (121) Breedon, S.; Cole-Hamilton, D. J.; Foster, D. F.; Schwarz, G. J.; Wills, M. *Angew. Chem., Int. Ed.* **2000**, *39*, 4106.
- (122) Cobley, C. J.; Klosin, J.; Qin, C.; Whiteker, G. T. *Org. Lett.* **2004**, *6*, 3277.
- (123) Clark, T. P.; Landis, C. R.; Freed, S. L.; Klosin, J.; Abboud, K. A. *J. Am. Chem. Soc.* **2005**, *127*, 5040.
- (124) Gual, A.; Godard, C.; Castellón, S.; Claver, C. *Adv. Synth. Catal.* **2010**, *352*, 463.
- (125) Zhang, X.; Cao, B.; Yan, Y.; Yu, S.; Ji, B.; Zhang, X. *Chem.—Eur. J.* **2010**, *16*, 871.
- (126) See Thaler, T.; Knochel, P. *Angew. Chem., Int. Ed.* **2009**, *48*, 645 and references cites therein.
- (127) Diéguez, M.; Deerenberg, S.; Pàmies, O.; Claver, C.; van Leeuwen, P. W. N. M.; Kamer, P. *Tetrahedron: Asymmetry* **2000**, *11*, 3161.
- (128) Diéguez, M.; Pàmies, O.; Net, G.; Ruiz, A.; Claver, C. *J. Mol. Catal. A: Chem.* **2002**, *185*, 11.
- (129) Robert, T.; Velder, J.; Schmalz, H.-G. *Angew. Chem., Int. Ed.* **2008**, *47*, 7718.
- (130) Knöbel, A. K. H.; Escher, I. H.; Pfaltz, A. *Synlett* **1997**, 1429.
- (131) (a) Alexakis, A.; Vastra, J.; Burton, J.; Benhaim, C.; Mangeney, P. *Tetrahedron Lett.* **1998**, *39*, 7869. (b) Alexakis, A.; Burton, J.; Vastra, J.; Benhaim, C.; Fournioux, X.; van den Heuvel, A.; Levêque, J.-M.; Mazé, F.; Rosset, S. *Eur. J. Org. Chem.* **2000**, 4011.
- (132) Hu, X.; Chen, H.; Zhang, X. *Angew. Chem., Int. Ed.* **1999**, *38*, 3518.
- (133) Yan, M.; Yang, L.-W.; Wong, K.-Y.; Chan, A. S. C. *Chem. Commun.* **1999**, 11.
- (134) Feringa, B. L.; Badorrey, R.; Pena, D.; Harutyunyan, S. R.; Minnaard, A. J. *Proc. Natl. Acad. Sci. U.S.A.* **2004**, *101*, 5834.
- (135) Reppe, W.; Magin, A. US Patent 2,577,208, 1951.
- (136) Stereochemical considerations for the alternating copolymerization of CO and disubstituted or further substituted alkenes are not relevant, since alternating copolymerization with this kind of alkene hardly proceeds.
- (137) (a) Nakano, K.; Kosaka, N.; Hiyama, T.; Nozaki, K. *Dalton Trans.* **2003**, 4039. (b) Nozaki, K. *Pure Appl. Chem.* **2004**, *76*, 541. (c) Nozaki, K. *Polym. J.* **2005**, *37*, 871.
- (138) (a) Nozaki, K.; Hiyama, T. *J. Organomet. Chem.* **1999**, *576*, 248. (b) Nozaki, K. *J. Polym. Sci., Part A: Polym. Chem.* **2004**, *42*, 215. (c) Nozaki, K. *Chem. Rec.* **2005**, *5*, 376. (d) Nakamura, A.; Ito, S.; Nozaki, K. *Chem. Rev.* **2009**, *109*, 5215.
- (139) Nozaki, K.; Sato, N.; Takaya, H. *J. Am. Chem. Soc.* **1995**, *117*, 9911.
- (140) Nozaki, K.; Sato, N.; Tonomura, Y.; Yasutomi, M.; Takaya, H.; Hiyama, T.; Matsubara, T.; Koga, N. *J. Am. Chem. Soc.* **1997**, *119*, 12779.
- (141) Nozaki, K.; Hiyama, T.; Kacker, S.; Horváth, I. T. *Organometallics* **2000**, *19*, 2031.
- (142) The chain-terminating step was supposed to be the β -hydride elimination from an alkylpalladium species.
- (143) Nozaki, K.; Kawashima, Y.; Nakamoto, K.; Hiyama, T. *Polym. J.* **1999**, *31*, 1057.
- (144) Nozaki, K.; Komaki, H.; Kawashima, Y.; Hiyama, T.; Matsubara, T. *J. Am. Chem. Soc.* **2001**, *123*, 534.
- (145) Iggo, J. A.; Kawashima, Y.; Liu, J.; Hiyama, T.; Nozaki, K. *Organometallics* **2003**, *22*, 5418.

- (146) (a) Nozaki, K.; Kawashima, Y.; Oda, T.; Hiyama, T.; Kanie, K.; Kato, T. *Macromolecules* **2002**, *35*, 1140. (b) Kawashima, Y.; Nozaki, K.; Hiyama, T.; Yoshio, M.; Kanie, K.; Kato, T. *J. Polym. Sci., Part A: Polym. Chem.* **2003**, *41*, 3556.
- (147) Kosaka, N.; Oda, T.; Hiyama, T.; Nozaki, K. *Macromolecules* **2004**, *37*, 3159.
- (148) (a) Nozaki, K.; Shibahara, F.; Elzner, S.; Hiyama, T. *Can. J. Chem.* **2001**, *79*, 593. (b) Fujita, T.; Nakano, K.; Yamashita, M.; Nozaki, K. *J. Am. Chem. Soc.* **2006**, *128*, 1968.
- (149) Nozaki, K. *J. Synth. Org. Chem., Jpn.* **2007**, *65*, 1108.
- (150) Nozaki, K.; Kawashima, Y.; Nakamoto, K.; Hiyama, T. *Macromolecules* **1999**, *32*, 5168.
- (151) Kawashima, Y.; Nozaki, K.; Hiyama, T. *Inorg. Chim. Acta* **2003**, *350*, 577.
- (152) (a) Frost, C. G.; Howarth, J.; Williams, J. M. J. *Tetrahedron: Asymmetry* **1992**, *3*, 1089. (b) Trost, B. M.; Van Vranken, D. L. *Chem. Rev.* **1996**, *96*, 395. (c) Trost, B. M.; Crawley, M. L. *Chem. Rev.* **2003**, *103*, 2921. (d) Trost, B. M. *J. Org. Chem.* **2004**, *69*, 5813. (e) Lu, Z.; Ma, S. *Angew. Chem., Int. Ed.* **2008**, *47*, 258.
- (153) (a) van Leeuwen, P. W. N. M.; Kamer, P. C. J.; Reek, J. N. H.; Dierkes, P. *Chem. Rev.* **2000**, *100*, 2741. (b) Birkholz, M.-N.; Freixa, Z.; van Leeuwen, P. W. N. M. *Chem. Soc. Rev.* **2009**, *38*, 1099.
- (154) (a) Rahman, M. M.; Liu, H. Y.; Eriks, K.; Prock, A.; Giering, W. P. *Organometallics* **1989**, *8*, 1. (b) Cobley, C. J.; Pringle, P. G. *Inorg. Chim. Acta* **1997**, *265*, 107. (c) Leyssens, T.; Peeters, D.; Orpen, A. G.; Harvey, J. N. *Organometallics* **2007**, *26*, 2637. (d) Gusev, D. G. *Organometallics* **2009**, *28*, 763.
- (155) The configuration of palladium complexes bearing an allyl ligand whose distal carbons are pointing in opposite direction to the substituents of the ligand backbone are referred to as *exo*; accordingly, when the allylic distal carbons point in the same direction as the ligand backbone substituents, the complex is described as *endo*.
- (156) Kagan, H. B.; Fiaud, J. C. *Top. Stereochem.* **1988**, *18*, 249.
- (157) Table 34 is not intended to provide a detailed comparison of the enantioselectivities obtained with P–OP ligands with those obtained with the many dozens of efficient ligands that have been developed up until now for this transformation. Due to space limitations, the authors have considered only the required set of ligands that allow comparison with the few results reported for P–OP ligands. The reader is referred to more specific reviews on allylic substitution for more detailed comparison with many kinds of highly efficient ligands (for example, see ref 152).
- (158) Fujii, K.; Kinoshita, N.; Tanaka, K. *Chem. Commun.* **1999**, 1895.
- (159) Yan, Y.-Y.; RajanBabu, T. V. *Org. Lett.* **2000**, *2*, 199.
- (160) von Matt, P.; Pfaltz, A. *Angew. Chem., Int. Ed. Engl.* **1993**, *32*, 566.
- (161) Yamaguchi, M.; Shima, T.; Yamagishi, T.; Hida, M. *Tetrahedron: Asymmetry* **1991**, *2*, 663.
- (162) Rabeyrin, C.; Sinou, D. *Tetrahedron: Asymmetry* **2003**, *14*, 3891.
- (163) See the following leading references, and references cited therein: (a) Beletskaya, I.; Pelter, A. *Tetrahedron* **1997**, *53*, 4957. (b) Carroll, A.-M.; O'Sullivan, T. P.; Guiry, P. J. *Adv. Synth. Catal.* **2005**, *347*, 609. (c) Guiry, P. J. *ChemCatChem* **2009**, *1*, 233. (d) Thomas, S. P.; Aggarwal, V. K. *Angew. Chem., Int. Ed.* **2009**, *48*, 1896. (e) Schiffner, J. A.; Muther, K.; Oestreich, M. *Angew. Chem., Int. Ed.* **2010**, *49*, 1194.
- (164) (a) Werle, S.; Fey, T.; Neudörfl, J. M.; Schmalz, H.-G. *Org. Lett.* **2007**, *9*, 3555. (b) Werle, S.; Fey, T.; Neudörfl, J. M.; Schmalz, H.-G. *Org. Lett.* **2007**, *9*, 4085.
- (165) Hayashi, T.; Matsumoto, Y.; Ito, Y. *J. Am. Chem. Soc.* **1989**, *111*, 3426.
- (166) Schnyder, A.; Hintermann, L.; Togni, A. *Angew. Chem., Int. Ed. Engl.* **1995**, *34*, 931.
- (167) Brown, J. M.; Hulmes, D. I.; Layzell, T. P. *J. Chem. Soc., Chem. Commun.* **1993**, 1673.
- (168) (a) Han, L.-B.; Mirzaei, F.; Zhao, C.-Q.; Tanaka, M. *J. Am. Chem. Soc.* **2000**, *122*, 5407. (b) Mirzaei, F.; Han, L.-B.; Tanaka, M. *Tetrahedron Lett.* **2001**, *42*, 297.
- (169) Xu, Q.; Han, L.-B. *Org. Lett.* **2006**, *8*, 2099.
- (170) Horiuchi, T.; Shirakawa, E.; Nozaki, K.; Takaya, H. *Tetrahedron: Asymmetry* **1997**, *8*, 57.
- (171) (a) Elmes, P. S.; Jackson, W. R. *J. Am. Chem. Soc.* **1979**, *101*, 6128. (b) Hodgson, M.; Parker, D.; Taylor, R. J.; Ferguson, G. *Organometallics* **1988**, *7*, 1761.
- (172) (a) Baker, M. J.; Pringle, P. G. *J. Chem. Soc., Chem. Commun.* **1991**, 1292. (b) Yan, M.; Xu, Q.-Y.; Chan, A. S. C. *Tetrahedron: Asymmetry* **2000**, *11*, 845.
- (173) Nozaki, K.; Lakshmi Kantam, M.; Horiuchi, T.; Takaya, H. *J. Mol. Catal. A: Chem.* **1997**, *118*, 247.
- (174) Zhou, H.; Hou, J.; Cheng, J.; Lu, S.; Fu, H.; Wang, H. *J. Organomet. Chem.* **1997**, *543*, 227.
- (175) Imada, Y.; Fujii, M.; Kubota, Y.; Murahashi, S.-I. *Tetrahedron Lett.* **1997**, *38*, 8227.
- (176) Loelsberg, W.; Ye, S.; Schmalz, H.-G. *Adv. Synth. Catal.* **2010**, *352*, 2023.
- (177) Noonan, G. M.; Newton, D.; Cobley, C. J.; Suarez, A.; Pizzano, A.; Clarke, M. L. *Adv. Synth. Catal.* **2010**, *352*, 1047.
- (178) Arribas, I.; Vargas, S.; Rubio, M.; Suárez, A.; Domene, C.; Álvarez, E.; Pizzano, A. *Organometallics* **2010**, *29*, 5791.
- (179) Doro, F.; Reek, J. N. H.; van Leeuwen, P. W. N. M. *Organometallics* **2010**, *29*, 4440.
- (180) Rubio, M.; Pizzano, A. *Molecules* **2010**, *15*, 7732.
- (181) Robert, T.; Abiri, Z.; Sandee, A. J.; Schmalz, H.-G.; Reek, J. N. H. *Tetrahedron: Asymmetry* **2010**, *21*, 2671.